

Some pages of this thesis may have been removed for copyright restrictions.

If you have discovered material in AURA which is unlawful e.g. breaches copyright, (either yours or that of a third party) or any other law, including but not limited to those relating to patent, trademark, confidentiality, data protection, obscenity, defamation, libel, then please read our [Takedown Policy](#) and [contact the service](#) immediately

TITLE PAGE

Gold Mineralisation in the Caledonides of the British Isles with Special Reference to the
Dolgellau Gold-belt, North Wales and the Southern Uplands, Scotland.

VOL. 1

JONATHAN NADEN

Doctor of Philosophy

THE UNIVERSITY OF ASTON IN BIRMINGHAM

APRIL 1988

This copy of the Thesis has been supplied on the condition that anyone who consults it is understood to recognise that its copyright rests with its author and that no quotation from this thesis and no information derived from it may be published without the author's prior, written consent.

Gold Mineralisation in the Caledonides of the British Isles with Special Reference to the
Dolgellau Gold-belt, North Wales and the Southern Uplands, Scotland.

JONATHAN NADEN

Doctor of Philosophy

1988

SUMMARY

Two aspects of gold mineralisation in the Caledonides of the British Isles have been investigated: gold-telluride mineralisation at Clogau Mine, North Wales; and placer gold mineralisation in the Southern Uplands, Scotland.

The primary ore assemblage at Clogau Mine is pyrite, arsenopyrite, cobaltite, pyrrhotine, chalcopyrite, galena, tellurbismuth, tetradymite, altaite, hessite, native gold, wehrlite, hedleyite, native bismuth, bismuthinite and various sulphosalts. The generalised paragenesis is early Fe, Co, Cu, As and S species, and later minerals of Pb, Bi, Ag, Au, Te, Sb. Electron probe micro-analysis (EPMA) of complex telluride-sulphide intergrowths suggests that these intergrowths formed by co-crystallisation/replacement processes and not exsolution. Minor element chemical variation, in the sulphides and tellurides, indicates that antimony and cadmium are preferentially partitioned into telluride minerals. Mineral stability diagrams suggest that during gold deposition $\log a_{\text{Te}_2}$ was between -7.9 and -9.7 and $\log a_{\text{S}_2}$ between -12.4 and -13.8. Co-existing mineral assemblages indicate that the final stages of telluride mineralisation were between c. 250 - 275°C. It is suggested that the high-grade telluride ore shoot was the result of remobilisation of Au, Bi, Ag and Te from low grade mineralisation elsewhere within the vein system, and that gold deposition was brought about by destabilisation of gold chloride complexes by interaction with graphite, sulphides and tellurbismuth.

Scanning electron microscopy of placer gold grains from the Southern Uplands, Scotland, indicates that detailed studies on the morphology of placer gold can be used to elucidate the history of gold in the placer environment. In total 18 different morphological characteristics were identified. These were divided on an empirical basis, using the relative degree of mechanical attrition, into proximal and distal characteristics. One morphological characteristic (a porous/spongy surface at high magnification) is considered to be chemical in origin and represent the growth of "new" gold in the placer environment. The geographical distribution of morphological characteristics has been examined and suggests that proximal placer gold is spatially associated with the Loch Doon, Cairnsphairn and Fleet grantoids.

Quantitative EPMA of the placer gold reveals two compositional populations of placer gold. Examination of the geographical distribution of fineness suggests a loose spatial association between granitoids and low fineness placer gold. Also identified was chemically heterogeneous placer gold. EPMA studies of these heterogeneities allowed estimation of annealing history limits, which suggest that the heterogeneities formed between 150 and 235°C.

It is concluded, on the basis of relationships between morphology and composition, that there are two types of placer gold in the Southern Uplands: (i) placer gold which is directly inherited from a hypogene source probably spatially associated with granitoids; and (ii) placer gold that has formed during supergene processes.

TO ANITA

Acknowledgements.

I am indebted to my two supervisors Drs. R.A. Ixer and D.J. Vaughan for their encouragement and constructive discussions during the writing of this thesis. I am also grateful to Dave Plant and Tim Hopkins at Manchester University who allowed me to use the Manchester microprobe. Thanks also go to J.F. Rottenbury for allowing access to Clogau Mine, and to Roger Howell and Eric Hartland at Aston University for technical support.

The research for this thesis was undertaken in the Department of Geological Sciences at Aston University, and was financed by a University Studentship.

Especial thanks go to Jennifer and David Howard for providing financial and moral support during the final stages of the production of this thesis, and without whose help the final completion of this thesis would not have been possible.

TABLE OF CONTENTS.

TABLE OF CONTENTS FOR VOLUME 1.

CHAPTER 1:

INTRODUCTION.....23

1.1. Aims and Scope of Thesis.....24

1.2. Outline of Thesis.25

CHAPTER 2:

THE OCCURRENCE OF GOLD IN THE BRITISH CALEDONIDES.....26

2.1. Introduction.27

2.2. Wales.27

2.3. Scotland.29

2.4. Ireland.30

2.5. England.31

2.6. Recent Discoveries of Gold.31

2.7. Summary.32

CHAPTER 3:

GEOLOGY OF THE HARLECH DOME.33

3.1. Introduction.34

3.2. Stratigraphy.34

3.3. Igneous Activity.36

3.4. Timing of Igneous Activity.36

3.5. Structure, Deformation and Metamorphism.37

3.6. Mineralisation in the Harlech Dome.39

3.7. Timing of Mineralisation.41

CHAPTER 4:

GEOLOGY, MINERALOGY AND MINERAL CHEMISTRY OF CLOGAU MINE.....

	42
4.1. Introduction.	43
4.2. Ore Mineralogy of No. 4 Level.	44
4.2.1. Rutile - arsenopyrite - pyrite/pyrrhotine - cobaltite Assemblage.	46
4.2.2. Chalcopyrite-pyrrhotine Assemblage.	46
4.2.3. Telluride Assemblages.	47
4.2.4. Other Occurrences of Native Gold and Tellurides.	52
4.2.5. Alteration Assemblages.	53
4.3. Paragenetic Interpretation.	53
4.4. Mineral Chemistry.	55
4.4.1. Introduction.	55
4.4.2. Cobaltite and Arsenopyrite.	58
4.4.3. Chemistry of Tellurobismuth, Tetradymite and Galena in the TellurideDominated Assemblage.	58
4.4.4. Comparison of Trace Element Distribution Between the Major Mineral Species in the Bismuth Telluride Assemblage.	62
4.4.5. Chemistry of Galena in the Sulphide-dominated Telluride Assemblage.	63
4.4.6. Chemistry of the Minor Phases.	64
4.4.7. Chemistry of Gold.	64
4.4.8. Chemistry of the Telluride and Sulphide Intergrowths.	65
4.5. Relationship Between Mineral Chemistry and Paragenesis.	67

CHAPTER 5:

CONDITIONS OF ORE FORMATION AT CLOGAU MINE..... 69

5.1. Introduction.	70
5.2. Thermochemical data for the systems Bi-Te-S, Bi-Te-Au, Pb-Te-S, Au-Ag-Te-S.	70
5.2.1. Calculation of activity data from Gibb's Free energy data.	71
5.2.2. Validity of calculated data.	72
5.2.3. Estimation of thermochemical data.	73
5.2.4. Validity of approximations.	76
5.2.5. Ranking of data.	77
5.2.6. Effect of pressure.	79
5.3. Conditions of Ore Formation at Clogau Mine.	79
5.3.1. Temperature.	80
5.3.2. Activity of Tellurium and Sulphur during Mineralisation.	80
5.4. Relationship Between Mineralisation at Clogau Mine and The Dolgellau Gold-belt.	83

CHAPTER 6:

DISCUSSION OF MINERALISATION AT CLOGAU MINE..... 84

CHAPTER 7:

GEOLOGY AND MINERALISATION OF THE SOUTHERN UPLANDS..... 88

7.1. Introduction.	89
7.2. Stratigraphy, Structure and Metamorphism.	89
7.2.1. Stratigraphy.	87
7.2.2. Structure.	91
7.3.2. Metamorphism.	95

7.3. Magmatism in the Southern Uplands.	95
7.3.1. Major intrusive complexes.	96
7.3.2. Minor Intrusions.	97
7.3.3. Dyke Swarms.	97
7.4. Mineralisation in the Southern Uplands.	98
7.4.1. Lead-zinc Vein Mineralisation.	99
7.4.2. Arsenic-antimony Mineralisation.	99
7.4.3. Porphyry-copper Style Mineralisation.	101
7.4.4. Iron-Cobalt-Nickel Mineralisation.	102
7.4.5. Gold Mineralisation.	103
7.5. Relationship between structure, rock type and mineralisation.	107

CHAPTER 8:

MORPHOLOGY, PETROGRAPHY AND COMPOSITION OF THE SOUTHERN UPLANDS PLACER GOLD: METHODOLOGY AND DISCUSSION.....	109
8.1. Introduction.	110
8.2. Morphology of Placer Gold.	110
8.3. Description of the Morphological Characteristics of Placer Gold from the Southern Uplands and North Wales.	114
8.3.1. Macro-morphological Characteristics.	114
8.3.2. Micro-morphological Features.	117
8.4. Summary and Discussion of Morphological Characteristics.	121
8.4.1. Macro-morphological Features.	121
8.4.2. Micro-morphological Features.	123
8.5. Petrography.	124
8.6. Composition of Native Gold.	124

8.7. "Concluding Remarks".	127
CHAPTER 9:	
MORPHOLOGICAL, PETROLOGICAL AND COMPOSITIONAL DATA FOR THE SOUTHERN UPLANDS PLACER GOLD.	129
9.1. Introduction.	130
9.2. Loch Doon-Glenkens Area.	130
9.2.1. General Geology and Distribution of Gold.	130
9.2.2. Morphology of the Loch Doon-Glenkens Placer Gold.	131
9.2.3. Scanning Electron Microscope Fineness Data for the Doon-Glenkens Placer Gold.	132
9.2.4. Petrography of The Doon-Glenkens Placer Gold .	133
9.2.5. Composition of the Doon-Glenkens Placer Gold.	134
9.3. Abington-Biggarr-Moffat Area.	136
9.3.1. General Geology and Distribution of Gold.	136
9.3.2. Morphology of the Abington-Biggarr-Moffat Placer Gold.	137
9.3.3. SEM Fineness Data for the Abington-Biggarr- Moffat Area.	137
9.3.4. Petrography of the Abington-Biggarr-Moffat Placer Gold.	138
9.3.5. Composition of the Abington-Biggarr-Moffat Placer Gold.	138
9.4. Comparison of the Doon-Glenkens and the Abington-Biggarr-Moffat Placer Gold.	138
9.5. Origin of the Southern Uplands Placer Gold.	139
CHAPTER 10:	
DISCUSSION OF THE SOUTHERN UPLANDS PLACER GOLD.	143
10.1. Critique of the Methodology Developed in Chapter 8.	144
10.2. Discussion of the Southern Upland Placer gold data.	145
10.3. Limitations of the Technique.	146

10.5. Future Work.	147
-------------------------	-----

TABLE OF CONTENTS FOR VOLUME 2.

FIGURES AND TABLES FOR CHAPTER 2:

THE OCCURRENCE OF GOLD ASSOCIATED WITH THE CALEDONIDES OF THE BRITISH ISLES.	15
------------------------------------------------------------------------------------------	-----------

Figure 2.1. Geographical distribution of gold occurrences in England, Wales and Southern Scotland.	16
---------------------------------------------------------------------------------------------------------	----

Figure 2.2. Geographical distribution of gold occurrences in Northern Scotland.	17
--------------------------------------------------------------------------------------	----

Figure 2.3. Geographical distribution of gold occurrences in Ireland.	18
----------------------------------------------------------------------------	----

Figure 2.4. Geographical distribution of gold mines in the Dolgellau Gold-belt.	19
--------------------------------------------------------------------------------------	----

Table 2.1. Table summarising the geological and mineralogical details of gold mineralisation in the Dolgellau Gold-belt.....	20
------------------------------------------------------------------------------------------------------------------------------	----

Figure 2.5. General geology surrounding Ogofau Mine, Dyfed, South Wales.....	
------------------------------------------------------------------------------	--

Figure 2.6. General geology associated with the Helmsdale placer gold deposit with approximate localities of recorded gold occurrences.....	23
---------------------------------------------------------------------------------------------------------------------------------------------	----

Table 2.2. Minor occurrences of gold in Scotland.....	24
-------------------------------------------------------	----

Figure 2.7. General geology associated with the Gold Mines River placer gold deposit with approximate localities of recorded gold occurrences.....	25
----------------------------------------------------------------------------------------------------------------------------------------------------	----

FIGURES FOR CHAPTER 3:

THE GENERAL GEOLOGY OF THE HARLECH DOME.....	26
-----------------------------------------------------	-----------

Figure 3.1. Stratigraphy of the Harlech Dome.....	27
---------------------------------------------------	----

Figure 3.2. General geology of the Harlech Dome.....	28
------------------------------------------------------	----

Figure 3.3. Outcrop of the Rhobell Fawr Volcanic Group and the western margin of the Aran Volcanic Group	29
----------------------------------------------------------------------------------------------------------------	----

Figure 3.4. Titanium versus zirconium scattergram for the intrusive rocks of the Harlech Dome.	30
-----------------------------------------------------------------------------------------------------	----

Figure 3.5. General geochemistry of the intrusive rocks.	31
---------------------------------------------------------------	----

Figure 3.6. Main structural features of the Harlech Dome.....	32
---------------------------------------------------------------	----

Figure 3.7. Rose diagram showing the spatial relationship between the minor faults, quartz veins and dykes in the Harlech Dome.	33
Figure 3.8. Geology surrounding the Coed-y-Brenin porphyry copper deposit	34
Figure 3.9. Geology surrounding the Glasdir copper body.....	35

FIGURES, PLATES AND TABLES FOR CHAPTER 4:

THE GEOLOGY, MINERALOGY AND MINERAL CHEMISTRY OF CLOGAU MINE.	36
Figure 4.1. Geology surrounding Clogau Mine.....	37
Figure 4.2. Sample location map, and general geology of No. 4 Level, Clogau Mine.	38
Figure 4.3. Schematic map of the geology of the ore shoot on No. 4 Level, Clogau Mine.	39
Plate 4.1. Bismuth tellurides and carbonate infilling fractures in quartz	40
Plate 4.2. Sericite laths included in galena	40
Plate 4.3. Thin veinlet of graphite in quartz with associated arsenopyrite locally altering to limonite, and gold.	41
Plate 4.4. Small rutile grains in shale inclusion.....	41
Plate 4.5. Galena replacing cobaltite and pyrrhotine.	42
Plate 4.6. Crossed nicols view of plate 4.5 showing the presence of arsenopyrite and bismuthinite	42
Plate 4.7. Euhedral cubes and rhombs of cobaltite locally cemented by chalcopyrite	43
Plate 4.8. Thin chalcopyrite vein in a micro-fracture in quartz.....	43
Plate 4.9. Pyrrhotine and chalcopyrite intergrown exhibiting mutual grain boundaries	44
Plate 4.10. Porous zoned pyrite replacing pyrrhotine	44
Plate 4.11. Triple point grain boundaries in tellurbismuth	45
Plate 4.12. Careous grain boundaries within tellurbismuth.....	45
Plate 4.13. Small galena inclusions forming along cleavage in tellurbismuth.....	46

Plate 4.14. Myrmekitic intergrowth of galena and tellurbismuth	46
Plate 4.15. Galena rim on tetradymite.	47
Plate 4.16. Careous boundary between tellurbismuth and tetradymite.....	47
Plate 4.17. Fingerprint intergrowth at the margin between tetradymite and quartz.....	48
Plate 4.18. Discrete galena grains in tellurbismuth.	48
Plate 4.19. Galena replacing tellurbismuth along cleavage.....	49
Plate 4.20. Small isolated grain of altaite in tellurbismuth.....	49
Plate 4.21. Altaite grain with small inclusion of native gold in tellurbismuth.....	50
Plate 4.22. Galena and altaite replacing tellurbismuth along cleavage	50
Plate 4.23a. Galena and hessite in tellurbismuth.	51
Plate 4.23b. Crossed polars view of figure 4.23a	51
Plate 4.24. Line of small hessite inclusions forming along a dissolution surface on tellurbismuth.....	52
Plate 4.25. Small isolated grain of native gold in tellurbismuth	52
Plate 4.26. Galena replacing pyrrhotine along grain boundaries	53
Plate 4.27. Cluster of ragged tetradymite laths and wehrlite in galena.....	53
Plate 4.28 Skeletal wehrlite, native bismuth and bismuthinite replacing galena.	54
Plate 4.29. Skeletal wehrlite replacing galena along cleavage.....	54
Plate 4.30. Small hessite grain in galena associated with cleavage.....	55
Plate 4.31. Native gold and ?Hedleyite in galena	55
Plate 4.32. Native bismuth forming along cleavage in galena.	56
Plate 4.33. Bismuthinite in galena.....	56
Plate 4.34. Veinlets of native gold in quartz	57
Plate 4.35. Gold cementing and replacing pyrite in quartz.	57
Plate 4.36. Veinlet of native gold in galena	58

Plate 4.37. Stibioiluzonite inclusions in galena.....	58
Plate 4.38. Tetrahedrite in a vug in quartz.	59
Plate 4.39. Pyrrhotine altering to pyrite and marcasite.	59
Plate 4.40. Covelline replacing galena.....	60
Plate 4.41. Arsenopyrite altering to limonite.	60
Table 4.3 Analytical details of electron probe micro-analyses.....	61
Figure 4.4. Line concentration profile across a cobaltite grain showing the variations in major element chemistry.	63
Figure 4.5. Line concentration profile across a cobaltite grain showing the variations in minor element chemistry.	63
Table 4.5. Summary Statistics of the major and minor element chemistry of tellurbismuth.....	64
Figure 4.6a. Histogram of the distribution of lead in tellurbismuth.....	65
Figure 4.6b. Histogram of the distribution of bismuth in tellurbismuth.....	65
Figure 4.6c. Histogram of the distribution of sulphur in tellurbismuth.	66
Figure 4.6d. Histogram of the distribution of tellurium in tellurbismuth.....	66
Figure 4.6e. Histogram of the distribution of antimony in tellurbismuth.	67
Figure 4.6f. Histogram of the distribution of cadmium in tellurbismuth.....	67
Figure 4.6g. Histogram of the distribution of silver in tellurbismuth.....	68
Table 4.6. Correlation matrix for the major and minor elements in tellurbismuth.	69
Table 4.7. Summary statistics of the major and minor element chemical data for Tetradymite.	69
Figure 4.7. X-Y plot showing the variation of the molar ratios of Bi, Te, S, Sb and Cd in tetradymite.	70
Figure 4.8. X-Y plots of the molar ratios (Bi+Pb)/(Te+Cd+Sb) and S/(Te+Cd+Sb) versus Total wt%.	70
Table 4.8. Correlation matrix for the major and minor elements in tetradymite.....	71

Figure 4.9a. Histogram showing the distribution of lead in tetradymite.	72
Figure 4.9b. Histogram showing the distribution of bismuth in tetradymite.	72
Figure 4.9c. Histogram showing the distribution of sulphur in tetradymite.	73
Figure 4.9d. Histogram showing the distribution of tellurium in tetradymite.	73
Figure 4.9e. Histogram showing the distribution of antimony in tetradymite.	74
Figure 4.9f. Histogram showing the distribution of cadmium in tetradymite.	74
Figure 4.9g. Histogram showing the distribution of silver in tetradymite.	75
Table 4.9. Summary statistics for the major and minor elements in galena.	76
Figure 4.10a. Line concentration profile across a tetradymite-galena-tellurbismuth intergrowth, showing the variation in antimony concentration between different minerals.	77
Figure 4.10b. Line concentration profile across a galena-tellurbismuth intergrowth, showing the variation in antimony concentration between the two minerals.	77
Figure 4.11. Histogram of the distribution of tellurium in galena from the tellurbismuth-dominated assemblage.	78
Figure 4.12. Histogram of the distribution of bismuth in galena from the tellurbismuth-dominated assemblage.	78
Table 4.10. Correlation matrix for major and minor element chemistry in galena from the tellurbismuth-dominated telluride assemblage.	79
Table 4.11. Summary statistics for the major and minor element concentrations in the fingerprint intergrowths.	79
Figure 4.13. Box plots showing the statistical variation of antimony between tellurbismuth, tetradymite, galena and the fingerprint intergrowths.	80
Figure 4.14. Box plots showing the statistical variation of cadmium between tellurbismuth, tetradymite, galena and the fingerprint intergrowths.	80
Figure 4.15. Box plots showing the statistical variation of silver between tellurbismuth, tetradymite, galena and the fingerprint intergrowths.	81
Table 4.12. Summary statistics for the major and minor element concentrations in galena from the sulphide-dominated telluride assemblage.	82

Figure 4.16. Histograms comparing the distribution of tellurium in galena between the two telluride assemblages.....	83
Figure 4.17. Histograms comparing the distribution of silver in galena between the two telluride assemblages.....	84
Figure 4.18. Histograms comparing the distribution of cadmium in galena between the two telluride assemblages.....	85
Figure 4.19. Histograms comparing the distribution of bismuth in galena between the two telluride assemblages.....	86
Table 4.13. Correlation matrix for the major and minor elements in galena from the sulphide-dominated telluride assemblage.....	87
Table 4.14a. Analyses of the minor tellurides, bismuthinite, and native bismuth from No. 4 Level.....	88
Table 4.14b. Analyses of the sulphosalts in BM kingsbury (K2).....	89
Figure 4.20. Histogram of the fineness of gold from No. 4 Level.	90
Figure 4.21. Histogram of the fineness of placer gold from the Hírgwm river.	90
Table 4.15. Summary statistics of fineness of native gold from No. 4 Level Clogau Mine, placer gold from the Hírgwm river, and the gold-bearing samples from the British Museum (Natural History) and the National Museum of Wales.....	91
Table 4.16. Fineness of gold in gold-bearing samples loaned from the British Museum (Natural History) and the National Museum of Wales.....	91
Figure 4.22. Line concentration profiles across a tellurbismuth-galena intergrowth showing the variation in major "cation" (Bi, Pb),"anion" (Te, S) and minor element (Sb, Cd) chemistries.....	92
Figure 4.23. Line concentration profile across a tellurbismuth-galena-tetradymite intergrowth showing the variation in major "cation" (Bi, Pb),"anion" (Te, S) and minor element (Sb, Cd) chemistries.	93
Figure 4.24. Line concentration profiles illustrating the variation in major "cation" (Bi, Pb) and "anion" (Te, S) chemistries.....	94
FIGURES AND TABLES FOR CHAPTER 5:	
CONDITIONS OF ORE FORMATION AT CLOGAU MINE.....	95

Table 5.1. Comparison of Gibbs Free energy between data calculated in this thesis and that by Barton and Skinner (1979).....	96
Table 5.2. Sulphidation and telluridation reactions investigated.	97
Figure 5.1.a Activity of tellurium plot for the telluridation of various compositions of electrum.	98
Figure 5.1b. Activity of tellurium-activity sulphur plot showing the method of calculation of tellurium activity in equilibrium with hessite and electrum.	99
Figure 5.2. Temperature-activity grid for the telluridation reactions	100
Figure 5.3. Temperature-activity grid for the sulphidation reactions	101
Figure 5.4. Mineral stability fields at 350°C and 1 atmosphere.....	102
Figure 5.5. Mineral stability fields at 300°C and 1 atmosphere.	103
Figure 5.6. Mineral stability fields at 250°C and 1 atmosphere.	104
Figure 5.7. Mineral stability fields at 200°C and 1 atmosphere.	105
Figure 5.8. Diagrammatic illustration of the stability ranges of the observed phases at Clogau Mine.	106
Table 5.3. Comparison of theoretically stable and unstable assemblages with actually observed assemblages.	107

FIGURES FOR CHAPTER 7:

THE GEOLOGY AND MINERALISATION OF THE SOUTHERN UPLANDS.	108
Figure 7.1. Fault bounded tracts and greywacke formations of the Southern Uplands.	109
Figure 7.2. Geology of the Leadhills-Wanlockhead mining district.	110
Figure 7.3. Distribution of arsenic-antimony mineralisation in the Southern Uplands.	111
Figure 7.4. Geology surrounding the Black Stockarton Moor sub-volcanic complex.	112
Figure 7.5. Geology of the Cu-Fe-As-Mo mineralisation at Caingarroch Bay.	113

Figure 7.6. Geology of the Fe-Co-Ni mineralisation at Talnotry.....	114
Figure 7.7. Geology of the gold mineralisation at the Fore Burn Igneous Complex...	115
Figure 7.8. Geology of the gold mineralisation at the margin of the Loch Doon granitoid Complex.	116
Figure 7.9. Relationship between structure intrusives and mineralisation.....	117

FIGURES, PLATES AND TABLES FOR CHAPTER 8:

MORPHOLOGICAL, PETROLOGICAL AND COMPOSITIONAL OF THE SOUTHERN UPLANDS PLACER GOLD; METHODOLOGY.....	118
Table 8.1. List of morphological characteristics of the Southern Uplands placer gold.....	119
Plates 8.1a to 8.1d SEM electronmicrographs of placer gold collected from the Hirgwm river, Bontddu, North Wales, 1km downstream from Clogau mine. These grains are used to illustrate the morphological characteristic of a glazed surface.	120
Plates 8.1e to 8.1h SEM electronmicrographs of placer gold collected from the River Mawddach by T.A. Readwin.....	121
Plates 8.2a to 8.2d SEM electronmicrographs showing the morphological features of lode gold dissolved from quartz using hydrofluoric acid.	122
Plates 8.3a to 8.3d SEM electronmicrographs of placer gold grains from the Southern Uplands which illustrate the macro-morphological feature of grains that preserve most of their original crystalline features.	123
Plates 8.4a to 8.4d SEM electronmicrographs of placer gold grains from the Southern Uplands that are used to illustrate the macro morphological feature of deformed crystalline texture.....	124
Plates 8.5a to 8.5d SEM electronmicrographs of placer gold grains from the Southern Uplands that are used to illustrate the macro-morphological feature of irregularly shaped gold grains.	125
Plates 8.6a to 8.6d SEM electronmicrographs of placer gold from the Southern Uplands that illustrates the macro-morphological feature subrounded and folded placer goldgrains.	126
Plates 8.7a to 8.7d SEM electronmicrographs of placer gold from the Southern Uplands that are used to illustrate the macro-morphological feature of placer gold grains with a generally elongate shape.....	127

Plates 8.8a to 8.8d SEM electronmicrographs of placer gold grains from the Southern Uplands which illustrate the macro-morphological feature of placer gold that is "nugget"-shaped.....	128
Plates 8.9a to 8.9d SEM electronmicrographs of placer gold from the Southern Uplands that illustrate placer gold that exhibits the macro-morphological feature of flake-shaped grains.	129
Plates 8.10a to 8.10d SEM electronmicrographs of placer gold grains from the Southern Uplands that are used to illustrate the micro-morphological feature of a smooth unworn surface at high magnification.....	130
Plates 8.11a to 8.11c SEM electronmicrographs of placer gold from the Southern Uplands that illustrate the micro-morphological feature of original inclusions.	131
Plates 8.12a to 8.12b SEM electronmicrographs of placer gold grains from the Southern Uplands that illustrate the micro-morphological feature of an irregular surface at high magnification.	132
Plates 8.13a to 8.13d SEM electronmicrographs of placer gold grains that show the micro-morphological feature of trapped mineral grains.	133
Plates 8.14a to 8.14d SEM electronmicrographs of placer gold grains from the Southern Uplands that exhibit the micro-morphological feature of a flaky surface at high magnification.	134
Plates 8.15a to 8.15d SEM electronmicrographs of placer gold grains from the Southern Uplands that exhibit the micro-morphological features of a surface that is generally smooth and worn at high magnification, and has random scratches on it.....	135
Plates 8.16a to 8.16d SEM electronmicrographs of placer gold grains from the Southern Uplands that show the micro-morphological feature of the formation of a dough like surface texture at high magnification.	136
Plates 8.17a to 8.17d SEM electronmicrographs of placer gold grains from the Southern Uplands which exhibit the micro-morphological feature of a porous surface at high magnification.....	137
Table 8.2. Relationship between macro- and micro-morphological characteristics.....	138

FIGURES, PLATES AND TABLES FOR CHAPTER 9:

MORPHOLOGICAL, PETROLOGICAL AND COMPOSITIONAL DATA FOR THE SOUTHERN UPLANDS PLACER GOLD.....139

Figure 9.1. Map showing the geology and the distribution of placer gold in the Loch Doon-Glenkens area.	140
Figure 9.2. Map showing the geology and the distribution of placer gold in the Abington-Biggarr-Moffat area.....	141
Figure 9.3. Histogram showing the distribution of macro-morphological characteristics of the Loch Doon-Glenkens placer gold.	142
Figure 9.4. Histogram showing the distribution of micro-morphological characteristics of the Loch Doon-Glenkens placer gold.	142
Figure 9.5. Geographical distribution of macro-morphological characteristics for the Loch Doon-Glenkens placer gold.	143
Figure 9.6. Geographical distribution of micro-morphological characteristics for the Loch Doon-Glenkens placer gold.....	144
Figure 9.7. Geographical distribution of placer gold preserving original morphological features.	145
Figure 9.8. Histogram showing the surface fineness distribution (from semi-quantitative energy dispersive analysis) of placer gold from the Loch Doon-Glenkens area.....	146
Figure 9.9. Geographical distribution of the surface fineness of placer gold from the Loch Doon-Glenkens area.	147
Plate 9.1. Backscattered electron image and X-ray ($\text{Ag}_{\text{L}\alpha}$) map of a silver-rich vein in a heterogeneous placer gold grain (sample no. C35).	148
Plate 9.2. Photomicrograph of a thin incomplete gold enrichment rim on a placer gold grain.	149
Plate 9.3. Backscattered electron image and X-ray ($\text{Bi}_{\text{M}\alpha}$) map of a native bismuth inclusion in a placer gold grain (sample no. C303).	150
Table 1. Summary statistics of the fineness of the Loch Doon-Glenkens placer gold.....	151

Figure 9.10. Histogram showing the core fineness distribution (from EPMA analysis) of placer gold from the Loch Doon-Glenkens area.	151
Figure 9.11. Geographical distribution of the core fineness of placer gold from the Loch Doon-Glenkens area.	152
Figure 9.12a. Line concentration profile showing the variation in silver content in placer gold from pan concentrate C18.	153
Figure 9.12b. Line concentration profile showing the variation in silver content in placer gold from pan concentrate C22.	153
Figure 9.12c. Line concentration profile showing the variation in silver content in placer gold from pan concentrate C22.	154
Figure 9.12d. Line concentration profile showing the variation in silver content in placer gold from pan concentrate C35.	154
Figure 9.12e. Line concentration profile showing the variation in silver content in placer gold from pan concentrate C37.	155
Figure 9.13. Annealing history limits for the heterogeneous placer gold from the Loch Doon-Glenkens area.	156
Figure 9.14. Histogram of the distribution of macro-morphological characteristics of the Abington-Biggarr-Moffat placer gold.	157
Figure 9.15. Histogram of the distribution of micro-morphological characteristics of the Abington-Biggarr-Moffat placer gold.	157
Figure 9.16. Geographical distribution of macro-morphological characteristics for the Abington-Biggarr-Moffat placer gold.	158
Figure 9.17. Geographical distribution of micro-morphological characteristics for the Loch Doon-Glenkens placer gold.	159
Figure 9.18. Histogram of the distribution of the surface fineness of the Abington-Biggarr-Moffat placer gold.	160
Table 9.2. Summary statistics of the core fineness of the Abington-Biggarr-Moffat placer gold.	160
Figure 9.19. Histogram of the distribution of the core fineness of the Abington-Biggarr-Moffat placer gold.	161

Figure 9.20. Geographical distribution of the core fineness of the placer gold from the Abington-Biggarr-Moffat area.....	162
----------------------------------------------------------------------------------------------------------------------------------	-----

Figure 9.21. Histogram showing the frequency distribution of the macro-morphological characteristics of placer gold from the Loch Doon-Glenkens and the Abington-Biggarr-Moffat areas.....	163
---------------------------------------------------------------------------------------------------------------------------------------------------------------------------------------------------	-----

Figure 9.22. Histogram of the morphological characteristics of placer gold with fineness <950.....	163
-----------------------------------------------------------------------------------------------------------	-----

Figure 9.23. Histogram of the morphological characteristics of placer gold with fineness >950.....	164
-----------------------------------------------------------------------------------------------------------	-----

APPENDICES.

Appendix 1a. Calculation of thermochemical data.	165
--------------------------------------------------------------	-----

Appendix 1b. Thermochemical Data.	174
-----------------------------------------------	-----

Appendix 2. Sample preparation techniques of the Southern Uplands placer gold for SEM and EPMA analyses.	189
----------------------------------------------------------------------------------------------------------------------	-----

Appendix 3. Method employed for the calculation of the annealing history limits for heterogeneous placer gold.	192
----------------------------------------------------------------------------------------------------------------------------	-----

Appendix 4a. Sample details for the material from Clogau Mine and Dogellau Gold-belt.	196
---------------------------------------------------------------------------------------------------	-----

Appendix 4b. Mineralogical data for chapter 4.	200
------------------------------------------------------------	-----

Appendix 5. Southern Uplands placer gold data.....	223
-----------------------------------------------------------	-----

CHAPTER 1.

INTRODUCTION.

1.1 Aims and Scope of Thesis.

Introduction.

The original aim of this study was to investigate the nature, occurrence and mineralogy of gold mineralisation in the Caledonides of the British Isles, but the availability of suitable material for study has restricted the detailed coverage to two areas: the vein quartz mineralisation of the Dolgellau Gold-belt in North Wales; and placer gold mineralisation from the Southern Uplands in Scotland. Although the detailed investigation is restricted to the above two areas, other occurrences of gold in the Caledonides of the British Isles are discussed.

Dolgellau Gold-belt.

The mineralogy of the vein quartz mineralisation at Clogau Mine has been studied in detail using reflected light and transmitted light microscopy. The mineral chemistry of Clogau Mine was studied using electron probe micro-analysis, and the variations in chemistry related to the observed mineralogy.

The aim of this section of the thesis is to establish the conditions of ore formation at Clogau Mine.

The Southern Uplands Placer Gold.

The study of the Southern Uplands placer gold forms the second part of this thesis. During an extensive stream sediment sampling survey of the Southern Uplands by the British Geological Survey, some one hundred and fifty placer gold grains were collected from over one hundred sites (all of the collecting sites are located by eight figure map references). The morphologies of these gold grains have been studied using scanning electron microscopy (SEM) with their compositions and homogeneity examined using reflected light microscopy and electron probe micro-analysis (EPMA).

The aim of this section of the thesis is to establish, firstly, if a study of placer gold and its associated stream sediments can yield information on the provenance of the placer gold and the type of original mineralisation that deposited the gold and, secondly,

if the composition of that placer gold can be related to the known geology of the Southern Uplands.

1.2 Outline of Thesis.

Chapter 2 is a general discussion on gold mineralisation in the British Isles, and for the reasons already mentioned the remainder of the thesis is divided into two sections: Chapters 3-6 deal with the gold mineralisation in the Dolgellau Gold-belt and Chapters 7 to 11 cover the investigation of the placer gold from the Southern Uplands.

Section on the Dolgellau Gold-belt.

Chapter 3 is a review of the literature that describes the geology and mineralisation in the Harlech Dome, of which the Dolgellau Gold belt comprises part. Chapter 4 presents the petrographic and mineral chemistry data on the vein quartz mineralisation at Clogau Mine. Chapter 5 presents the interpretation of the data on the conditions of ore formation from a thermochemical standpoint, and in Chapter 6 possible genetic models for the gold mineralisation in the Dolgellau Gold-belt are discussed.

Section on the Southern Uplands Placer Gold.

Chapter 7 is a synopsis of the geology and mineralisation relevant to the geographical distribution of the placer gold. In Chapter 8 the methodology employed in investigating the Southern Uplands material is discussed; Chapter 9 presents the data obtained from the placer gold in terms of its morphology and composition; and Chapter 10 is a critical assessment of the data obtained in Chapter 9.

CHAPTER 2.

THE OCCURRENCE OF GOLD ASSOCIATED WITH THE CALEDONIDES OF THE BRITISH ISLES.

2.1 Introduction.

Gold mineralisation in the British Isles is not to be found on the scale of the world's great mining districts, but the British Isles has produced gold from antiquity to the present day. Most of this gold has been mined in the last four hundred years, with the majority of the production in the nineteenth and early twentieth centuries.

The main areas where gold has been mined are the Southern Uplands (alluvial gold) and Sutherland (alluvial gold) in Scotland; Avoca in County Wicklow, Eire (alluvial gold); and Gwynedd and Dyfed in Wales (lode gold). Apart from these areas, there are a number of minor occurrences that have not been mined. The geographical distribution of all known gold occurrences is shown in Figures 2.1.to 2.3

The geological setting and the mining history of these occurrences of gold will be discussed for each region in turn.

2.2 Wales.

The major occurrence of gold in Wales, indeed in the British Isles, is in the area surrounding Dolgellau in Gwynedd, North Wales . Here gold occurs in quartz veins in a narrow belt stretching from Bontddu in the east through Dolgellau, and then northwards towards Trawsfynydd. The other occurrence in Wales is in quartz veins and pyritised shales at Ogofau in Dyfed.

Gwynedd.

Gold, silver and base metals have been mined in the Gwynedd since the middle of the nineteenth century, although there is evidence that base metals were mined much earlier (Readwin, 1888). The discovery of gold in 1844 was vehemently disputed by a Mr. Dean and a Mr. Roberts (Morrison, 1975). After this discovery, during the period 1847 to 1935, some thirty mines (not all operational at the same time) exploited quartz plus sulphide veins for gold, silver and base metals, with varying degrees of success.

These veins are in Cambrian shales, siltstones and grits, which contain basic to intermediate sills, dykes and laccoliths for which the mining term is "greenstones".

The geographical distribution of these mines is shown in Figure 2.4, and the general geology, mineralogy and production figures are given in table 2.1. The estimated total production of the area is 3,685 Kg of gold from 325,000 tonnes of ore (Allen and Jackson, 1985). Most of this production has been from Clogau Mine (2296 Kg) at the southern end of the Dolgellau Gold-belt, and Gwynfynydd Mine (1162 Kg) at its northern end. Although the mining district has been virtually shut-down since 1935, both the above mines have produced gold after this date, and in 1986 both mines were operational on a small scale.

A fuller account of the history and discovery of mines in the Dolgellau region is given in Hall (1975) and Morrison (1975).

Dyfed.

The Ogofau gold mine lies to the northeast of the village of Pumpisaint, about ten miles northwest of the town of Llandovery in Dyfed, central Wales (fig. 2.5).

The mine area lies on the northwestern flank of the Towy anticline, in a mineralised zone lying close to the boundary between Ordovician and Silurian shales and siltstones. Gold occurs with pyrite and arsenopyrite in quartz veins and pyritic shale bands, with minor hydromuscovite, galena and sphalerite and rare cookeite. These veins and pyritised shale bands form "saddle reef" structures in the crests of minor folds (Steed *et al.*, 1976)

The workings at Ogofau mine show evidence of three periods of operation: the first and most extensive was in Roman times; the second between 1872 and 1912; and the third between 1930 and 1940. The ore was of low grade, generally less than 1.4 ppm gold, and since 1905 approximately 37 Kg of gold have been recovered from 5,800 tonnes of ore (Steed and Annels, 1980).

Other localities of gold in Wales.

Gold is known to occur in the gossan of the copper deposit at Parys Mountain, Anglesey; two assays show gold associated with bismuthinite, pyrite, chalcopyrite and quartz at Rhosmynach Fawr and pyrite at Llangaffo (Greenly, 1919).

2.3 Scotland.

All of the gold that has been mined in Scotland has come from alluvial workings in two areas: the Leadhills-Wanlockhead district in Lanarkshire and the area surrounding Helmsdale in Sutherland. Active mining took place in these two areas during the middle of the sixteenth century and between 1868 and 1870 respectively. The Leadhills-Wanlockhead district produced gold worth £100,000 (at sixteenth century prices) and the Helmsdale area produced 191 Kg of gold (Maclaren, 1902).

Southern Uplands.

Apart from the Leadhills-Wanlockhead district, gold has been reported from the following areas of the Southern Uplands: Dumfries, Kirkcudbright, Wigtown, Ayr, Selkirk and Peebles (Lindsay, 1867). During the 1970's the Mineral Reconnaissance Programme of the British Geological Survey confirmed this widespread occurrence of alluvial gold (Dawson *et al.*, 1977, 1979), and located "in situ" gold mineralisation at the southern margin of the Loch Doon granitoid complex (Leake *et al.*, 1981), and in the area of the Fore Burn igneous complex (Allen *et al.*, 1982). At both of these localities gold is associated with disseminated arsenopyrite. This style of mineralisation could be a possible source for the Southern Uplands placer gold.

Sutherland.

Alluvial gold is restricted to two localities: firstly, the tributary streams flowing into the Ullie or Helmsdale; and to two streams, the Kildonan Burn and Blackwater, flowing into Loch Brora (fig. 2.6). The rocks associated with the Sutherland placer gold district are Moinian schists, quartzites, granulites and migmatites.

During mining activities, gold was found in the stream beds and the alluvium bordering the streams. The richest alluvium (an irregular bed of ferruginous sand and gravel) was close to the bedrock. Gold, however, was not restricted to this horizon, and some nuggets were obtained from alluvium above this bed, and from among the roots of peat and heather which cover the alluvium (Read, 1931).

Other gold occurrences in Scotland.

A number of minor occurrences of gold in Scotland that have not been mined are shown in table 2.2.

2.4 Ireland.

Most of the gold that has been mined in Ireland has come from alluvial deposits in the Gold Mines River and from gossans near Avoca, County Wicklow (fig.2.7). This area has probably produced gold since prehistoric times (Holland, 1979), but the main enterprise in recent history was from 1795 to 1865 when the area produced between 211 Kg and 266 Kg of gold (Maclaren, 1902).

The rocks associated with the alluvial gold are Silurian slates and sandy shales. Close to the alluvial deposits is the base metal deposit of Avoca, where gold has been found in the associated gossans and from assays of pyrite concentrates (Maclaren, 1902). Maclaren (1902) suggested that the Avoca deposit could be a possible source for the alluvial gold in Gold Mines River. However, a more recent study by Macardle and Warren (1987) on the Gold Mines River placer gold and associated bedrock concluded that the source for the Goldmines River placer gold was locally derived from iron-copper mineralisation hosted in volcanic rocks. They based their conclusions on the gold content (0.16 - 0.21ppm) of the iron formation associated with these volcanic rocks.

2.5 England.

There are no historical records of any significant gold production in England. There are a number of authentic reports of the occurrence of gold (Maclaren, 1902). Most of the localities of this gold are in the Hercynian terrain of Devon and Cornwall. The only occurrences of gold in the Caledonian area in England are those from the Lake District.

Gold has been found in the veins at Seathwaite Tarn where a few grains were found associated with Cu-Fe sulphides, and in the veins at Paddy End, Coniston, where it is associated with bismuth telluride and cobaltite (Stanley, 1979).

2.6 Recent Discoveries of Gold.

Since 1982, a number of mining companies have been involved in exploration for gold in Scotland and Ireland. This has resulted in the discovery of several small deposits, none of which were in production in 1987. These deposits are near Perth and Oban (Scotland); in the Sperrin Mountains, County Fermanagh (Northern Ireland), and Clontibret, County Monaghan (Eire).

Perth.

Colby Resources Corporation and East West Resources Corporation were, in 1986, drilling four targets near Perth in Dalradian metasediments (Mining Annual Review, 1986).

Oban.

Ennex International have defined a small ore zone in an area between Pitlochry and Oban. The ore zone is 110m long and 2m wide and grades at 15.5 ppm gold and 45 ppm silver. BP Minerals were, in 1986, drilling a gold-prospect at Kilmelford near Oban (Mining Annual Review, 1986).

Sperrin Mountains.

Ennex International have delineated an ore body in Dalradian metasediments, which comprises sixteen gold-bearing quartz veins, with reserves of 487,000 tonnes, grading at 9.2 ppm gold (Mining Annual Review, 1986).

Clontibret.

Gold at Clontibret is associated with antimony and arsenic vein mineralisation in Silurian greywackes. This gold is found associated with disseminated arsenopyrite and pyrite, where it occurs as small (20µm) inclusions. Assays indicate that some of the gold is locked in the sulphides either in solid solution or as submicroscopic grains (Steed, 1982).

2.7 Summary.

All of the gold that has been mined in the British Isles has come from mineralisation in rocks or alluvial deposits associated with rocks of Lower Palaeozoic age. The majority of gold has come from quartz veins in the Cambrian sediments of the Harlech Dome, and from the alluvial deposits associated with Silurian and Ordovician greywackes of the Southern Uplands, but recent discoveries indicate that, in the future, gold may be produced from mineralisation in the Dalradian metasediments.

CHAPTER 3.

**GENERAL GEOLOGY OF
THE HARLECH DOME.**

3.1 Introduction.

The rocks of the Harlech Dome were first described by Murchison (1839) and Sedgwick (1844), and formed a major part of their "Silurian controversy". It was not until the early part of the twentieth century that the stratigraphy was described in detail by Andrew (1910) and by Cox and Wells (1927). The first combined structural and stratigraphic synthesis was undertaken by Matley and Wilson (1946). More recent work by Allen and Jackson (1978, 1985) and Allen *et al.* (1981a) has re-examined the geology of the Harlech Dome in detail.

3.2 Stratigraphy.

The strata of the Harlech Dome comprise mainly Cambrian clastic sedimentary and volcanic rocks, which are divisible into three main groups: the Harlech Grits Group (Allen and Jackson, 1985); the Mawddach Group (Allen *et al.*, 1981a); and the Rhobell Fawr Volcanic Group (Wells, 1927 and Kokelaar, 1977, 1979). For the sake of brevity, the details of the stratigraphy of the two sedimentary groups are illustrated in Fig. 3.1, which was compiled using the literature already cited. The outcrops of the various formations are shown in Fig. 3.2.

3.3 Igneous Activity.

Introduction.

The nature of the igneous activity in the Harlech Dome is discussed in more detail than the sediments as it may have an important bearing on the different styles of mineralisation that are present in the Harlech Dome.

Much of the Cambrian sedimentary sequence has been intruded by sills, dykes and laccoliths. These intrusions were termed "greenstones" by earlier workers (Ramsay, 1881; Andrew, 1910; Cox and Wells, 1927; and Matley and Wilson, 1946). Although these rocks are metamorphosed, Allen *et al.* (1976) were able to classify them according

to their geochemistry into dolerites, microdiorites and microtonalites. Some of these intrusives are weakly mineralised and form the Coed-y-Brenin porphyry copper deposit (Rice and Sharp, 1976).

Cropping out on the eastern margin of the Harlech Dome is the Rhobell Fawr Volcanic Group (Fig. 3.3). These volcanic rocks comprise a sequence of basalts, andesites, and minor rhyolites, which were extruded sub-aerially on to already eroded Cambrian sediments. This volcanism commenced in the Tremadoc and continued into the Arenig (Kokelaar, 1977,1979).

Flanking the Harlech Dome in the south east is the Aran Volcanic Group (cf. Fig. 3.3); this is an alternating sequence of acid and basic volcanics intercalated with sediments. These overlie unconformably the Rhobell Fawr Volcanic Group and the Cambrian sediments (Dunkley, 1979).

Geochemistry of the igneous rocks.

Intrusive rocks.

The intrusive rocks in the Cambrian have been studied by Allen *et al.* (1976) Allen and Jackson (1985) and Rice and Sharp (1976); the intrusives associated with the Rhobell Fawr Volcanic Group and Aran Volcanic Group by Kokelaar (1977) and Dunkley (1979). Allen and Jackson (*op. cit.*) recognised two geochemically distinct populations: a Ti-rich group of predominantly basic composition associated chemically with the Aran Volcanic Group, and a Ti-poor group, which includes rocks of basic and intermediate compositions; of the two populations the Ti-poor group is volumetrically the more important. Allen and Jackson (1985) suggest on the evidence of trace element distributions of Ti and Zr (Fig. 3.4) that these Ti-poor intrusives are genetically linked with the intrusives of the Coed-y-Brenin porphyry copper deposit, and that their overall geochemistry (Fig. 3.5) define the group as a calc alkaline suite emplaced in an island arc environment rather than a continental margin setting.

Extrusive rocks.

Kokelaar (1977,1979) classified the volcanic rocks of the Rhobell Fawr Volcanic Group, using Ti-Y-Zr discriminant diagrams, as being transitional between low-K tholeiites and calc alkaline basalts, and concluded that the Rhobell Fawr Volcanic Group consistently show characteristics of typical island arc destructive plate margin volcanism. Kokelaar (1979) also found that the intrusions in a peripheral belt along the east and southeast of the Harlech Dome are chemically and petrographically similar to intrusions in the sub-volcanic complex at Rhobell Fawr, and postulated that these intrusions may have acted as feeders to the Rhobell Fawr Volcanic Group.

Dunkley (1979) classified the Aran Volcanic Group and associated intrusives as a suite that is essentially tholeiitic in character. They are chemically distinct from the Rhobell Fawr Volcanic Group, the Aran Volcanic Group having formed in a back arc basin in which extension was insufficient to form new oceanic crust.

3.4 Timing of Igneous Activity.

The timing of the vulcanism that gave rise to the Rhobell Fawr Volcanic Group and the Aran Volcanic Group is stratigraphically constrained. The Rhobell Fawr Volcanic Group formed between the late Tremadoc and the early Arenig and the Aran Volcanic Group formed between the Arenig and Llanvirn-Caradocian times. Radiometric dating of the Rhobell Fawr Volcanic Group by Beckinsale and Rundle (1980) and Kokelaar *et al.* (1982) using K-Ar methods gave age ranges of 477 ± 12 Ma and 508 ± 11 Ma. The latter of these two ages is the more reliable, as the age determinations were undertaken on unaltered primary pargasite phenocrysts. The age of the intrusive suite in the Cambrian sediments is, however, more problematical as there are no available radiometric age data, but the petrographic, chemical and field data of Allen *et al.* (1976) and Allen and Jackson (1985) suggest that there are two major magmatic episodes, both related to vulcanism and both pre-dating the regional cleavage, metamorphism and vein quartz mineralisation. Allen and Jackson (*op. cit.*) consider that the first magmatic episode is associated with Rhobell Fawr vulcanicity, giving rise to the low Ti suite of sills, dykes and laccoliths

(this suite includes the igneous rocks of the Coed-y-Brenin porphyry copper deposit), and that the second magmatic episode is related to the Aran vulcanicity - producing the high Ti suite of intrusions.

3.5 Structure, Deformation and Metamorphism.

Structure and deformation.

The earliest interpretations of the structure of the Harlech Dome were by Salter (1865) and Ramsay (1881). However it was not until Matley and Wilson (1946) remapped the Harlech Dome that the structure of the area was understood. More recent work by Allen and Jackson (1985) has expanded the studies of earlier workers, and it is mainly from this study that the following structural synopsis is taken. The main structural features of the Harlech Dome are shown in Figure 3.6.

Folding.

In the western area, Matley and Wilson (1946) identified four major structures (cf. Fig. 3.6): the Dolwen Pericline, the Caerdeon Syncline, the Traeth Bach Syncline and the Coastal Syncline. The Dolwen Pericline comprises a set of *en echelon* parallel folds, which give the major axis of the fold a sinusoidal trace. The Caerdeon Syncline is similarly made up of a number of smaller folds; at its northern end its axis is offset and truncated by a number of folds and the Traeth Bach Syncline is probably a continuation of this fold. In the eastern area, four phases of folding have been identified (Allen and Jackson, 1985).

Faulting.

The complex pattern of faulting in the Harlech Dome is shown in Fig. 3.6. An understanding of the relative chronology of this fault pattern is important as the vein quartz mineralisation is fault controlled, and only certain sets of faults carry mineralisation (Matley and Wilson, 1946; Gilbey, 1969; Ashton, 1976; Allen and Jackson, 1985).

The faults in the Harlech Dome have been divided into major and minor faults by Matley and Wilson (1946). The major faults trend between 345° and 040°, and are generally over 2 Km in length with strike-slip movements of up to 3.5 Km. Matley and Wilson (1946) termed these faults "meridional". Allen and Jackson (1985) further subdivided these meridional faults in terms of their directions and type (reverse or normal faults) into "Reversed Faults", "NNE Faults", "NNW Faults" and North Faults". The relative chronology of these faults is not well understood, but the NNW grouping of faults shows evidence of movement over an extended period of time. For example, a NNW fault, the Trawsfynydd fault, is exposed in Gwynfynydd Mine and is observed to displace gold-bearing quartz veins, whereas further south the NNW faults pre-date the intrusion of the Craiglaseithen microtonalite laccolith, which in turn pre-dates the vein quartz mineralisation. This prolonged period of movement is also suggested since the NNW faults generally have a greater throw in the Cambrian sediments than in the overlying Rhobell Fawr Volcanic Group, which indicates that some of these faults were active prior to vulcanism (Allen and Jackson, 1985). None of the meridional faults carry economic mineralisation.

Within the area bounded by the Moelefre Fault in the east and Trawsfynydd and Dowas/Afon Wen fault line in the west are numerous minor normal faults. These minor faults carry the economic mineralisation. Many of these minor faults are terminated against meridional faults, for example, in the north east of the area where a number of minor faults terminate against the Trawsfynydd Fault (Fig. 3.6).

The minor faults follow two complementary directions (330° and 060°). These two directions coincide with the major trends of the dolerite dykes and quartz veins in the area (Fig. 3.7). Dykes are preferentially found in faults trending 330° and quartz veins in faults trending 060°. Commonly both dyke and vein occupy the same fault, and where this is the case the vein always post-dates the dyke (Allen and Jackson, 1985).

The relative chronology of the major and minor faults is well illustrated in the two major mines in the area, the Gwynfynydd and Clogau Mines, where the main lodes

are offset by a major cross-cutting fault in each case; the Trawsfynydd fault at Gwynfynydd and the Bryntyrion fault at Clogau. These faults show that the final movements on the major faults postdated the minor faults and the vein quartz mineralisation.

Metamorphism.

Metamorphism of the rocks of the Harlech Dome was first recognised by Greenly (1897), and the maximum grade of this metamorphism is lower greenschist facies (Allen and Jackson, 1985). Estimates of the timing of peak metamorphism in Wales are given by Fitch *et al.* (1969) using Rb-Sr and K-Ar dating of metamorphic minerals. These results give two age populations 420 to 400 ± 10 Ma (late Silurian to early Devonian) and a subsidiary grouping at 390 ± 10 Ma.

3.6 Mineralisation in the Harlech Dome.

Introduction.

In the Harlech Dome there are three distinct styles of mineralisation: firstly, porphyry copper mineralisation (Rice and Sharp, 1976); secondly, mineralised intrusion breccias (Allen and Easterbrook, 1978); and, thirdly, vein quartz mineralisation (Andrew, 1910; Gilbey, 1969; Ashton, 1976; Bottrell, 1986; and Bottrell *et al.*, 1988).

Porphyry copper mineralisation.

The discovery of copper mineralisation at Coed-y-Brenin by Riofinex Ltd., during an exploration programme lasting from 1968 to 1973, was the first record of porphyry style mineralisation in Great Britain (Rice and Sharp, 1976). The mineralised body is spatially associated with the Afon Wen microtonalite intrusion (Fig. 3.8), which is thought to be comagmatic with the Rhobell Fawr Volcanic Group (Rice and Sharp, *op. cit.*; Allen *et al.*, 1976; Allen *et al.*, 1978 and Allen and Jackson, 1985).

The deposit consists only of the hypogene zone. The mineralisation occurs along small joints and fractures and as disseminations in the microdiorite. The main ore

minerals are chalcopyrite and its alteration products with minor amounts of molybdenite. In places the deposit also contains recoverable amounts of gold (up to 0.5ppm).

Allen *et al.* (1976) showed that the Afon Wen microdiorite is not unique, and that several nearby intrusions contain high levels of copper (0.27-0.67 wt% copper). Locally, copper mineralisation is visible along joints and fractures.

Mineralised breccia pipes.

Allen and Easterbrook (1978) showed that the Glasdir copper body (Fig. 3.9), which from 1872 to 1914 produced 13077 tons of copper concentrate (grading on average 9 to 10% copper, with by-product gold and silver) is a mineralised breccia pipe, shaped like a flattened inverted cone.

The ore, which never contained more than 2% copper overall (Phillips, 1918), contained pyrite, marcasite, arsenopyrite with minor sphalerite and chalcopyrite. Shepherd and Allen (1985), in a fluid inclusion study of the mineralisation in the Harlech Dome, showed that the fluids that produced both the Coed-y-Brenin and Glasdir copper mineralisation were similar in composition, and they concluded that the two deposits were probably formed by the same mineralising event.

Vein quartz mineralisation.

The vein quartz mineralisation will only be dealt with briefly, as it is discussed in detail in the following chapter.

The mineralisation occurs in a belt (cf. Fig. 2.4). Most of the veins occur in faults, and metal sulphide mineralisation is usually confined to vein intersections in the Clogau Shales and the Maentwrog Formation. In the south of the belt, the mineralisation comprises a chalcopyrite-pyrrhotine assemblage with minor amounts of lead-zinc sulphides, native gold and tellurides, while in the north, galena and sphalerite form the dominant sulphides with minor copper-iron sulphides, gold and sulphosalts.

3.7 Timing of Mineralisation.

The different styles of mineralisation have been radiometrically dated by Moorbath (1962), Ineson and Mitchell (1975) and Allen and Jackson, (1985).

The above studies found two distinct age groupings one at 410 Ma and another at 370 Ma, which reflect real geological events and not argon loss (Allen and Jackson, 1985). The former age is coincident with that of peak metamorphism obtained by Fitch *et al.* (1969). The simplest interpretation of these data is that the earlier age records the metamorphism and the later age records the vein quartz mineralisation, with both of these events overprinting the earlier porphyry copper and intrusion breccia mineralisation. According to geochemical evidence, the earlier events are approximately contemporaneous with Rhobell Fawr volcanism, dated at 508 Ma (Kokelaar *et al.*, 1982). This interpretation, however, is not consistent with the data, as all three styles of mineralisation record both groups of dates, whereas if the above interpretation were correct, the vein quartz mineralisation would record the 370 Ma group of dates only. Thus, the 410 Ma group probably record the vein quartz mineralisation and the 370 Ma group a later geological event.

CHAPTER 4.

GEOLOGY AND MINERALOGY OF CLOGAU MINE.

4.1 Introduction.

Clogau mine is situated on the southern margin of the Harlech Dome on the northern side of the Mawddach estuary. Figure 4.1 illustrates the geology of the area around the mine. Here, a quartz lode is associated with two dolerite sills that have intruded the Clogau Shales. Where gold has been found in any quantity the following empirical observations have been made: (i) the wallrocks are composed of Clogau Shales and/or dolerites; (ii) the ore shoots are often associated with cross-cutting faults; (iii) gold mineralisation is often associated with various telluride minerals; and (iv) the quartz is often blue-grey in colour with books and ribbons of included wallrock (Andrew, 1910). When the lode passes into the Gamlan Series it is generally no longer auriferous (Gilbey, 1969).

A recently worked-out ore shoot on the lowest level (N^o. 4 level) of the Llechfraith section of the mine (fig. 4.2) has been studied in detail. The lode is not a simple quartz vein; the quartz within the lode pinches and swells and is commonly interleaved with the wallrock. The thickness of the lode varies along the length of the mining level from quartz veins 2-5cm thick interleaved with wallrock shales to a thick (2m) quartz vein. Two types of quartz are present on N^o. 4 Level: (i) a blue-grey quartz with included books and ribbons of Clogau Shale; this quartz carries the highest gold values and is also the most sulphide-rich; and (ii) a barren pure white quartz, which has no associated gold values and a low sulphide content (the mining term for this barren quartz is "white elephant"). Barren quartz commonly cuts out the blue-grey quartz; this is most clearly seen at the eastern end of the ore shoot (cf. Fig.4.2) where the barren quartz swells to 2m in thickness and occupies the whole of the mine level.

The geology of the ore shoot is illustrated schematically in figure 4.3. The hanging-wall rocks comprise Clogau Shales and the footwall rocks consist of altered dolerite. In the centre of the lode is a thin (0.25-0.50m) highly altered dolerite dyke for which the mining term is "Clogau Stone". This dyke, although impersistent in lateral and vertical extent, is present on most levels in the mine and occupies the same fault as the

lode quartz; it pre-dates the main mineralisation as vein quartz can clearly be seen cutting the dyke. Alteration of the shale is restricted to local bleaching, and the widespread development of sericite, rutile and minor chlorite. Gangue minerals associated with vein quartz are, in order of decreasing abundance: various carbonates, sericite, chlorite and graphite. All four minerals occur in the blue-grey mineralised quartz (i.e., the quartz that is associated with the highest gold grades and highest sulphide content). However, only carbonate and sericite are associated with the barren quartz. Carbonate forms along microfractures and in voids in the quartz (plate 4.1). It is commonly associated with sulphides, which occupy the same microfractures and voids. Sericite has a similar occurrence, except that where sericite is associated with sulphides it forms lath-shaped inclusions within the sulphides (plate 4.2), whereas the carbonate is only rarely included in the sulphides. Chlorite and graphite are restricted in their occurrence and are usually only found associated with thin (~1mm) slivers of shale within mineralised quartz. However, graphite also forms small (<10µm long) laths in the sulphides, and very thin (10µm) impersistent veinlets in quartz (plate 4.3). These veinlets are commonly associated with various sulphides, and more rarely with native gold.

Material was collected from ore that had been removed from the ore shoot on No. 4 Level; this material consisted of vein quartz containing abundant tellurides. *In situ* samples were collected from the barren quartz and the sulphide-rich quartz (for the location of the samples see fig. 4.2). The material collected was then prepared for ore microscopic examination and subsequent electron probe micro-analysis. Also studied were two polished sections of a mill concentrate containing abundant gold (these sections were used to characterise compositional variations in the gold from the ore shoot), and material from the British Museum (Natural History) and the National Museum of Wales.

4.2 Ore Mineralogy of No. 4 Level.

Introduction.

All observations, unless otherwise stated, were made using oil immersion lenses, and identification of all the phases was confirmed by electron probe

micro-analysis.

In most of the sections examined the opaque minerals constitute 5-10% of any one sample, and only locally do the opaque minerals comprise up to 20% of a sample.

The ore mineralogy of No. 4 Level comprises five distinct mineral assemblages. The general mineralogy of these assemblages is as follows:

(i) an arsenopyrite, pyrite/pyrrhotine, cobaltite and rutile assemblage (rutile here refers to all TiO_2 minerals, as it was not determined which particular TiO_2 polymorph was present). This assemblage occurs as impregnations of the wallrocks and veinlets in quartz.

(ii) A chalcopyrite-pyrrhotine assemblage, which occurs in voids and microfractures in the blue-grey quartz.

(iii) A complex telluride assemblage containing lead, bismuth, silver, antimony, tellurium, sulphur minerals plus native bismuth and native gold. This assemblage also occurs in voids and microfractures in the blue-grey quartz. However, where the telluride and chalcopyrite-pyrrhotine assemblages occur together the telluride assemblage replaces the chalcopyrite-pyrrhotine assemblage.

(iv) A chalcopyrite-pyrrhotine assemblage associated with the barren quartz, which occurs in vugs, voids and microfractures in the barren quartz.

(v) An alteration assemblage comprising marcasite-pyrite intergrowths (probably after pyrrhotine) and secondary copper sulphides and hydrated iron oxides.

In the description, below, of the various assemblages, special attention is paid to the telluride assemblages, as these are associated with gold mineralisation.

4.2.1 Rutile - arsenopyrite - pyrite/pyrrhotine - cobaltite Assemblage.

The occurrence of rutile is restricted to the wallrocks and wallrock inclusions in the quartz veins. Rutile forms small needles (10µm long) and clusters of needles (up to 100µm in diameter) (plate 4.4). Rutile also locally occurs rimming pyrrhotine.

In the samples examined from № 4 Level arsenopyrite was only observed in two samples. In sample JN 39 arsenopyrite occurs as a vein in quartz and is heavily brecciated (no other sulphides were observed). However, in sample JN 12, arsenopyrite occurs with major amounts of cobaltite, and minor pyrite and pyrrhotine. Arsenopyrite, cobaltite and pyrite all occur as euhedral crystals (mainly rhombs, cubes and pyritohedra) and locally these minerals are cemented by pyrrhotine, with the arsenopyrite/cobaltite being preferentially replaced by galena (plate 4.5). Plate 4.6 is a crossed nicols view of plate 4.5 and shows other phases to be present; the cobaltite is intergrown with arsenopyrite (showing blue anisotropy colours) and the galena has inclusions of bismuthinite (showing grey-white anisotropy colours). In other cobaltite-rich samples (e.g., SB 128 COB) cobaltite is locally replaced and cemented by chalcopyrite (plate 4.7) and/or pyrrhotine.

4.2.2 Chalcopyrite-pyrrhotine Assemblage.

Chalcopyrite with very rare inclusions of sphalerite occurs in small veins (2-3mm long by 0.1-1mm wide) (plate 4.8) and as discrete rounded to angular (50-500µm) grains in quartz, associated with microfractures. Pyrrhotine occurs with chalcopyrite and is locally intergrown with it, exhibiting mutual grain boundaries (plate 4.9). The proportion of chalcopyrite to pyrrhotine varies from polished sections that contain mainly chalcopyrite to sections that consist mainly of pyrrhotine. Pyrrhotine is commonly associated with "porous" zoned pyrite and marcasite which have replaced pyrrhotine (plate 4.10).

4.2.3 Telluride Assemblages.

Introduction.

Two types of telluride assemblage are present at Clogau mine: (i) a tellurbismuth-dominated assemblage with minor galena, tellurides of silver and lead, and native gold; and (ii) a sulphide-dominated telluride assemblage with minor tellurides and rare gold. The bismuth telluride assemblage comprises the following minerals: major tellurbismuth (Bi_2Te_3), minor tetradyte ($\text{Bi}_2\text{Te}_2\text{S}$) and galena with minor amounts of hessite (Ag_2Te), altaite (PbTe) and native gold. The sulphide-dominated telluride assemblage comprises the following minerals: major galena, with minor tetradyte, wehrlite (BiTe_{1-x}), hessite, native bismuth, bismuthinite and very rare native gold. In both assemblages, in the material studied, no Au, Au-Ag tellurides (e.g., calaverite, krennerite or sylvanite) or maldonite (Au_2Bi) were observed.

Tellurbismuth-dominated Assemblage.

Tellurbismuth is the most abundant telluride, and generally accounts for 70-80% of the opaque minerals in any one section. Tellurbismuth usually forms prismatic subhedral crystals (0.5-3mm long) infilling voids associated with microfractures within the quartz (cf. plate 4.1). Optically, in plane polarised reflected light, tellurbismuth is characterised by its high reflectance, pure white colour, and under crossed polars by its moderate brown-orange anisotropy. Aggregates of tellurbismuth show annealing textures, exhibited as triple point boundaries (plate 4.11), and replacement textures (careous boundaries) (plate 4.12). Carbonate is commonly associated with tellurbismuth, which infills the same type of voids and microfractures as the tellurbismuth (cf. plate 4.1). The textural relationships between tellurbismuth and the other tellurides and sulphides are complex, varying from small (5-50 μm) isolated inclusions to arrays of very small (5-10 μm) inclusions aligned along the cleavage of tellurbismuth (plate 4.13), and also from coarse myrmekitic intergrowths (plate 4.14) to very fine scale (<3 μm) admixtures of tellurides and sulphides. These textures are described more fully when the minerals that

are intergrown with tellurbismuth are discussed.

Tetradymite is the second most abundant phase in the telluride assemblage and accounts for approximately 5-10 modal percent of the bismuth telluride assemblage. Tetradymite has a similar habit and occurrence to tellurbismuth in that it generally forms subhedral prismatic grains (100-1000 μ m long). Tetradymite is distinguished in plane polarised reflected light from tellurbismuth by its slightly lower reflectance and green-grey tint, and under crossed polars by its stronger anisotropy. Where it occurs against tellurbismuth, it is nearly always rimmed by a thin (10-40 μ m wide) incomplete rim of galena (plate 4.15). When this rim is completely absent the boundary between tetradymite and tellurbismuth locally exhibits replacement textures. However, it is not possible to unequivocally determine which phase is replacing which (plate 4.16). Where tetradymite occurs against quartz the margin of the tetradymite grain commonly comprises a thin (5-10 μ m wide) zone that consists of a complex myrmekitic intergrowth of blue-grey galena and silver-grey bismuth telluride. This fingerprint intergrowth is also commonly present at the contact between tetradymite and tellurbismuth (plate 4.17). The nature of this intergrowth was examined using electron probe micro-analysis techniques and is discussed more fully in section 4.4.8 of this chapter.

Galena is approximately equal in abundance to tetradymite (5-10 modal percent). Against the high reflectance tellurides, it appears to the eye as a blue-grey low reflectance phase instead of a steel-silver grey phase of moderate reflectance (cf. plate 4.15), and forms several types of intergrowth with the two major tellurides. The major occurrence of galena associated with tellurbismuth is as small (20-50 μ m) isolated anhedral grains. These isolated grains tend to occur at grain boundaries between tellurbismuth and quartz (plate 4.18) or at tellurbismuth - tellurbismuth grain boundaries within clusters of tellurbismuth crystals. Galena also occurs as a myrmekitic intergrowth with tellurbismuth (cf. plate 4.14) and replaces tellurbismuth along cleavage (plate 4.19). The textural relationships between galena and tetradymite are described in the tetradymite section.

In plane polarised reflected light, altaite is characterised by its high reflectance

(approximately equal to that of tellurbismuth and slightly higher than tetradymite) and duck egg blue-green colour, and under crossed polars it is isotropic. The occurrence of altaite is similar to that of most of the galena, that is, it generally occurs as small (10-30 μ m) isolated anhedral grains at grain boundaries within tellurbismuth (plate 4.20) and at the contact between tellurbismuth and quartz. However, compared with galena its abundance is very low, forming less than 0.1 modal percent of tellurides and sulphides in any one section. Altaite is also associated with very small (<5 μ m) grains of native gold (plate 4.21), and is locally observed in contact with galena (plate 4.22).

Hessite is a very minor (<0.1%) constituent of the bismuth telluride assemblage. The optical properties of hessite in plane polarised light are very similar to those of galena. The reflectivities of the two phases are very similar and there is only a slight colour difference between the two minerals. In this association hessite has a slight brown tint as opposed to the blue grey colouration of galena. However, under crossed polars the two minerals are easily distinguished because hessite is strongly anisotropic, exhibiting blue-red anisotropy colours and is polysynthetically twinned. Hessite occurs as small anhedral grains that are located at the grain boundaries of the major phases (plates 4.23a, 4.23b and 4.24).

In the material collected from the ores shoot on № 4 Level all of the telluride-bearing samples contain very small amounts of native gold, which occurs as small (<10 μ m) grains (plate 4.25). These grains are generally deep yellow in colour, indicating that the gold is of high fineness (the native gold grains were too small to analyse using electron probe micro-analysis techniques, thus it was not possible to ascertain the exact fineness of the native gold). As with the other minor phases associated with tellurbismuth and tetradymite, native gold forms as isolated grains located at grain boundaries within the tellurbismuth, and in mutual contact with hessite and altaite. In the two milled concentrates containing abundant gold from the ore shoot on № 4 Level, the milling process had destroyed any textural relationships between the native gold and the tellurides. However, the colour of the native gold exhibits a variation from deep yellow to a paler yellow showing that the gold associated with the ore shoot does vary in

composition.

The Sulphide-dominated Telluride Assemblage.

Two large hand samples (approximately 1Kg) were collected from the ore shoot, and the eastern end of No. 4 Level. The sample from the eastern end of No. 4 Level contains galena and Fe-Cu sulphides, and the sample from within the ore shoot contains galena and Fe-Co sulphides and sulpharsenides. In the sample collected from within the ore shoot the sulphide-dominated telluride assemblage replaces cobaltite, pyrite and arsenopyrite, and in the other sample the sulphide-dominated telluride assemblage replaces pyrrhotine and chalcopyrite. A third sample, predominantly made up of galena in quartz, but containing appreciable gold (approximately 15 modal percent) was obtained from the British Museum (Natural History) (labelled BMNH Kingsbury, Clogau Mine).

In the sulphide-dominated telluride assemblage galena is the major phase comprising 90 to 95 modal percent of the opaque phases present, and, because the high reflectance tellurides are low in abundance, galena, to the eye, exhibits normal optical properties. Galena generally occurs along fractures in the quartz and replaces the quartz, is associated with thin (1-2mm thick) slivers of shale wallrock, and replaces the chalcopyrite-pyrrhotine and the arsenopyrite - cobaltite - pyrite / pyrrhotine assemblages (plate 4.26 and cf. plate 4.6). Tellurides, native bismuth and bismuth sulphides form as small (10-40 μ m) isolated inclusions, myrmekitic intergrowths, or skeletal and ragged prismatic crystals.

Tetradymite forms ragged elongate and stubby prismatic subhedral grains (plate 4.27), the margins of which, against galena, locally show replacement textures, but it is not possible to determine which phase is being replaced. The cores of tetradymite commonly comprise either galena or bismuthinite. Generally tetradymite is only intergrown with galena and bismuthinite and fine grained intergrowths consisting of galena and tetradymite, plus bismuth tellurides and native bismuth are rare.

Wehrlite has optical properties that are very similar to tellurbismuth and the two minerals can only be properly distinguished by electron probe micro-analysis. However, in all the phases analysed, using electron probe micro-analysis, which exhibited optical properties of wehrlite/tellurbismuth, a chemical composition corresponding closely to that of wehrlite was observed (table 4.1). Hence it is assumed that the majority of the bismuth telluride in the sulphide-dominated telluride assemblage is wehrlite and not tellurbismuth. Wehrlite occurs in two main types of textural intergrowth: firstly, it forms as small (20-50µm) anhedral inclusions in galena and secondly, it occurs as skeletal prismatic crystals (plates 4.28 and 4.29). In both of these intergrowths wehrlite is commonly associated with native bismuth.

Hessite appears to be the least common of the tellurides in the sulphide-dominated telluride assemblage. However, the similarity of optical properties in plane polarised light to galena may have caused the underestimation of the abundance of hessite. Hessite occurs as small (10-40µm) isolated anhedral grains within the galena (plate 4.30). The cores of some of the skeletal wehrlite crystals in plane polarised light exhibit blue-red anisotropy that shows the cores of the grains to consist of a fine (<2µm) interlocking mosaic of crystals. These cores are tentatively identified as hessite (there are no analytical data for the cores of these grains to confirm this observation).

Hedleyite has very similar optical properties to tellurbismuth and wehrlite and can only be positively identified using electron probe micro-analysis. Hedleyite was found as small (20µm) inclusions in galena in sample BMNH Kingsbury, Clogau Mine (K3) (plate 4.31).

In plane polarised light native bismuth has a high reflectance (similar to the reflectance of the bismuth tellurides), and a distinct to strong bireflectance, and shows polysynthetic twinning. However, it rapidly tarnishes and usually exhibits a distinct cream tint. It commonly also "polishes out" leaving a pitted area in the section with only very small (<10µm) flecks of native bismuth left intact. Native bismuth occurs as small (10-40µm) isolated anhedral grains in galena. The contact between native bismuth and

galena, generally, shows no reaction rim to form bismuthinite, but native bismuth and bismuthinite are commonly intergrown in an interlocking mosaic (plate 4.32). In plane polarised reflected light bismuthinite exhibits strong bireflectance and, under crossed polars, strong anisotropy. The major occurrence of bismuthinite is as small (10-14 μ m) anhedral grains and as interlocking aggregates of grains included in galena (plate 4.33). Minor amounts are associated with tetradymite where bismuthinite forms in the cores of tetradymite crystals.

In the two samples examined, native gold was not observed in the cobaltite-bearing sample from within the ore shoot, but was present in the sample collected from outside the ore shoot. Here, native gold occurs as very rare minute (<2 μ m) grains associated with graphitic wallrock inclusions.

4.2.4 Other Occurrences of Native Gold and Tellurides at Clogau Mine.

A number of native gold/telluride-bearing samples from Clogau Mine (table 4.2) were provided by the National Museum of Wales and the British Museum (Natural History), the precise locations of these samples in the mine workings are not known. In the telluride-bearing samples the occurrence of the sulphide and telluride minerals is as recorded in the material from N^o. 4 level. However, one sample contained abundant gold (approximately 5-10% of the whole sample) and no tellurides. The opaque mineralogy of this sample comprises: major gold, pyrite, arsenopyrite and galena with minor sulphosalts (boulangerite, tetrahedrite and stibioluzonite). Here, the native gold has four types of occurrence: (i) forming along microfractures in the quartz (plate 4.34); (ii) associated with graphitic wallrock inclusions (cf. plate 4.3); (iii) forming emulsoid droplets, symplectite-like intergrowths, and veinlets with pyrite and galena (plates 4.35 and 4.36); and (iv) forming veins in arsenopyrite. Pyrite and arsenopyrite occur as medium-sized (50-500 μ m) euhedral crystals associated with graphitic wallrock inclusion and microfractures in the quartz (cf. plate 4.3). Galena and the sulphosalts occur infilling vugs and voids in the quartz (plate 4.37 and 4.38).

4.2.5 Alteration Assemblages.

In the pyrrhotine-chalcopyrite assemblage pyrrhotine is commonly altered to a mixture of pyrite and marcasite (plate 4.39). This type of alteration was the only type of alteration observed in material collected from N^o. 4 Level. However, one sample (BM Kingsbury, Clogau Mine from the British Museum (Natural History)) exhibited a degree of supergene alteration, with galena altering to covellite (plate 4.40), and pyrite and arsenopyrite to limonite (plate 4.41).

4.3 Paragenetic Interpretation.

Considering the complex nature of the various intergrowths described in the two precious metal assemblages there is little justification in assigning a precise paragenetic position to each individual mineral. However, the textural and paragenetic relationships between the different assemblages indicate the following:

- (i) the mineralised quartz is earlier than the barren quartz.
- (ii) All of the sulphides and tellurides are later than the mineralised quartz.
- (iii) The tellurbismuth and sulphide-dominated telluride assemblages are later than the iron-nickel-cobalt and copper-iron assemblages, and earlier than the barren quartz.
- (iv) Because of the close spatial association of graphite with sulphides, tellurides and gold, the graphite may have played a role in sulphide/telluride/gold deposition, acting as a reductant to destabilise metal complexes in hydrothermal solution.
- (v) In the tellurbismuth-dominated assemblage bismuth tellurides with a high bismuth:tellurium ratio (wehrlite and hedleyite), bismuthinite, and native bismuth are absent whereas these phases are present in the sulphide-dominated assemblage and

tellurbismuth is absent. This indicates that the fluid which deposited the two assemblages had different tellurium to sulphur ratios, this ratio being high when the tellurbismuth assemblage was deposited, and lower when the sulphide-dominated assemblage was deposited. The detailed aspects of this varying tellurium ratio are discussed from a thermodynamic standpoint in Chapter 5.

The deposition of the mineralised quartz is interpreted as the earliest phase of vein mineralisation, as all other minerals contained in quartz are related to microfractures within it; this especially applies to the euhedral sulphides (pyrite and arsenopyrite), which on the basis of crystal shape could be interpreted as being paragenetically earlier. However, close petrographic study reveals that these euhedral crystals are always related to microfractures within the quartz, and hence the euhedral habit of these sulphides is due either to recrystallisation or to their power of crystallisation. The widespread development of "book and ribbon" textures in the mineralised quartz indicates that deposition of mineralised quartz was episodic, with the repeated re-opening of veins and renewed deposition of quartz between leaves of wallrock. Most of the mineralised quartz has suffered post-depositional deformation, as evidenced by the lack of vugs and its recrystallised nature.

The two telluride assemblages are interpreted as being later than the sulphides associated with the mineralised quartz and earlier than the barren quartz for the following reasons. Firstly, tellurides were never found associated with the barren quartz and, secondly, where the telluride assemblages are observed associated with the pyrrhotine - chalcopyrite or the arsenopyrite - pyrite - cobaltite assemblages, the telluride assemblages are always seen to replace them. In the telluride assemblages, as there are few textures that are of unambiguous interpretation (e.g., veining of one mineral by another) the interpretation of the various textures is equivocal; for example, the isolated galena inclusions that occur at grain boundaries and along cleavage planes in tellurbismuth could be interpreted in one of the following ways, each of which on petrographic grounds is equally valid:

(i) exsolution, where lead and sulphur have moved by diffusion to form galena at grain boundaries and along cleavage planes in tellurbismuth;

(ii) by replacement of tellurbismuth along lines of weakness, that is, grain margins and cleavage planes.

The identification of two types of textures in the telluride assemblage, the dissolution textures between grains of tellurbismuth along which other tellurides, galena and gold have been deposited, and the annealing textures between tellurbismuth grains, are indicative of the complex nature of the processes that have taken place. The dissolution textures show that deposition of the various minerals in the telluride assemblages is not simple sequential precipitation of ore minerals from solution, and the annealing textures show that primary textural features have been modified since deposition.

There is no textural evidence to unambiguously assess the exact paragenetic relationship between the sulphides and the associated carbonate which occupies the same fractures, except that the carbonate is not earlier than the associated tellurides, because the telluride assemblage is never seen veining or replacing the carbonate. The carbonate may be roughly contemporaneous or much later, the fluids depositing the carbonate having utilised the same fractures in the quartz.

4.4 Mineral Chemistry.

4.4.1 Introduction.

Analytical Details

The mineral chemistry of the opaque phases at Clogau Mine was investigated using electron probe micro-analysis. The micro-analyses were undertaken using two instruments: a two spectrometer fully automated Cameca Camebax and a Cambridge Instruments Microscan V. The Microscan V was used exclusively to identify mineral

phases, and the Cameca was used to gather the data for the line scan profiles and the random spot analyses. Data gathered on the two instruments were not combined in any manipulation of the data so as to avoid any instrument bias. All analyses were undertaken using an operating voltage of 20Kv, and beam currents of 500nA (Microscan V) and 25nA (Cameca).

Electron probe micro-analysis was employed to investigate: (i) the chemical variation in minor element distribution between minerals; (ii) the variation in chemistry across the complex telluride-sulphide intergrowths described earlier in this chapter and (iii) to positively identify unknown minerals. Analytical details, such as, the elements analysed for, the standards used for analysis, the peaks used for analysis, the detection limits for each element, and the analytical error for each element associated with a particular mineral are presented in table 4.3.

Analytical Problems.

Analytical problems were encountered in obtaining totals between 98 and 102 wt% on tellurbismuth using the Cameca Camebax. The totals obtained were consistently low by approximately 1-2 wt%. These problems are not due the analysed material, as analyses of galena directly adjacent to tellurbismuth or tetradymite being analysed gave totals between 99 and 101 wt% with correct stoichiometries, and analyses of the same material on the Microscan V gave totals between 99 and 101 wt% (table 4.4), also giving correct stoichiometries. Thus the problem must lie in the ZAF data reduction procedure. This problem can be traced to the amount of bismuth present in the analyses; stoichiometric tellurbismuth contains 52.20 wt% bismuth, whereas the total amount of bismuth present from the microprobe analyses undertaken on the Cameca Camebax is 50.04 ± 1.62 (± 2 sigma)wt%, approximately 2% lower than stoichiometric tellurbismuth. A similar but less extreme problem was also encountered with analyses of tetradymite. However, due to the presence of major amounts of lead (up to 10 wt%) substituting for bismuth, an accurate assessment of how much bismuth is "missing" from tetradymite is difficult to assess, but it should be in the same order as that for tellurbismuth (i.e., 1-2wt%).

However, the above problems do not pose problems if the data comparisons are relative, as the same errors in the ZAF correction procedure will apply to all of the comparisons that are made. But care should be taken in interpreting data which are used to examine the variation in stoichiometry of minerals.

Objectives.

The objective in examining the minor element chemistry of the major minerals was to see if partitioning of minor elements could be related to mineral species by:

- (i) comparing the concentration of minor elements between minerals of similar major element chemistry (e.g., cobaltite and arsenopyrite; tellurbismuth and tetradymite).
- (ii) Comparing the concentration of minor elements between the same minerals in different assemblages (e.g., between galenas in the telluride-dominated assemblage and in the sulphide-dominated telluride assemblage).

The chemistries of the complex intergrowths were examined to try and determine whether the intergrowths were formed by exsolution, replacement or co-crystallisation processes based on the following criteria:

- (i) exsolution processes leave a characteristic major element pattern; away from an exsolved body, the host mineral will contain significant amounts of the major elements of the exsolved mineral, but adjacent to the exsolved mineral the concentration of those elements will decrease due to the diffusion of atoms to form the exsolved phase.
- (ii) Replacement processes also form a characteristic major and minor element profile; away from the replacing mineral the host mineral only contains small amounts of the major elements contained in the replacing phase; however, close to the replacing mineral the concentration of these elements will increase. This profile is opposite to the chemical profile produced by exsolution.

(iii) In co-crystallisation processes, as there is no scavenging or introduction of new elements to either mineral, it is expected that no enrichment or depletion of elements would be observed adjacent to the grain boundaries of the minerals involved in the intergrowths.

The above criteria are somewhat idealised, but they do provide a framework for interpreting the variations in chemistry of the complex sulphide-telluride intergrowths.

4.4.2 Chemistry of Cobaltite and Arsenopyrite.

One large (150 μ m) zoned grain (cobaltite rim, arsenopyrite core) from sample JN 12 was analysed for arsenic, nickel, cobalt, sulphur, copper, antimony and gold (gold was always below the detection limits of the technique). Each analysis was made at 75 μ m intervals to produce a line concentration profile (figs. 4.4 and 4.5).

The major element chemistry shows sympathetic relationships between cobalt and nickel. Iron generally exhibits an antipathetic relationship with the other major elements. The minor elements copper silver and antimony do not show close sympathetic or antipathetic relationships between each other, but antimony shows a sympathetic relationship with iron. The cobaltite contains significant amounts of iron (3.4 to 7.75 wt%; mean=5.64wt%; median=5.45) and nickel (2.92 to 10.77wt %; mean=6.61wt%; median=5.70), whereas the arsenopyrite contains only minor amounts of nickel (below detection limits to 3500ppm; mean=1500ppm; median=1400ppm). Silver and copper show their highest concentrations at grain boundaries (Ag: up to 2800ppm and Cu: up to 1200ppm).

4.4.3. Chemistry of Tellurbismuth, Tetradymite and Galena in the Telluride-dominated Assemblage.

Tellurbismuth, tetradymite and galena were analysed for bismuth, tellurium, sulphur, cadmium, antimony, silver and gold (gold was always below the detection limits

of the technique). Two analytical approaches were adopted.

(i) Random spot analyses were undertaken to determine minor element partitioning between the different bismuth tellurides and sulphotellurides, and to examine if the minor element chemistry of an individual mineral species exhibits systematic variations that can be related to petrographic observations. For example, there is petrographic evidence that there are two generations of tellurbismuth, as shown by the presence of dissolution textures (cf. plate 4.12). Therefore, it may be expected that the two generations of tellurbismuth, identified petrographically, would have different minor element chemistries. Similarly, it may also be expected that galena from the two telluride assemblages would also have different minor element chemistries.

To obtain a representative sample of the tellurides from the ore shoot for the above investigation, six small (10-15g) telluride-bearing quartz samples were chosen at random. The tellurides were then extracted by dissolving the quartz in HF according to the method of Neuerberg (1979), and the resulting telluride concentrate was mounted in epoxy resin and polished for electron probe micro-analysis.

(ii) The complex intergrowths were analysed in detail by undertaking quantitative analyses at approximately 1-10 μ m intervals along a line perpendicular to the observed intergrowth. The chemistry of these intergrowths is described in section 4.4.3 of this chapter.

The summary statistics on the chemistry of tellurbismuth are presented in table 4.5. Tellurbismuth always contains minor amounts of antimony (range = 4700 - 8900ppm, mean = 7500ppm, median = 7600ppm) and cadmium (range = 2100 - 5100ppm, mean = 3610ppm, median = 3600ppm), and rarely minor quantities of silver (range = below the detection limits of the technique to 7900ppm, median and mean = below the detection limits of the technique). Lead is also locally present (range = below the detection limits of the technique to 7.82 wt%, mean=0.42 wt%, median = below the detection limits of the technique). The major element chemistry shows little variation (Bi

= 43.80 - 55.44 wt%, mean = 49.73, median = 50.01 wt%; Te = 45.84 - 47.31 wt%, mean = 46.49 wt%, median = 46.58). Histograms (figs. 4.6a to 4.6g) of the frequency distribution of the concentration data for each element show that except for silver none of the elements are bimodally distributed, indicating that chemically there is no difference between the two generations of tellurbismuth observed petrographically. A correlation matrix (table 4.6) shows a negative correlation of .779 between bismuth and lead, and a positive correlation of 0.86 between silver and lead, indicating that lead probably substitutes for bismuth, and to account for the charge deficit (bismuth is 3^+ , and lead is 2^+) silver (1^+) accompanies lead in the substitution. No similar correlations were observed between antimony and cadmium.

The summary statistics for the major and minor element chemistry of tetradymite are presented in table 4.7. The minor element chemistry of cadmium, antimony and silver in tetradymite show similar ranges and means as they do in tellurbismuth (Sb: range = below detection to 8800ppm, mean = 7500ppm, median = 7500; Cd: range = below detection limit to 3700ppm, mean = 3200ppm, median = 3100ppm; and Ag: range = below detection limit to 1200ppm, mean and median = below detection limit). However, the concentration of lead is significantly higher (range = 0.58 to 10.93wt%, mean = 7.56wt%, median = 7.94wt%) than in tellurbismuth. The major element chemistries of bismuth, tellurium and sulphur show a significant variation (Bi: range = 48.95 - 56.17wt%; Te: range = 28.97 - 35.16wt%; and S: range = 3.69 - 5.56wt%). Figure 4.7 illustrates this variation diagrammatically; the molar ratios of bismuth:tellurium and sulphur:tellurium vary from 0.47 to 0.69 (S:Te) and 0.45 to 1.16 (Bi:Te). As the total wt% for the tetradymites varies from 97 to 101wt% it could be argued that variation in the molar ratios of Bi:Te and S:Te is due to the variation in total wt%. To show that the variation in Bi:Te and S:Te are real and not an artifact of the analyses the two molar ratios were plotted against total wt% to examine if there were any correlations between the molar ratios of Bi:Te and S:Te. Figures 4.8 shows that there are no correlations that would account for the observed variation illustrated in figure 4.7.

A correlation matrix (table 4.8) for all the elements analysed shows good

correlations between lead and bismuth (-.731), lead and tellurium (-.821), and bismuth and tellurium (.809), but no correlation ($0.5 < R < -0.5$) between the minor elements (antimony, cadmium and silver), and the minor and major elements. The good correlations between the major elements suggest that a complex series of substitutions occur. That is, as lead increases, the amount of sulphur increases and accompanying these increases the concentration of bismuth and tellurium decrease. Histograms (figs. 4.9a to 4.9g) showing the compositional variations in tetradymite show that none of the elements are bimodally distributed. This indicates that the variation in tetradymite chemistry is not due to deposition from different solutions with different sulphur to tellurium ratios but from one solution in which the ratio of sulphur to tellurium varied during the deposition of tetradymite.

The summary statistics for the major and minor element chemistry of galena are presented in table 4.9. The minor element chemistry of cadmium and antimony in galena is significantly different from that in tellurbismuth and tetradymite; the overall content and mole percent is lower than in the two tellurides. This difference is well illustrated by a line concentration profile (figs. 4.10a and 4.10b) across a telluride-galena intergrowth. These line concentration profiles show that antimony is preferentially concentrated in the bismuth tellurides. However, there is no significant difference in silver content. The tellurium content in galena shows a bimodal distribution; in approximately 50% of the analysed galena grains, tellurium is below the detection limits of the technique (fig. 4.11). Bismuth exhibits a wide variation in concentration from 5300ppm to 4.04wt% (fig 4.12). A correlation matrix (table 4.10) for all the elements analysed shows no significant correlations ($0.5 < R < -0.5$) between any of the elements.

The summary statistics of the fingerprint intergrowths are given in table 4.11. The major elements (lead, bismuth, tellurium and sulphur) show a wide variation in concentration. This variation is to be expected because the intergrowth comprises two minerals that are intergrown on a scale that does not allow direct determination of each mineral species using electron probe micro-analysis, and each analysis is an analysis of differing proportions of the two minerals. However the molar ratios Bi/Te and Pb/S are

fairly constant ($\text{Bi:Te} = 0.885$ to 0.925 ; and $\text{Pb:S} = 1.0$ to 1.1). The lead to sulphur ratio is very close to that of galena, and because the lower reflectance phase in the "fingerprint" intergrowths (cf. plate 4.17) has similar optical properties to that of galena in plane polarised light, it is reasonable to assume that this phase is galena. Therefore the other phase involved in the intergrowth must be a bismuth telluride with a molar ratio of Bi:Te of less than 1; this corresponds to wehrlite (BiTe_{1-x}).

The minor element distributions of antimony, cadmium and silver in the fingerprint intergrowth are broadly similar to those of galena, but the lack of data prohibit any detailed comparison.

4.4.4 Comparison of minor Element Distribution Between the Major Mineral Species in the Bismuth Telluride Assemblage.

Box plots (figs. 4.13 to 4.15) show the statistical distributions of the minor element data between galena, the fingerprint intergrowths, tetradymite and tellurbismuth. In these box plots, the box represents the spread of the data between the lower and upper quartiles (i.e., 50% of the data), the line through the box shows the median of the data, the ticks represent the 95% confidence limits and the circles show the data points that lie outside the 95% confidence limits.

The distribution of cadmium and antimony content between the various mineral phases shows a sequential increase in concentration from galena to tellurbismuth. In the four mineral species and intergrowths examined tetradymite has a range in cadmium contents that has affinities with both galena and tellurbismuth. This suggests that tetradymite may have formed by replacement of galena or tellurbismuth.

The distribution of silver content does not show a distinct trend; the median value is close to, or at, the detection limits of the technique, and a number of silver values fall outside the 95% confidence limits.

The statistical distributions of antimony and cadmium indicate that these

elements are preferentially partitioned into tellurium-rich minerals.

4.4.5 Chemistry of Galena in the Sulphide-dominated Telluride Assemblage.

The summary statistics of galena are given in table 4.12. Locally galena contains significant amounts of bismuth (range = 0.53 to 4.04wt%, mean = 0.45wt%, median = 0.85wt%).

The frequency distribution of tellurium (fig. 4.16) is bimodal in both assemblages with both maxima (one below the detection limits of the technique and the other at 3500ppm) almost exactly coincidental. The range of antimony values (excluding one analysis at 7000ppm) in the two assemblages are very similar (below detection to 1500ppm).

However the range in silver content (below detection to 1.28wt%) of galena in the sulphide-dominated assemblage is significantly broader than in galena from the tellurbismuth-dominated assemblage (below detection to 1900ppm). Comparison of the two distributions (fig. 4.17) shows that the distribution of high silver content in galena from the sulphide-dominated assemblage has a range of values from .30 to 1.28. This range in silver values are absent from galena in the tellurbismuth-dominated assemblage. A similar distribution pattern is also observed when the concentrations of bismuth between the two assemblages are compared; in the sulphide-dominated assemblage there are a range of bismuth concentrations from 1.5 to 3.3 wt%, which are absent from the galenas in the tellurbismuth-dominated assemblage. The comparison of the distribution of cadmium concentrations is illustrated in figure 4.19; the range of cadmium concentration in the two assemblages is very similar (below the detection limits to 2400ppm in the tellurbismuth-dominated assemblage and below the detection limits to 3000ppm in the sulphide-dominated assemblage). A correlation matrix for all the elements analysed shows no significant correlations ($0.5 < R < -0.5$) between any of the elements (table 4.13).

The similarity between the tellurium and cadmium contents of galena in both the precious metal assemblages (i.e., the frequency distribution is bimodal and the modes have very similar values) suggests that similar processes have formed both assemblages. The difference in the distribution of bismuth concentrations can be explained by the presence of major amounts of tellurbismuth and tetradyomite, in the telluride-dominated assemblage, using most of the available bismuth. Whereas in the sulphide-dominated assemblage, in which bismuth minerals are of minor occurrence, excess bismuth is taken into solid solution in galena. A similar explanation can be used for the differences in the concentration of silver in galena between the two assemblages; in the tellurbismuth-dominated assemblage there are significant amounts of hessite and native gold, but in the sulphide-dominated assemblage native gold is very rare and hessite was only observed in small amounts. Therefore, it may be expected that silver will be preferentially partitioned into hessite and native gold. Thus as most of the silver will be used to form these minerals, galena in the tellurbismuth-dominated assemblage will have a low silver content, but in the sulphide-dominated assemblage galena can take up silver in solid solution as native gold and hessite are rarer in this assemblage.

4.4.6 Chemistry of the Minor Phases.

All of the minerals that could not be positively identified optically were analysed to confirm their composition. The minerals identified using electron probe micro-analysis were altaite, hessite, native bismuth, bismuthinite, bournonite, boulangierite and tetrahedrite. These minerals are of very low abundance and commonly small (10-40µm). A small number of analyses were undertaken on each mineral so as to confirm optical identification; these analyses are presented in tables 4.14.a and 4.14b

4.4.7 Chemistry of Gold.

Two mill concentrate samples CMC1 and CMC2 from the ore shoot on N^o 4 Level containing abundant gold were analysed for gold, silver and copper. The fineness

(fineness = $\text{wt\% Au} / (\text{wt\% Au} + \text{wt\% Ag})$) of the gold varies from 823 fine to 969 fine with a mean of 929 fine. The copper content varies from below the detection limits of the technique to 4900ppm with a mean below the detection limits of the technique. Figure 4.20 shows that the fineness distribution is bimodal with one population centred on 838 fine (mid-point of the interval 825 to 850) and the other on 938 fine (mid-point of the interval 925 to 950). The bimodal distribution of fineness indicates that, chemically, there are two distinct populations of gold; this confirms the petrological observations. This difference in chemistry could be related to: (i) two different fluids with different gold-silver ratios; or (ii) a single fluid where the co-precipitation of hessite preferentially sequesters silver from the ore fluids, hence increasing the fineness of the gold. For comparison, the compositions of gold from the samples provided by the British Museum (Natural History) and the National Museum of Wales were analysed (table 4.15). The fineness of gold from these samples is in the same range as the gold from No. 4 level (table 4.16). Placer gold from the Hirgwm river, which cuts the main lode, was also analysed as this gold should provide a sample representative of gold from the rest of the mine. Figure 4.21 illustrates the distribution of the fineness of the placer gold showing that it has a similar variation in fineness to the gold analysed from No.4 Level. The similarity in frequency distributions between gold from No. 4 Level and the placer gold from the Hirgwm river, combined with the similar range in composition for the museum gold indicates that the observed variation in fineness in samples from No. 4 Level is probably representative of the whole mine.

4.4.8 Chemistry of the Telluride and Sulphide Intergrowths.

Introduction.

The three types of telluride intergrowth described earlier in this chapter were examined using electron probe micro-analysis. These intergrowths are small (10-30 μm) inclusions in tellurbismuth (cf. plate 4.18), galena rims on tetradymite (cf. plate 4.15), and the fingerprint intergrowths on the margins of tetradymite grains (cf. plate 4.17). For each intergrowth examined, quantitative analyses for bismuth, tellurium, lead, sulphur, antimony, cadmium and silver were made at approximately 1 μm intervals along a line

running approximately perpendicular to the intergrowth. The detection limits of the technique and analytical errors for each element are the same as those for the random spot analyses.

Tellurbismuth-galena intergrowths.

Figure 4.22 shows the variation between: lead and bismuth; sulphur and tellurium; and cadmium and antimony across a galena-tellurbismuth intergrowth.

The concentration of lead in tellurbismuth is always low (generally below the detection limits of the technique). However, there are always significant amounts of bismuth in galena (approximately 5000ppm). Before a grain boundary is encountered there is little variation in the lead or bismuth content, and the only variations that were observed are those attributable to mineral phase changes; the boundaries are sharp, with the chemical changes from galena to tellurbismuth occurring over distances of one analysis (8 μ m). The other elements analysed show the same variations as lead and bismuth. There are no variations close to grain boundaries that would indicate whether the galena formed from exsolution or replacement. However the low lead content in tellurbismuth indicates that the inclusions could not have formed by exsolution, but the question as to whether the galena inclusions form by replacement or co-crystallisation processes is equivocal.

Tellurbismuth-galena-tetradymite Intergrowths.

Figure 4.23 shows the compositional variation between: lead and bismuth; sulphur and tellurium; and cadmium and antimony across a complex intergrowth.

On the left tellurbismuth and tetradymite are in direct contact and on the right there is a rim of galena between the tellurbismuth and tetradymite. Within the three phases there is little variation in either lead or bismuth content and, as with the tellurbismuth intergrowths, changes in chemistry only occur at phase boundaries over short distances (5 or 10 μ m). However, unlike tellurbismuth, tetradymite contains appreciable lead and it is therefore possible that the galena formed by exsolution from tetradymite with

subsequent annealing destroying any local depletion of lead caused by the exsolution of galena.

"Fingerprint" Intergrowths.

Figure 4.24 shows the variation in lead and bismuth, and sulphur and tellurium concentrations across a fingerprint intergrowth.

In the "fingerprint" intergrowth sulphur varies sympathetically with tellurium, whereas in the other two intergrowths described, tellurium and sulphur vary antipathetically. This indicates that a different process has formed this type of intergrowth. Amongst the minor elements, antimony varies sympathetically with bismuth. This relationship is similar to the other two intergrowths, and is consistent with the observation that antimony preferentially partitions into bismuth minerals.

4.5 Relationship Between Mineral Chemistry and Paragenesis.

The chemical relationships in the telluride assemblages generally show no significant difference between the two telluride assemblages; indeed, there are a number of striking similarities between the composition of the galena in the two assemblages suggesting that similar processes have operated in forming the two assemblages. Within the bismuth telluride assemblage, the optical observation that there are at least two generations of tellurbismuth is not reflected in the chemistry; this shows that the different generations of tellurbismuth must have been deposited from chemically similar fluids. In mineral species where bimodal distributions in minor element chemistry were observed, there is generally no association of one population with any particular intergrowth or assemblage. The line concentration profiles show that the galena inclusions in tellurbismuth were not formed by exsolution (this is consistent with the textural observation of galena, hessite and gold forming along dissolution surfaces in tellurbismuth), and that tetradymite did not form by exsolution from tellurbismuth because the elements required to form galena and tetradymite (lead and sulphur) from

tellurbismuth are not present in tellurbismuth. The formation of the galena rims and fingerprint intergrowths associated with tetradymite are more problematical, because tetradymite contains lead and sulphur which are required to form the intergrowths and annealing processes could have modified the original chemical profiles. Thus it is not possible to say unequivocally whether exsolution, replacement or co-crystallisation processes formed the intergrowths. However, the similarity in minor element chemistry between the galena rims and isolated inclusions indicates that similar processes have operated in the two types of intergrowth, and as the isolated inclusions were not formed by exsolution then it is more probable that the galena rims and fingerprint intergrowths were formed by either replacement or co-crystallisation processes.

If it is assumed that replacement and co-crystallisation processes formed the two telluride assemblages then the following hypothesis can be put forward. Firstly, bismuth and tellurium were removed into solution. The bimodal distribution of tellurium concentrations indicates that tellurium could have been removed from some galenas. The increase in bismuth and tellurium content of the solution allows the formation of the bismuth tellurides by replacement of sulphides, or as discrete bismuth and tellurium minerals in voids and microfractures elsewhere in the lode. This process would result firstly in the formation of lead-rich tetradymite. Secondly, tellurbismuth and any lead or sulphur in the fluids that cannot be incorporated into the bismuth telluride minerals would be left as galena inclusions at grain boundaries. This replacement/co-crystallisation model is supported by the observation that bismuth tellurides are observed replacing galena along cleavage planes (cf. plate 4.29) in the galena assemblage. A consequence of this type of process is that the total amount of tellurium in solution increases and, if it reaches a high enough level, altaite will form instead of galena. The detailed consequences of changing the tellurium content in the fluid are discussed in the following chapter.

CHAPTER 5.

CONDITIONS OF ORE FORMATION AT CLOGAU MINE.

5.1 Introduction.

The ore mineral assemblages at Clogau Mine contain phases that occur in the systems Bi-Te-S, Bi-Te-Au, Au-Ag-Te-S, and Pb-Te-S. In order to estimate the conditions of formation of these assemblages in terms of the activities of tellurium and sulphur, a number of phase diagrams have been constructed. These diagrams are of the type:

- (a) Log Activity of S_2 or Te_2 versus Temperature.
- (b) Log Activity of S_2 versus Log Activity Te_2 .

For the majority of simple sulphides and oxides, such diagrams are already published in the literature, but there are few diagrams for the tellurides. Therefore, these diagrams have been constructed from thermochemical data available in the literature, and where no appropriate thermochemical data exist, estimations have been made.

5.2 Thermochemical data for the systems Bi-Te-S, Bi-Te-Au, Pb-Te-S, Au-Ag-Te-S.

Introduction.

The following section describes the methods used to construct the activity diagrams, and critically assesses the data obtained from the calculations. The calculations are of essentially two types: firstly, calculation of Gibbs Free energy data from heat capacity data, and standard enthalpies and entropies of formation at 298 K; and, secondly, the estimation of thermochemical data.

The detailed description of the calculations employed to obtain the Gibbs Free energy data from heat capacity, enthalpy and entropy data is in Appendix 1a, and all of the thermochemical data that have been generated using the various methods are tabulated in Appendix 1b.

5.2.1 Calculation of activity data from Gibbs Free energy data.

The Gibbs Free energy for a sulphidation reaction is given by the following equation:

$$\text{Log } a_{\text{S}_2} = \Delta G_{\text{T(reaction)}}/4.576T \quad (\text{eq.5.1})$$

Equation (5.1) can be used for any sulphidation reaction as long as the Gibbs Free energy for the sulphidation reaction is calculated in terms of 1 mol of $\text{S}_2(\text{g})$. The same criteria apply to telluridation reactions, and an analogous equation may be written for the activity of tellurium:

$$\text{Log } a_{\text{Te}_2} = \Delta G_{\text{T(reaction)}}/4.576T \quad (\text{eq.5.2})$$

if both tellurium and sulphur are involved in a reaction, then the activities of those substances are related to the Gibbs Free energy of that reaction by the following equation:

$$\text{Log } a_{\text{Te}_2} - \text{Log } a_{\text{S}_2} = \Delta G_{\text{T(reaction)}}/4.576T \quad (\text{eq.5.3})$$

Equation (5.3) holds true if the Gibbs Free energy of reaction is calculated from reactions written in terms of 1mol of $\text{Te}_2(\text{g})$ forming 1mol of $\text{S}_2(\text{g})$. Using equations (eq.5.1), (eq.5.2) and (eq.5.3) enables the construction of two types of petrogenetic diagram from Gibbs Free energy data: a temperature-activity plot, and an activity - activity plot, at a given temperature. The plotting of such diagrams requires a large number of data points, and hence a computer program was devised, using the calculation procedure outlined in Appendix 1a, to facilitate the exercise.

The computer program produces The Gibbs Free energy for a substance at temperature T K, and the calculation of activity data was achieved from the Gibbs Free energy data by using the *Statworks*TM statistical package on an *Apple Macintosh* microcomputer.

5.2.2 Validity of calculated data.

To test the validity of the method of calculation the Gibbs Free energy data obtained are compared to those published by Barton and Skinner (1979). In table 5.1, reactions 5.1 to 5.4 compare the data obtained by the method described in this thesis and the data of Barton and Skinner (1979). In these reactions the original data source is the same (Mills, 1974), whereas for reactions 5.5 and 5.6 (table 5.1) the original data sources are different. In the latter two reactions the data source used in this thesis is Mills (1974), whereas Barton and Skinner (*Op. Cit.*) use Barton and Toulmin (1964) for reaction 5.5 and Craig and Barton (1973) for reaction 5.6.

For all of the above reactions, Barton and Skinner (*Op. Cit.*) state that the uncertainty in determining the Gibbs Free energy of reaction is within 1 kcal. Thus for reactions 5.1 to 5.4, where the data sources are identical, the Gibbs Free energy of reaction for the two methods are generally within 0.1 kcal, which is well within the error of determination. For reaction 5.5, the agreement between the two methods is not as good as for the first four reactions (± 0.5 kcal). The reason for this seems to be due to a typographical error in the text of Mills (1974, p.104); in the text the heat capacity expression $C_p = 1.819 + 53.0 \times 10^{-3}T$ is quoted, while in the Appendix, $C_p = -1.819 + 53.0 \times 10^{-3}T$ is the actual expression used to calculate the G-function and tabulate thermochemical data for Ag_2S .

A more extreme problem arises when the two data sets for reaction (5.6) are considered. The errors here are of the order of 10kcal. This discrepancy can be traced to the data for the enthalpy of formation of $\text{Bi}_2\text{S}_3(\text{s})$. Mills (1974) selects a value of $48.2 \text{ kcal mol}^{-1}$ for ΔH_{f298} , whereas the data of the majority of other workers suggest that the true value is some 10 kcal mol^{-1} lower. If the value -33900 ± 250 (Robie and Waldbaum, 1968) is selected instead of the value proposed by Mills (1974), then the results are in much closer agreement (± 0.5 cal). The value selected by Mills (1974) was discarded for calculations of thermochemical data of bismuthinite, as the data of other

workers suggest that the true value is some 10 kcal mol⁻¹ lower.

The above critique shows that the method chosen in this thesis to calculate thermochemical data is valid for the reactions which are shown in table 5.1, and hence it should also be valid for reactions where no comparisons are available in the literature. Where thermochemical data in the literature are insufficient to allow thermochemical calculations of the type outlined in Appendix 1a, estimations of thermochemical properties have been made to enable the estimation of Gibbs Free Energy data. The estimation of thermochemical data is the subject of the next section.

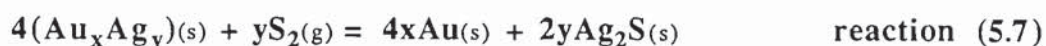
5.2.3 Estimation of thermochemical data.

A number of equilibria in the systems Bi-S-Te, Au-Bi-Te and Au-Ag-S-Te are of interest when considering the ore assemblages at Clogau Mine, but thermochemical data for these equilibria are not adequate enough to allow the calculation of Gibbs Free energy data over a range of temperatures. The equilibria of interest are as follows:

- (i) electrum/argentite/acanthite/hessite;
- (ii) the bismuth sulphotellurides and bismuth tellurides.

Estimation of thermochemical data for the electrum (Au,Ag), argentite/acanthite (Ag₂S) hessite (Ag₂Te) equilibria.

Barton and Toulmin (1964) have investigated the following equilibrium:



and determined log a_{S_2} over the temperature range 160°C (433K) to 423°C (696K) for electrum compositions over the range of 5.77 weight percent silver to pure silver. If the activity of S₂(g) and Te₂(g) in the following equilibrium:



can be determined with reasonable accuracy (which they can by using the data of Mills, 1974) then it is possible to determine, graphically, the activity of $\text{Te}_2(\text{g})$ in the following reaction:



this involves applying the data of Barton and Toulmin (1964) in the following way. At a specified temperature and composition of electrum, reaction (5.7) will have a unique, and known, activity of $\text{S}_2(\text{g})$, and hence the activity of $\text{S}_2(\text{g})$ in reaction (5.8) is also known. Therefore, the activity of $\text{Te}_2(\text{g})$ in equilibrium with electrum, hessite and Ag_2S at the specified temperature can be determined, and thus the activity of $\text{Te}_2(\text{g})$ in reaction (5.9) in equilibrium with hessite and an electrum of known composition can be calculated. This is shown graphically in figures 5.1a and 5.1b. To facilitate this graphical interpolation, a series of equations were derived from the data of Barton and Toulmin (1964) and Mills (1974), and a computer program devised to calculate the activity of tellurium in equilibrium with hessite (Ag_2Te) and electrum of a known composition.

Therefore, it is a simple matter to construct an activity S_2 - activity Te_2 grid, contoured in terms of electrum composition, which is much more relevant to natural systems, as gold is nearly always alloyed with silver in nature. Also, if the composition of electrum in equilibrium with hessite in a natural system is known, the petrogenetic grid can provide a reasonable estimate of tellurium activity at the time of ore deposition.

Estimation of thermochemical data for bismuth sulphotellurides.

In order to obtain thermochemical data for sulphotellurides, the method employed by Craig and Barton (1973), who estimated thermochemical data for

sulphosalts, was utilised. Craig and Barton (1973) used the sum of the Gibbs Free energy data for the end-member metal sulphide and semi-metal sulphide, combined with a Gibbs Free energy of mixing term based on ideal mixing assuming no enthalpy of mixing. They quote the following equation for the Gibbs Free energy:

$$\Delta G^{\circ} = N_a \Delta G_a + \dots + N_i \Delta G_i + (1.20 \pm 0.8)(N_a R T \ln a + \dots + N_i R T \ln i) \quad (\text{eq.5.4})$$

where N_i is the mole fraction of the i th simple sulphide component, R is the gas constant and T the temperature in degrees Kelvin. Thus, considering the sulphotelluride tetradyomite ($\text{Bi}_2\text{Te}_2\text{S}$), which is present at Clogau Mine, the following reaction may be written for its formation:



By applying equation (eq.5.4) to reaction (5.10) the equation for the Gibbs Free energy of tetradyomite is as follows:

$$G_T = \left[1/3G_T(\text{Bi}_2\text{S}_3) + 2/3G_T(\text{Bi}_2\text{Te}_3) \right] + (1.20 \pm 0.8) \left[1/3RT \ln(1/3) + 2/3RT \ln(2/3) \right]$$

Therefore:

$$G_T = 1/3 \left[G_T(\text{Bi}_2\text{S}_3) + 2G_T(\text{Bi}_2\text{Te}_3) \right] - 1.526T \quad (\text{eq.5.5})$$

Hence thermochemical data for tetradyomite can be estimated using equation (eq.5.5).

Estimation of thermochemical data for maldonite (Au_2Bi).

Barton and Skinner (1979) quote the Gibbs Free energy of reaction for the formation of gold and bismuthinite by the sulphidation of maldonite over the temperature range 113-371°C:



$$G_T = -54145 + 41.44T \quad (\text{eq.5.7})$$

Equation (eq.5.7) gives the Gibbs Free energy change for reaction (5.11) at any temperature in the given temperature range, and as the Gibbs Free energies for the substances (except maldonite) are known over that temperature range; then the Gibbs Free energy of maldonite is given by the following equation:

$$\begin{aligned} G_T(\text{Au}_2\text{Bi}) &= 2G_T(\text{Au}) + 1/2G_T(\text{Bi}_2\text{S}_3) - 3/4G_T(\text{S}_2) \\ G_T(\text{Au}_2\text{Bi}) &= 4060 - 31.08T \end{aligned} \quad (\text{eq.5.8})$$

5.2.4 Validity of approximations.

Electrum (Au,Ag) - argentite/acanthite (Ag_2S) - hessite (Ag_2Te) equilibria.

As the electrum tarnish method of Barton and Toulmin(1964) is used to calibrate the activity of sulphur in other sulphidation reactions, the errors involved in this half of the estimation are small. Other inaccuracies which are involved are firstly, the precision in determining the Gibbs Free energy of the equilibrium in reaction (5.8). Barton and Skinner (1979) estimate that data obtained from Mills (1974) are accurate to ± 1 kcal which is equivalent to ± 1.36 log activity units at 298K and to ± 0.36 log activity units at 600K. Secondly, there are the errors caused by the solubility of gold in hessite. These errors are difficult to quantify as there are no experimental data, although, by analogy with Ag_2S , the errors involved will be small, probably in the order of ± 0.5 log activity units. Hence, this method is valid as a first approximation.

Sulphotelluride approximations.

Craig and Barton (1973) stated that the approximations which they made could not be rigorously tested for most sulphosalts due to the paucity of empirical data. However, they compared an experimentally determined tie-line switch where the low temperature assemblage silver-matildite is replaced by the high temperature assemblage argentite - bismuth liquid with the theoretical determination of the same tie line switch.

Experimentally, this switch was observed at $343 \pm 3^\circ\text{C}$, and the appropriate sulphidation reactions yielded a calculated temperature for the reaction of 339°C , which is in very close agreement with the experimentally determined temperature. This shows that the estimation of thermochemical data using the method of Craig and Barton (1973) is applicable as a first approximation.

Maldonite approximation.

Barton and Skinner (1979) estimated the error in determining the Gibbs Free energy for reaction (5.11) at $\pm 1\text{kcal}$. The accuracy of determining the Gibbs Free energy of the individual substance in reaction (5.11) is also $\pm 1\text{kcal}$. Therefore, the accuracy of estimating thermochemical data for maldonite is of the same order.

5.2.5 Ranking of data.

For the final construction of activity - temperature, and activity - activity diagrams, the following ordering of data was used:

- (i) actual experimental determination of the activity of sulphur or tellurium at the required temperatures.
- (ii) Thermodynamic data at 298K, extrapolated to higher temperatures using data for heat capacity, entropy and enthalpy of phase transitions. Selected data in this category are always the most recent or the most reliable where there is a conflict of data (the data in Mills (1974) were used almost exclusively in this category).
- (iii) Estimated thermochemical data. Data in this class fall into two categories: (a) estimation of the Gibbs Free energy of a substance using the method of Craig and Barton (1973) and (b) extrapolation of thermochemical data in a system of type 1 or 2 to one where there are no thermochemical data, but where the two systems can be related by a common reaction of type 1 or 2.

In the above three data types, the order of preference that was used to construct the activity diagrams is: firstly, experimental determination of data at the required temperatures; secondly, thermochemical data at 298 degrees kelvin extrapolated to higher temperatures; and thirdly, estimated thermochemical data. For example, in reaction (5.5) (the sulphidation of silver to form acanthite) the experimental data of Barton and Toulmin (1964), which are of type 1, are used to calculate the activity of sulphur rather than the data of Mills (1974), which are of type 2.

Table 5.2 shows the reactions which have been investigated, the type of data used, the source of the data used, and the temperature range under investigation. The numbering of reactions in table 5.2 refers to the reaction lines on the activity- activity grids for sulphur and tellurium.

The activity-temperature grids for the reactions involving tellurium are shown in figure 5.2. The corresponding activity-temperature grids for sulphur are shown in figure 5.3. These grids were constructed from the data in Appendix 1b. The important reactions to note are the sulphidation and telluridation of native bismuth to form bismuthinite and tellurbismuth respectively plus the sulphidation and telluridation of maldonite to form bismuthinite + native gold and tellurbismuth + native gold. These reactions indicate that in the sulphide dominated assemblage where native bismuth occurs maldonite would be the stable gold mineral and not native gold. This association is supported by the phase equilibrium study of Gather and Blachnik (1974) of the system Au-Bi-Te which showed that the stable assemblages in this system are native gold-tellurbismuth-calaverite, native gold-tellurbismuth and native bismuth-maldonite-hedleyite. Because of the above theoretical mineral associations all sections containing native bismuth were carefully examined for the presence of maldonite. In all of the sections examined no maldonite or native gold was observed. This indicates that the fluids which deposited the native bismuth did not carry any significant gold.

Another set of important reactions are the sulphidation of native bismuth to form bismuthinite and the sulphidation of pyrrhotine to form pyrite as there is a tie line switch

at 243°C where the assemblage pyrrhotine-bismuthinite switches to the assemblage pyrite and native bismuth. Three of these minerals were observed in one sample (JN 12) in which pyrrhotine and bismuthinite were observed in contact (cf. plates 4.5 and 4.6) but native bismuth and pyrrhotine were not observed in contact. The presence of bismuthinite in contact with native bismuth within the same sample suggests that temperatures during ore deposition were between 243°C (the temperature of the tie line switch) and below 271°C (the melting point of native bismuth).

The activity - activity grids for sulphur and tellurium are shown in figures 5.4 to 5.7 and were constructed between 350°C and 200°C with a temperature interval of 50 °C between each diagram to show the phase interaction at different temperatures.

5.2.6 Effect of Pressure.

All of the diagrams have been calculated at a pressure of one atmosphere. The effect of elevated pressure has been ignored, as for many of the phases under consideration there are no molar volume data. Therefore, the calculation of volume changes during a reaction is impossible. Barton (1970) has shown that for many sulphidation reactions the change in volume is small and hence the effect of pressure is negligible.

The discussion of the relevance of the constructed diagrams to the natural assemblages is the subject of the next section.

5.3 Conditions of Ore Formation at Clogau Mine.

5.3.1 Temperature.

Bottrell (1986) and Bottrell *et al.* (1988) using fluid inclusion geothermometry and barometry stated that gold was deposited at Clogau Mine between 300 and 320°C at a pressure of about 1.8 Kb. However, as already stated the presence of native bismuth, pyrrhotine and bismuthinite associated with the gold-bearing ore shoot at Clogau Mine

suggests that at least some of the mineralising event took place below these temperatures. But, in the material containing the above assemblages, native gold was not actually observed, indicating that although the occurrence of the above minerals is closely spatially associated with gold-telluride mineralisation, precipitation of gold from solution may have ceased by the time temperatures were below 300°C.

5.3.2 Activity of Tellurium and Sulphur During Mineralisation.

The paragenesis and mineral chemistry of the studied ore shoot shows a sequence of mineralogical changes from minerals with high lead:bismuth ratios and high sulphur:tellurium ratios, to minerals with low lead:bismuth and low sulphur:tellurium ratios. This is the sequence in the tellurbismuth-dominated assemblage: galena - "fingerprint" intergrowth - tetradymite - tellurbismuth, with gold and altaite generally associated with tellurbismuth as opposed to tetradymite. Figures 5.4 to 5.7 are four isothermal sections showing mineral stabilities in activity Te_2 - activity S_2 space. The reactions that give the activities of sulphur and tellurium in the bismuth telluride assemblage are:

reaction 9	$FeS + Te_2 = FeTe_2 + 1/2 S_2$	No iron telluride.
reaction 8	$Fe + 1/2 S_2 = FeS$	
reaction 1	$2Bi + 3/2 Te_2 = Bi_2Te_3$		
reaction 13	$2Bi + Te_2 + 1/2 S_2 = Bi_2 Te_2 S$	No native bismuth (only applies to the tellurbismuth assemblage).
reaction 4	$2Bi + 3/2 S_2 = Bi_2S_3$		
reaction 10	$FeS + 1/2 S_2 = FeS_2$	Pyrrhotine as opposed to pyrite is associated with the tellurbismuth assemblage.
reaction 12	$Au + Te_2 = AuTe_2$	No calaverite.
reaction 7	$Ag_2Te + 1/2 S_2 = Ag_2S + 1/2 Te_2$	No acanthite/argentite.
reaction 5	$4Ag + Te_2 = 2Ag_2Te$	No native silver

The limits of the above reactions are outlined on each figure in a bold polygon. Assuming that gold and hessite were precipitated approximately contemporaneously and in

equilibrium, then the approximate range of activity of tellurium during gold deposition, as given by the range in gold composition ($N_{Ag} = 0.1$ to 0.3) (cf. section 5.2.3), is -7.9 to -9.7 log activity units at 300°C .

In all four diagrams, the stability field of altaite never overlaps with the stability field of tetradymite. Thus, tetradymite and altaite, at a given activity of tellurium and sulphur, cannot co-exist (the stable assemblage being tetradymite and galena, a commonly observed assemblage). This explains why altaite is always observed included in tellurbismuth and not tetradymite. By analogy, as gold has the same occurrence as altaite (with respect to tetradymite and tellurbismuth), then the activity of tellurium - activity of sulphur ratio, during gold deposition may have been similar to that during altaite deposition; that is, greater than one. The occurrence of gold and galena is not incompatible with this, because galena is stable throughout all of the tetradymite field and a small portion of the tellurbismuth field and can co-exist with altaite. The main iron sulphide in the ore shoot is pyrrhotine, but the local occurrence of pyrite indicates that the activity of sulphur was close to the pyrite-pyrrhotine buffer, hence the location of the stippled area of probable formation in figures 5.4 to 5.7 close to the pyrite-pyrrhotine reaction line.

The isothermal sections show conclusively that the observed mineral species could not be formed from a fluid whose total tellurium concentration remained fixed, because at a constant temperature the formation of an assemblage comprising altaite, tellurbismuth, galena and tetradymite (the tellurbismuth-dominated assemblage), and an assemblage consisting of galena, tetradymite, werhlite and native bismuth (the sulphide-dominated assemblage) requires a large change in the activity of tellurium so that the different mineral species in each assemblage can form. Neither can the observed assemblages be formed by reducing temperature at a constant activity of tellurium and sulphur, because examination of the isothermal sections shows that as the temperature falls calaverite and not native gold becomes the stable gold mineral. As calaverite is not observed in any of the sections examined, nor, for that matter, are any gold-silver tellurides (e.g., sylvanite or krennerite) observed, it is unlikely that this process could

have formed the observed mineral species.

To produce the observed mineral assemblages the ratio of the activity of sulphur to the activity of tellurium combined with temperature must change in a manner which allows the formation of altaite, the mineral which requires the highest activity of tellurium, and then native bismuth, the mineral that is stable at lowest activity of tellurium. These two minerals can be produced by holding the ratio of activity of tellurium to activity of sulphur constant, and allowing the temperature to fall or holding the temperature constant and allowing the ratio of activity of tellurium - activity of sulphur to decrease. This produces the idealised sequence illustrated in fig. 5.8. The minerals are presented in order of appearance and the length of each line shows the stability range of each mineral; where lines overlap, the minerals associated with that overlap can co-exist. For example, altaite-gold-tellurbismuth form a stable assemblage at a given activity of tellurium and sulphur, whereas the assemblage tetradyomite-altaite-gold cannot co-exist stably. Table 5.3 lists a number of mineral associations some of which are stable and some of which are unstable, each assemblage in bold type face is an assemblage that was observed in polished section. The strong correlation between stable theoretical assemblages and actual observed assemblages suggests that decreasing activity of tellurium and falling temperature have caused the observed mineral assemblages.

In the above discussion there are no paragenetic relationships associated with the formation of individual mineral species because there is no unambiguous textural information within the two telluride assemblages to suggest the correct paragenetic sequence. However, this does not detract from the fact that the observed mineral assemblages can be produced by changes in tellurium activity and temperature.

5.4 Relationship Between Mineralisation at Clogau Mine and The Dolgellau Gold-belt.

Shepherd and Allen (1985), in a fluid inclusion study of the Dolgellau Gold-belt, concluded that gold mineralisation at Gwynfynydd mine was the result of an externally-derived oxidised gold-bearing fluid reacting with graphite in the wallrocks and precipitating its gold due to the destabilisation of either gold-chloride or gold-bisulphide complexes. This is the same model as proposed by Bottrell (1986) and Bottrell *et al.* (1988). Thus, it would seem that the overall process of gold mineralisation in the Dolgellau Gold-belt is similar for all the occurrences of vein quartz-hosted gold mineralisation (minor gold mineralisation is associated with the copper deposits at Coed-y-Brenin and Glasdir). Gilbey (1969) recognised that: (i) the vein quartz-hosted gold mineralisation in the Dolgellau Gold-belt is zoned with respect to the base metal mineralogy of the veins; in the south-west of the Dolgellau Gold-belt a chalcopyrite-pyrrhotine assemblage dominates and gives way, in the north-east, to a sphalerite-galena assemblage; and (ii) in the south-west, native gold is associated with bismuth tellurides and galena while, in the north-east, native gold is associated with galena, sphalerite and argentiferous tetrahedrite. Thus, although the fluid inclusion data of Shepherd and Allen (1985), Bottrell (1986) and Bottrell *et al.* (1988) show that the same overall process formed the gold, the difference in mineralogy between the two main gold producers in the Dolgellau Gold-belt suggests that, in terms of their metal content, compositionally different fluids were involved in gold mineralisation, with gold being deposited from a tellurium-bearing fluid in the south and an antimony-bearing fluid in the north.

CHAPTER 6

DISCUSSION OF MINERALISATION AT CLOGAU MINE.

Bottrell (1986) and Bottrell *et al.* (1988) in a fluid inclusion study of Clogau Mine examined the fluid chemistry of the same ore shoot on No.4 Level that was studied in this thesis. They concluded that the gold mineralisation at Clogau Mine was the result of an externally derived gold-bearing oxidised aqueous fluid reacting with the Clogau shales to produce an immiscible $\text{H}_2\text{O}-\text{CH}_4$ fluid. Deposition of gold was ascribed to the de-stabilisation of either AuCl_2^- or $\text{Au}(\text{HS})_2^-$ complexes due to fluid interaction with the shale wallrocks. Deposition of gold took place at c.300-320°C and at a pressure of c.1.8Kb. Bottrell (1986) and Bottrell *et al.* (1988) also observed that high gold values were associated with high total CH_4 and low CO_2/CH_4 ratios. The localisation of gold mineralisation associated with these methane and carbon dioxide values was thought to be the result of increased interaction between wallrock and gold-bearing fluid. However Seward (1973, 1984) has examined the role of AuCl_2^- and $\text{Au}(\text{HS})_2^-$ complexes in the transportation of gold in hydrothermal solution over a wide range of P-T conditions, and concluded that the bisulphide complex was the dominant complex under reducing conditions (f_{S_2} close to the pyrite pyrrhotine buffer) at temperatures below 350-400°C, and the chloride complexes may be important under oxidising conditions (f_{O_2} close to the magnetite hematite buffer). Thus for the conditions of ore formation at Clogau Mine it would seem probable that the bisulphide complex was the dominant, but not the only ligand for gold transport.

This model implies that gold was deposited from one fluid with the abundance of tellurides, sulphides and gold being directly related the amount of gold-bearing fluid passing through a particular section of the mine, and the amount of wallrock available to bring about gold precipitation. The areas of the mine that would have had the maximum wallrock available for reaction and the highest permeability to allow fluid to pass through are the cross-cutting faults. However, the data presented here suggest that replacement and remobilisation processes had a role to play in gold mineralisation. For example the

dissolution textures in the tellurbismuth assemblage show that the ore fluids at different stages in the mineralisation must have been capable of both precipitating and dissolving the same ore minerals. This observation tends to imply that two compositionally different fluids were involved in mineralisation, but the fluid inclusion data of Bottrell (1986) and Bottrell *et al.* (1988) show no evidence to suggest that separate fluids were involved in mineralisation. Therefore, any model proposed for the gold mineralisation at Clogau Mine must be compatible with what appear to be two conflicting sets of data.

This paradox can be resolved by proposing the following hypothesis. Firstly a gold-bearing oxidised aqueous fluid is introduced and reacts with the graphite in the shale wallrocks precipitating its dissolved metal content due to the de-stabilisation of chloride and/or bisulphide complexes as proposed by Bottrell (1986) and Bottrell *et al.* (1988). In this model, reaction could proceed until all of the available graphite has been consumed. The vein is then isolated from the fluid, and subsequent deformation and fracturing re-opens the vein. However, as there is no graphite available to cause the precipitation of metals from solution, and if the fluid is not saturated with respect to its dissolved metal content, the fluid will re-dissolve some or all of the previously precipitated metals. This process increases the metal content of the fluid and when this modified fluid encounters fresh wallrock it precipitates its metals. Movement of this fluid will be along zones of weakness, such as fractures in vein quartz and, along cross-cutting faults. Also, within these fault zones, the wallrocks will be heavily brecciated and hence provide large amounts of wallrock for metal complex de-stabilisation reactions to take place. Thus these fault zones will act as geochemical traps because all of the graphite will not be consumed, and hence metal-bearing fluids entering a fault zone will precipitate their metals.

The above model of reaction of wallrock graphite with auriferous fluids is not the only way that gold can be deposited from hydrothermal solution. Bancroft and Jean (1982) and Jean and Bancroft (1985) investigated experimentally the deposition of gold from solutions of KAuCl_4 and $\text{KAu(CN)}_2\text{Br}$ (with gold concentrations of 1, 10 and 100ppm) on

the surfaces of the following sulphides: pyrite, pyrrhotine, galena and sphalerite. They observed that elemental gold was precipitated very rapidly on the surface of all the minerals investigated from the chloride solutions, but in the gold-cyanide solutions gold was present on the surface as the gold complex AuCN^- , and not as elemental gold. They proposed that reactions of gold chloride complexes by oxidation of sulphide ions at the surface of the minerals were responsible for the precipitation of gold. The close association of gold and pyrite (cf. plate 4.35), gold and galena (cf. plate 4.36) suggests that reduction of gold-chloride complexes may have brought about the deposition of gold.

Also Lebedeva (1982) investigated the role of tellurbismuth and native bismuth in gold deposition and found that gold was preferentially precipitated by tellurbismuth. This is consistent with the petrographic observation that native gold is associated with tellurbismuth and not native bismuth; also the observation that native gold occurs at grain boundaries in tellurbismuth indicates that tellurbismuth may have acted as a precipitant for gold.

It is concluded that:

- (i) gold mineralisation at Clogau mine took place at temperatures c. 300°C and pressures of c. 1.8Kb, but the presence of native bismuth associated with gold mineralisation indicates that the last stages of precious metal mineralisation may have been as low as c. 250°C .
- (ii) The range of gold compositions, within the ore shoot on No. 4 Level, in equilibrium with hessite indicate that gold deposition took place at $\log a_{\text{Te}_2}$ between -7.9 and -9.7 at 300°C , and the presence of pyrite and pyrrhotine indicates that the $\log a_{\text{S}_2}$ was close to the pyrite-pyrrhotine buffer ($\log a_{\text{S}_2} = -12.4$ at 300°C and -13.8 at 250°C).
- (iii) The high grade telluride ore-shoots are the result of remobilisation of gold, tellurium, bismuth and lead from elsewhere in the lode to zones where increased interaction between wallrock and fluid is more probable
- (iv) Precipitation of gold was caused by fluid interaction with graphite in the wallrock, and reactions involving pyrite and /or pyrrhotine, tellurbismuth and galena destabilising gold bisulphide and/or gold chloride complexes.

CHAPTER 7.

**GEOLOGY AND
MINERALISATION IN THE
SOUTHERN UPLANDS,
SCOTLAND.**

7.1 Introduction.

Until recently, the evolution of the Southern Uplands was regarded as involving accretion during early Palaeozoic subduction of Iapetus oceanic crust beneath the southern margin of the Laurentian continent (e.g., McKerrow *et al.* 1977; Leggett *et al.*, 1979a, 1979b; Knipe and Needham, 1985; Needham and Knipe, 1986; Leggett, 1987). In this model, the accretion of the sedimentary wedge is regarded as starting in the Llanvirn and continued until Wenlockian time. This resulted in the formation of at least ten tectonostratigraphically distinct units of ocean floor sediments and trench-fill turbidites. Accretion was terminated by end-Silurian early Devonian continental collision (Soper and Hutton, 1984).

However Stone *et al.*, (1987) and Morris (1987) have proposed an alternative interpretation of the evolution of the Southern Uplands, namely that the Southern Uplands formed in a deformed back-arc basin. The major lines of evidence cited for the existence of a volcanic arc, of which there are no extant remains, are the two distinct petrofacies of greywackes and their opposing transport directions.

7.2 Stratigraphy, Structure and Metamorphism.

7.2.1 Stratigraphy.

The rocks of the Southern Uplands consist of pelagic and hemipelagic ocean floor sediments, spilites, cherts and trench-fill turbidites, the latter being volumetrically the more important. The sequence of rocks is divided into three tectonically bounded belts:

(i) the Northern Belt, which comprises Ordovician rocks, and is bound by the Southern Uplands fault in the north and the Kingledores Fault in the south.

(ii) The Central Belt, which is composed of mainly Silurian rocks, but rocks of Ordovician age (the Moffat Shales) occur within the Central Belt as small, isolated,

elongate inliers. The Central Belt is bounded by the Kingledores Fault in the north and the Riccarton Line in the south.

(iii) The Southern Belt, which is composed mainly of Wenlock rocks, which occur to the south of the Riccarton Line (Craig, 1983).

Northern Belt.

The Northern Belt is composed mainly of sequences of greywacke and finer grained interbeds that are essentially of Ordovician age. Locally conglomeratic beds and limestones occur. Volcanic rocks in the Northern Belt, usually associated with cherts, are of various ages (Craig, 1983).

The greywackes of the Northern Belt are divided according to modal mineralogical composition into a number of formations that are petrographically distinct from each other. This distinction enables a lithostratigraphic correlation to be erected. North of the Leadhills Line the mineralogical composition of the greywackes is dominated by continental clastic material, and south of the Leadhills Line clasts of basic material dominate (Kelling, 1961, 1962; Floyd, 1982; Stone *et al.*, 1987; and Morris, 1987). The intervening shales are correlated according to their graptolite faunas.

Central Belt.

The Central Belt is defined, in the north, by the Silurian-Ordovician boundary, and in the south by the occurrence of Wenlock rocks. Both boundaries are faults: the Kingledores Fault in the north and the Riccarton line in the south.

The northern section of the Central Belt comprises greywacke sequences, and in the southern part of the belt, south of the Moffat Shales, arenites dominate. The greywacke and the arenite-dominated sequences are Silurian in age, and the Moffat Shales, which occur as thin elongate inliers of mudstones, grey cherts, tuffs, and black pyritiferous shales, are Ordovician in age.

Southern Belt.

The Southern Belt was originally defined on the basis that it only contains Wenlock rocks: the Riccarton Beds and the Raeberry Castle Beds. Subsequently it was shown that the Raeberry Castle Beds are Llandovery in age (Clarkson *et al.*, 1975).

The Raeberry Castle Beds comprise fine grained sequences divided by lenticular conglomerates. The Riccarton Beds are more uniform in grain size and bedding than the Raeberry Castle Beds, with only occasional thick greywackes (Craig, 1983).

7.2.2 Structure.

The structural detail of the Southern Uplands has been extensively studied (e.g., Leggett *et al.*, 1979a; Knipe and Needham, 1985; Needham and Knipe, 1986). In the accretion model of the Southern Uplands Needham and Knipe (1986) tentatively suggest that the observed deformation features could be subdivided into the following categories: downslope gravity-driven deformation, accretion-related deformation, collision-related deformation and post-collision readjustments.

Downslope gravity-driven deformation results in both extension and deformation structures, depending on the position of the sediment in the slump sheet.

Deformation that was related to accretion produced a series of strike-parallel fault-bounded tracts (fig. 7.1). The faults that bound each individual tract are steep, back-rotated thrust faults. These thrust faults are commonly associated with imbricate fans (Needham and Knipe, 1986). The tracts internally become younger to the northwest, but overall the tracts progressively young to the south. Folding within the individual tracts takes the form of upright, asymmetric, southeast-verging folds with northeast-southwest trending axes. The wavelengths of the folds are between 2m and 500m and display flattened parallel morphologies. The associated cleavage is slaty in the interbedded shales and spaced in the greywackes. This cleavage is axial planar in the Ordovician of the Northern Belt, but exhibits a clockwise transection in rocks further south.

The structures that are possibly related to collision deformation indicate a reversal in transport direction (Needham and Knipe, 1986). In the Silurian, later deformation is represented by *en echelon* northwest-directed shear zones, that cause localised refolding, and minor northwest-directed thrusts. These structural features truncate earlier structures. In the Ordovician, the later deformation is restricted to a series of faults, many of which form conjugate pairs. These faults have a shallow dip to the northwest and southeast. They cut the steep bedding and cleavage, and cause the cleavage locally to become crenulated.

Needham and Knipe (1986) consider that the dominant set of faults indicates overriding to the northwest, whereas the conjugate sets indicate horizontal shortening.

The youngest deformation is related to the following structures: shear zones along reactivated thrust faults, kink bands, sigmoidal tension gashes and shear bands in black shales. Needham and Knipe (1986) suggest that this last phase of deformation is related to sinistral strike-slip motion.

It is generally agreed that the main deformation of the Southern Uplands gave rise to ten tectonically bound tracts. However, there are two alternative interpretations as to the deformational mechanism that produced this structural outcrop pattern: (i) deformation was caused by subduction-related accretion of fore-arc material on to a continental margin (e.g., McKerrow *et al.* 1977; Leggett *et al.*, 1979a, 1979b; Leggett *et al.*, 1982; Knipe and Needham, 1985; Needham and Knipe, 1986 and Leggett, 1987); and (ii) the model of Stone *et al.* (1987) and Morris (1987) who consider that the main deformation is the result of an imbricate thrust belt initiated in a back-arc position .

Accretion Model.

The original simple accretionary model of McKerrow *et al.* (1977), Leggett *et al.* (1979a, 1979b) and Leggett *et al.* (1982) has been substantially modified firstly to take into account the presence of basal rocks (the Moffat Shales and associated igneous

rocks), which should have been subducted (Leggett, 1987), within the imbricate belt, and secondly to take into account the mode of closure of Iapetus.

The presence of basal rocks within the accretionary wedge is explained by Leggett (1987) by the incorporation of the basal rocks into the wedge by complex underthrusting and tectonic shuffling of sediments at the boundary between the accretionary prism and the subducted oceanic crust.

The closure of Iapetus was not simple orthogonal collision as originally envisaged by McKerrow *et al.* (1977); this is indicated by the post-collision deformation features described by Needham and Knipe (1986). Needham and Knipe (*op. cit.*) interpret the post-collision deformation features in the Southern Uplands as representing a large scale pop-up structure between a forethrust, the Iapetus suture, and a backthrust which emplaced the Southern Uplands northwestward over the Midland Valley continental basement. Closure also involved an appreciable amount of sinistral strike-slip movement which took place parallel to the ancient continental margin, with the major movement taking place along strike-parallel faults such as the Kingledores fault that separates the Northern and Central Belts (Leggett, 1987).

Back-arc Model.

Although Stone *et al.* (1987) and Morris (1987) do not agree with the accretionary prism model for the evolution of the Southern Uplands, they do not dispute the general structural interpretation of the Southern Uplands which comprises at least ten tectonostratigraphically bound units that internally young to the northwest, even though the sequence as a whole becomes progressively younger to the south. Stone *et al.* (1987) and Morris (1987) state that the observed structural pattern can be equally well explained by using a thin-skinned thrusting model. The reason for invoking a thin-skinned tectonic model for the evolution of the Southern Uplands is that new data suggest that the greywackes in the Northern Belt were deposited in a back-arc environment rather than in a fore-arc/subduction environment. The data that Stone *et al.* (1987) and Morris (1987) use involves palaeocurrent directions that indicate different provenances of greywackes of

very contrasting composition: the northerly derived greywackes, north of the Leadhills Line, consist of dominantly acidic (continental material), and the southerly derived greywackes, south of the Leadhills Line, comprise dominantly andesitic detritus (arc material). The greywackes of differing composition and provenance are interpreted as having formed in a back-arc basin. Stone *et al* (1987) and Morris (1987) then use a thin-skinned tectonic model to produce the observed structural pattern in the Southern Uplands, because it is implicit in their back-arc interpretation of the Southern Uplands that the Southern Uplands could not have formed by accretion, and hence a new deformation model (thin-skinned tectonics) has to be invoked. Stone *et al.* (1987) and Morris (1987) also cite another line of evidence to refute the accretionary prism model; namely, the presence of a suite of lamprophyre dykes which were derived from deep within the mantle (Rock, 1984 and Rock *et al.*, 1986). This type of magmatism that has no modern analogues in accretionary prisms (Rock, 1987).

Closure of Iapetus during the Llandovery, in the back-arc model according to Stone *et al.*, (1987), caused cessation of subduction and transfer of the compressional regime into the back-arc basin. This resulted in the initiation of a southeastward propagating thrust stack that overrode the eroded remains of the volcanic arc. This thrust stack provided the detritus for a foreland basin which now forms the late Llandovery and later sequences. Mid- to end-Silurian sinistral strike-slip movements produced a transpressional regime that reactivated old structures, allowing the intrusion of dykes and granites. However, according to Morris (1987) closure did not proceed in the above manner and climactic deformation is expressed as a transpressive imbricate thrust stack that is principally end-Silurian in age, pre-dating the mid-Wenlock sediments. The driving force behind the end-Silurian deformation in this model was the interaction between Laurasia and Cadomia.

It is not within the scope of this thesis to discuss the merits of the above two models, and the differences between them. However, it is important to note, when considering the influence that structure has had upon mineralisation, that: (i) there are major structural divides that coincide with the Leadhills Line and the Kingledores Fault,

which could be deep seated; (ii) The strike-parallel faults have an appreciable shear component to them; and (iii) the above two points are common to all the proposed models.

7.2.3 Metamorphism.

The rocks of the Southern Uplands have undergone very low grade metamorphism. Prehnite occurs in both lavas and greywackes across most of the Northern and Central Belts. Prehnite is found with pumpellyite in all of the lavas, but in the greywackes this association tends to be restricted to rocks that are rich in basic clasts. Accompanying the formation of the above two minerals, the feldspars have been albitised, and the new mineral assemblages comprise albite, quartz, prehnite, pumpellyite, chlorite, sericite (phenicia), sphene, calcite and haematite. This paragenesis indicates pressure-temperature conditions of approximately 300°C and 2.5 Kb (Oliver and Leggett, 1980).

7.3 Magmatism in the Southern Uplands.

Introduction.

The granites (*sensu lato*) in Scotland have been divided into the "Older" forceful granites, that were intruded during metamorphism and deformation, and the "Newer" permitted granites, which were intruded after metamorphism and deformation. The "Newer" granite suite are subdivided according to whether or not they contain inherited zircons. Generally only the "Newer" granites to the north of the Highland Boundary Fault contain inherited zircons.

In the Southern Uplands there are several important representatives of the "Newer" post-orogenic granite suite that do not contain inherited zircons. These are: the Cairnsmore of Cairnsphairn, the Loch Doon, the Cairnsmore of Fleet and the Criffel-Dalbeattie granitoids. Accompanying these large plutons are a number of minor granitoid intrusions. Also throughout the Southern Uplands are numerous felsite and

lamprophyre dykes (the former being far more abundant).

7.3.1 Major intrusive complexes.

The Loch Doon granite consists of a genetically related magma suite that ranges in composition from hypersthene diorite at the margins through quartz monzonite to granodiorite at the centre. The contacts between the various rock types are generally gradational (Brown *et al.*, 1979a). The Loch Doon Pluton is also notable for its high xenolith content. Two types of xenolith have been recognised; hornfelsed greywackes and those of igneous derivation. The geochemistry of the Loch Doon pluton shows normal calc-alkaline trends. Brown *et al. (op. cit.)* interpret this as indicating that the Loch Doon pluton formed by a process of fractionation, not multiple intrusion as originally proposed by Gardiner and Reynolds (1937) and later developed by Deer (1935) for the Cairnsmore of Carsphairn pluton.

The Cairnsmore of Fleet pluton consists of a fine grained granite core surrounded by coarse grained granite (Parslow, 1968). Parslow (1971) concluded that the Fleet pluton was formed mainly by multiple intrusion, but magmatic differentiation also played a role in forming the observed zonation.

The Criffel-Dalbeattie pluton comprises an outer granodiorite that, for the most part, surrounds an asymmetrically placed central core. The boundary between the two rock types was shown by Stephens and Halliday (1980), on geochemical grounds, to be abrupt and thus the intrusion to be composite.

Halliday *et al.* (1980) in a Rb-Sr and oxygen isotopic study dated the Doon, Criffel and Fleet intrusions at 408 ± 2 Ma, 397 ± 2 Ma and 392 ± 2 Ma respectively. Halliday *et al.* (1980) concluded the Loch Doon magmas were mainly derived from successive melting of a largely basic or ultrabasic source with only a minor contribution from partial melting of sediments. A similar model was proposed for the source of the Criffel and Fleet magmas, with melting probably originating at greater depths than the Lower Palaeozoic.

7.3.2 Minor Intrusions.

The minor intrusive rocks range in composition from granite to diorite. The larger intrusions at Portencorkie, Priestlaw and Cockburnlaw are compositionally zoned. Portencorkie has an inner and younger adamellite body and an outer diorite zone; Priestlaw is mainly composed of a hornblende-biotite-granodiorite with hybridisation at the margins giving the rock a dioritic composition; and Cockburnlaw has an hornblende-adamellite core which passes in to granite and micro-granite, with the outer zone being a hybrid diorite with xenoliths of basic and sedimentary rocks (Cooper *et al.*, 1982).

A significant number of these minor intrusions are hydrothermally altered and have associated pyrite and, locally, copper mineralisation. Alteration and mineralisation were recorded at the following intrusions: Mains of Dhuloch, Mochrum, Priesthope, Lamberton Moor, Broad Law, Glenluce, Priestlaw, Cockburn Law and Mull of Galloway. The last four of these contain minor copper mineralisation (Cooper *et al.*, 1982).

7.3.3 Dyke Swarms.

Within the Southern Uplands are several hundred dominantly NE-trending dykes which intrude the rocks of all three belts in the Southern Uplands. The dykes range in composition from basic potassium-rich biotite lamprophyres, hornblende lamprophyres and appinites to dykes that are rhyolitic in composition (63-71% silica). The lamprophyres are restricted in distribution to a narrow zone 10km wide, which stretches across the Southern Uplands and runs past the northern end of the Fleet pluton to an area surrounding the Loch Doon pluton. Outside these two areas lamprophyres are rare. Emplacement of the lamprophyres took place between Wenlock and early Devonian times. The earliest phase of dyke intrusion post-dates the main deformation but pre-dates

thrusting (Barnes *et al.*, 1986, and Rock *et al.*, 1986).

Barnes *et al.* (1986) and Rock *et al.* (1986) conclude on geochemical and field evidence that the presence of lamprophyres within the Southern Uplands is incompatible with the accretion model. Their reasons are as follows: (i) the geochemical data from the lamprophyres are not consistent with subduction; (ii) lamprophyres are generated from deep within the mantle and yet they are found within 25km of the supposed Iapetus suture, whereas in modern analogues they are found at large (300km) distances away from the suture; (iii) the dykes represent intrusion into an extensional regime but to be related to subduction they would have to be intruded into a compressional regime; and (iv) the lamprophyres of the Southern Uplands and the Lake District are geochemically of the same suite yet they supposedly lie on opposite side of the suture.

In conclusion Barnes *et al.* (1986) and Rock *et al.* (1986) state that at least part of the greywacke terrain of the Southern Uplands cannot be related to subduction and that the lamprophyres are more likely to be related to a transcurrent regime, as are many other lamprophyre swarms.

7.4 Mineralisation in the Southern Uplands.

Introduction.

Within the Southern Uplands there are several styles of mineralisation: lead-zinc mineralisation at Leadhills-Wanlockhead and Newton Stewart; arsenic-antimony mineralisation at Glendinning and Hare Hill (the Knipe); porphyry copper style mineralisation at Black Stockarton Moor and Carngarroch Bay; iron-cobalt-nickel mineralisation at Talnotry; and gold mineralisation at the Foreburn Igneous Complex (*in situ*), the southern margin of the Loch Doon granitoid (*in situ*), the Leadhills-Wanlockhead district (placer gold) and minor localities (placer and *in situ*) throughout the Southern Uplands.

7.4.1 Lead-zinc Vein Mineralisation.

Lead-zinc mineralisation in the Southern Uplands occurs in the Leadhills-Wanlockhead area (fig. 7.2), and in the area surrounding Newton Stewart. The mineralisation in both areas typically occurs in banded fissure-filling veins. At Leadhills, the veins are located within the Leadhills Imbricate Zone and vary in width from 5cm to 5m and comprise brecciated greywacke cemented by dolomite, calcite and quartz. The veins contain vertical stringers of galena and sphalerite. Although galena (which is often argentian) and sphalerite are the main ore minerals, 57 mineral species have been identified in the mining area; most of these minerals are secondary in origin. However the non-secondary minerals include rare niccolite, rammelsbergite and cobaltite (Temple, 1956; MacKay, 1959; Dunham *et al.*, 1979). Despite the widespread occurrence of placer gold in the Leadhills district, gold has never been found associated with the lead-zinc mineralisation in the Leadhills-Wanlockhead mining district.

K-Ar dating of the mineralisation at Leadhills-Wanlockhead by Ineson and Mitchell (1975) gave ages ranging from 343 ± 8 to 297 ± 4 Ma. This age range indicates a mid-Carboniferous mineralising event.

7.4.3 Arsenic-antimony Mineralisation.

Introduction.

Arsenic-antimony mineralisation occurs at a number of localities in the Southern Uplands. The major occurrences are the stratabound and vein mineralisation at Glendinning and the vein mineralisation at the Knipe (Hare Hill) (fig. 7.3)

Glendinning.

Gallagher *et al.* (1983) have described in detail the arsenic-antimony mineralisation at Glendinning and identified a stratabound pyrite-arsenopyrite assemblage that is overprinted by a later vein quartz-dolomite-sulphide-antimonide assemblage.

The mineralisation, which comprises mainly stibnite and quartz, is contained within a steeply dipping N-S quartz vein. The ore contains minor amounts of gold (0.5ppm) and silver (2ppm) (Muir, 1972, and Duller, 1984).

7.4.3 Porphyry copper-Style Mineralisation.

Black Stockarton Moor.

At Black Stockarton Moor, disseminated and veinlet iron and copper sulphide mineralisation occurs. The mineralisation is located within a Caledonian subvolcanic complex intruded into Lower Palaeozoic greywackes (fig. 7.4) (Leake and Brown, 1979; Brown *et al.*, 1979b).

The subvolcanic complex comprises the following features: (i) intersecting porphyritic microgranodiorite dyke swarms of at least three different stages; (ii) granodiorite sheet intrusions; (iii) small granodiorite stocks; (iv) breccia pipes; (v) vent agglomerates of basic igneous rocks; and (vi) a small number of basic dykes. The early features (the first dyke phase, granodiorite sheet intrusions, granodiorite stocks, breccia pipes and vent agglomerates) pre-date the Criffel-Dalbeattie granodiorite, and the later stages of dyke-emplacement post-date the granodiorite complex.

The mineralisation at Black Stockarton Moor was divided into four zones on the basis of the abundance and nature of the opaque minerals by Brown *et al.* (1979b). These zones are hematite plus minor pyrite, pyrite plus hematite with minor copper minerals, pyrite plus minor copper mineralisation, and minor pyrite plus several copper minerals. Accompanying this mineralisation are three widespread zones of hydrothermal alteration. These consist of: (i) an outer propylitic zone with jasperoid, epidote, chlorite, actinolite and calcite in the sedimentary rocks, and chlorite and calcite in the igneous rocks; (ii) an inner propylitic zone with similar characteristics to the outer zone but characterised by the additional presence of dolomite and sericite in the sedimentary rocks, and the appearance of sericite and disappearance of calcite in the igneous rocks; and (iii) a sericitic zone dominated by the presence of sericite together with dolomite and calcite. Very small

amounts of gold (0.06ppm) associated with antimony, and to a lesser extent arsenic, have been recorded at Black Stockarton Moor (Brown *et al.*, 1979b).

Cairngarroch Bay.

Allen *et al.* (1981b) identified patchy but pervasive Cu-Fe-As-Mo mineralisation associated with two intrusion complexes (the Bay Complex and the Glen Complex) at Cairngarroch Bay (fig. 7.5). The mineralisation is accompanied by irregular enrichment of potassium, barium and strontium.

The two intrusion complexes comprise a number of minor intrusions, ranging in composition from granodiorite to diorite. Sulphide mineralisation occurs as disseminations within the intrusives, along fracture surfaces and in quartz and calcite veinlets. Mineralisation is associated with brecciation and sericite/calcite alteration of the intrusives. The primary sulphide assemblage consists of mainly pyrite with minor amounts of chalcopyrite and pyrrhotine with rare secondary malachite. Duller (1984) has reported small quantities of gold (0.5ppm) and silver (2ppm) at Cairngarroch Bay.

Allen *et al.* (1981b) consider that the presence of potassic alteration and an inner zone of Cu-Mo mineralisation at Cairngarroch Bay conform to the Lowell and Guilbert (1970) model of porphyry copper mineralisation. However, with the alteration zonation being incomplete and not pervasive, and the very low copper and molybdenum values, Allen *et al.* (1981b) interpret the mineralisation at Cairngarroch as possibly representing a "failed porphyry system".

7.4.4 Iron-Cobalt-Nickel Mineralisation.

Iron-cobalt-nickel mineralisation is located at Talnotry mine 8.5 km north east of Newton Stewart in Kirkcudbrightshire (fig. 7.6). The geology of the mine, and the surrounding area is described in detail by Wilson and Flett (1921), Jones (1924),

Gregory and Leitch (1927), Gardiner and Reynolds (1937) and Stanley *et al.* (1987)

The mineralisation occurs in an altered basic igneous sheet at the contact with the surrounding greywackes. This complex is within the metamorphic aureole of the Cairnsmore of Fleet pluton, and the Talnotry Thrust Zone. The ore mineral assemblage comprises chalcopyrite, nickel-bearing pyrrhotine, niccolite, arsenopyrite and smaltite.

Between 1885 and 1900, one hundred tons of ore were mined, but never removed from the mine. Assays of the ore material from the mine dump by Wilson (1920) show both gold (1.5ppm) and silver (250ppm) to be present. A recent study by Stanley *et al.* (1987) has shown that native gold is present at Talnotry. Very minor amounts of gold are associated with chalcopyrite, pyrrhotine, pentlandite and various nickle-sulpharsenides; also small quantities (3000 to 9000ppm) of platinum group elements were associated with cobaltian gersdorffite

Electromagnetic geophysical surveys undertaken by the BGS (Parker, 1977) in the area surrounding Talnotry show that the orebody is of limited extent.

There are two views as to the origin of the deposit: (i) that the deposit was formed by magmatic segregation (Wilson and Flett, 1921; Stanley *et al.*, 1987); or (ii) the deposit was formed by contact metasomatic/hydrothermal processes (Gregory, 1928). Stanley *et al.* (1987) concluded that the deposit is magmatic in origin on the basis that macroscopic and microscopic ore textures in the pyrrhotine-rich samples are strongly indicative of formation from an immiscible sulphide melt

7.4.5 Gold Mineralisation.

The major locality of placer gold mineralisation in the Southern Uplands is in the Leadhills-Wanlockhead district. However minor placer gold mineralisation occurs throughout the Southern Uplands (Dawson *et al.*, 1977; Dawson *et al.*, 1979). The detailed aspects of this mineralisation are the subjects of Chapters 8 and 9.

Vein gold mineralisation has been recorded associated with the Fore Burn igneous complex (Allen *et al.*, 1982), and at the southern margin of the Loch Doon granitoid complex (Dawson *et al.*, 1977; Leake *et al.*, 1981). Gold exploration in the Southern Uplands by BP Minerals International Ltd., since 1983, has located gold mineralisation associated with the Cairnsmore of Cairnsphairn intrusive complex, and the small intrusives at Hare Hill and Broad Law (Sharp, 1986).

The Fore Burn Igneous Complex.

The Fore Burn igneous complex lies in a graben-like structure between two northeast-trending faults: the Southern Uplands Fault to the south, and an unnamed fault to the north. The unnamed fault to the north separates the early Devonian rocks of the graben from the mainly conglomeratic Ordovician rocks of the Big Hill of the Baing (fig. 7.7). The complex itself comprises mainly intrusive rocks of intermediate composition (quartz-microdiorite, tonalite, feldspar-porphyry, porphyritic-hypersthene-microdiorite and microtonalite) intruded into andesites, basaltic andesites and sedimentary rocks of Ordovician age. Both the complex and the country rocks are tourmalinised (Eyles *et al.*, 1929, 1949; Allen *et al.*, 1982).

Allen *et al.* (1982) recognised three types of mineralisation and alteration:

- (i) pervasive replacement of feldspars and matrix by sericite or muscovite, and muscovite associated with some chlorite and various amounts of disseminated sulphide.
- (ii) Tourmalinisation; the tourmaline generally forms radiating aggregates, but occasionally in some rocks it is disseminated. The radiating aggregates of tourmaline commonly contain pyrite and minor amounts of chalcopyrite with rare galena and sphalerite, the latter two minerals occurring as blebs in pyrite. Other sulphides that have been recorded associated with tourmalinisation are arsenopyrite and tennantite-tetrahedrite. Apatite is also present and locally abundant.
- (iii) The last type of mineralisation occurs as veins and veinlets of quartz and carbonate, which

in places form a cross-cutting stockwork. The veins and veinlets rarely exceed 15 cm in thickness and within the veins tourmaline and sulphides are common. The main gangue minerals are quartz, tourmaline, chlorite, sericite and carbonate. The main sulphides are chalcopyrite, pyrite and arsenopyrite, with rare cobaltite. Small amounts of gold and tennantite are found as inclusions in chalcopyrite. Post-dating these veins and veinlets are barren veins and veinlets of carbonate and sericite.

Allen *et al.* (1982) conclude that the mineralisation at Fore Burn fits a porphyry copper model better than any other, with the mineralisation being similar in style to that at Mount Nausen described by Sawyer and Dickinson (1976). At Mount Nausen, quartz and tourmaline in breccia pipes are surrounded by zones of mineralised rock. The main orebody is Cu-Mo-Au, and veins peripheral to it contain gold and silver with arsenopyrite, stibnite, galena and sphalerite.

The Loch Doon Granitoid Complex.

Leake *et al.* (1981) described three types of mineralisation from outcrop material and from seven boreholes within the contact zone (which comprises metasomatised and hornfelsed greywackes) of the Loch Doon granitoid: disseminated arsenic-gold mineralisation, vein arsenic-gold mineralisation and base metal mineralisation. The general geology of the the Loch Doon gold mineralisation is illustrated in figure 7.8. Mineralisation is located at the margin of the Loch Doon complex within the rectangle marked on figure 7.8.

(i) The disseminated arsenic-gold mineralisation, identified in two of the seven boreholes by Leake *et al.* (1981), shows a spatial relationship to a swarm of monzonitic intrusions. Sulphide mineralisation mainly occurs as pyrrhotine, arsenopyrite and pyrite disseminated within the margins of the intrusions and as arsenopyrite disseminations in the surrounding hornfels. Arsenic levels in the mineralised rocks attain levels of 3000 ppm, these levels are generally higher in the hornfelsed greywackes than in the igneous rocks. Gold values associated with this mineralisation reach 0.14 ppm. However, no free gold or gold minerals and no significant enrichment of base metals were observed.

(ii) Vein arsenic-gold mineralisation was identified by Leake *et al.* (1981) in six of the seven boreholes and a number of surface outcrops. This mineralisation occurs as quartz veins up to 30 cm thick surrounded by a zone, 80 cm thick, of veined and mineralised rock containing arsenopyrite and rare native gold. Arsenopyrite is located mainly at the margins of the quartz veins, but also occurs as veins and stringers within the main body of the quartz veins. The native gold is mainly found in the vein quartz, but gold does occasionally occur as small blebs in the arsenopyrite. Arsenic values reach as high as 3.5% and gold values reach 8.8 ppm. Other elements associated with this mineralisation are lead, bismuth and silver, which attain values of 1600 ppm, 125 ppm and 90 ppm respectively.

(iii) Base metal mineralisation was found by Leake *et al.* (1981) in four of the seven boreholes drilled. The mineralisation takes the form of sphalerite and galena with minor marcasite or pyrite and chalcopyrite in carbonate veinlets or in carbonate-rich breccia zones. The mineralisation has a random distribution and does not appear to be related to any particular rock type .

Leake *et al.* (1981) consider that the gold mineralisation at Loch Doon can be attributed to metasomatic and hydrothermal events within an evolving cycle of magmatism.

Hare Hill.

The discovery of gold values in grab samples from altered intrusive rocks in the area of Hare Hill close to the Knipe antimony mine (cf. fig.7.3) was made by BP Minerals International Ltd. in 1983. Diamond drilling has shown that minor gold mineralisation (gold was present at the 0.5ppm level or higher) is located within N-S structures in the Knipe granodiorite. The mineralisation is associated with intense alteration, which involves potassium enrichment, major sodium depletion, minor calcium/magnesium depletion, and arsenopyritisation of the wall rocks. The ore assemblage consists of major arsenopyrite and pyrite, minor stibnite, and rare chalcopyrite, sphalerite, and galena (Sharp, 1986).

Broad Law.

The Broad Law intrusive is a biotite microgranodiorite. Gold mineralisation, as at Hare Hill, is associated with intense wallrock alteration which consists of sericitisation, with minor chloritisation, carbonatisation, silicification and disseminated arsenopyrite and pyrite. Geochemically, the observed alteration assemblage involves potassium enrichment with major sodium depletion and minor calcium and magnesium depletion, introduction of silica, sulphur and arsenic. The ore mineralogy at Broad Law is less complicated than at Hare Hill and consists of disseminated arsenopyrite and pyrite, associated with vein quartz and carbonate containing pyrite and arsenopyrite (Sharp, 1986).

Cairnsmore of Cairnsphairn.

Two zones of gold mineralisation associated with the Cairnsmore of Cairnsphairn intrusive complex were discovered by BP Minerals International Ltd.. The first zone is hosted entirely within the intrusive complex and is intimately associated with a porphyritic felsite dyke, and the second zone is greywacke hosted at a faulted contact, within the Leadhills Imbricate Zone, between the intrusive and surrounding sediments. Mineralisation and alteration follows similar patterns to the mineralisation Broad Law and Hare Hill (Sharp, 1986).

7.5 Relationship Between Structure, Rock Type and Mineralisation.

Figure 7.9 shows the spatial relationship between: (i) the major intrusive complexes; (ii) the main structural elements, that is the thrust (strike-parallel) faults of Leggett *et al.* (1979b); and (iii) the localities of the various types of mineralisation discussed above.

The map illustrates that there is a spatial relationship between structure, magmatism and mineralisation. The different types of mineralisation, with the exception of the straiform As-Sb mineralisation at Glendinning, lie on or close to a major strike-parallel fault, and most of the localities of gold mineralisation are spatially associated with faulting, and an intrusive body or complex. An exception is the

Leadhills-Wanlockhead placer gold district which has no associated intrusive body. Gold mineralisation is also associated with the Moffat Shales at Glenhead Burn, Cairnsmore of Carsphairn and in the Leadhills-Wanlockhead district. Therefore, it would seem possible, based on empirical observations, to delineate three styles of gold mineralisation/association with the common feature that all the styles are spatially associated with a steep back-rotated thrust fault. These styles are as follows: (i) gold mineralisation which is granite-hosted (e.g., Cairnsmore of Cairnsphairn); (ii) gold found at the contact between an intrusive body and the Moffat Shales (e.g., Loch Doon); and (iii) placer gold that is associated with the Moffat Shales (e.g., Leadhills).

CHAPTER 8.

MORPHOLOGY, PETROGRAPHY AND COMPOSITION OF PLACER GOLD; METHODOLOGY.

8.1 Introduction.

This chapter describes the methodology adopted in this work for examining placer gold from the Southern Uplands, Scotland, and the Dolgellau Gold belt, North Wales. The placer gold was examined in three stages: firstly, shape and surface composition were studied using scanning electron microscopy (SEM); secondly, the petrography of sectioned and polished grains was examined; and thirdly, internal variations in composition were analysed using electron probe micro-analysis. The details of sample preparation and analysis techniques are given in Appendix 2. The approach used at each stage is described separately, and the efficacy of each technique and the reasons for adopting a technique are discussed. Particular attention is paid to the analysis of shape variation in the placer gold, as this is used as a basis for investigating the mobilisation of placer gold from lode deposit into the placer environment.

8.2 Morphology of Placer Gold.

Placer gold forms essentially as the result of weathering, that is the mechanical breakdown and the chemical dissolution of a pre-existing deposit. The gold is then redistributed and concentrated by mainly alluvial, eluvial, and chemical processes. During transport in the fluvial environment, originally crystalline gold is deformed, abraded, and comminuted on the stream bed by saltation and "sand blasting". The pronounced malleability of particulate placer gold leads to the acquisition of characteristic morphological features during transport.

Hallbauer (1981), Utter (1979), and Hallbauer and Utter (1977), in a thematic set of papers, examined the surface textures and morphology of Recent placer gold and gold grains from the Witwatersrand quartz-pebble conglomerates using scanning electron microscopy. In their 1977 paper, they examined the morphological characteristics of Recent placer gold which was collected at known distances from lode gold deposits, and in that work they attempted to correlate the morphological features of placer gold grains with their known distances of transport. They showed that placer gold

undergoes characteristic morphological and textural changes during abrasion, deformation, and comminution in the fluvial environment, and that these changes can indicate the proximity of placer gold to its original source. The features which Hallbauer and Utter (1977) related to transport distances are as follows:

(i) gold that has only travelled short distances (1-5km).

Such gold characteristically has an overall jagged morphology and irregular surface, and retains well-defined crystalline features; also the presence of a "glazed" surface is diagnostic of grains that have travelled short distances.

(ii) Gold that has travelled 5-15km.

Placer gold that has travelled relatively short distances shows an overall flaky and jagged appearance, deformation of the original crystalline texture, and a general elongate shape.

(iii) Placer gold which has travelled intermediate distances (up to 30km).

Placer gold in this category has random scratches on the surface, and bent and hammered edges that sometimes "trap" other mineral grains. Some grains show remnants of original crystalline texture. Towards the upper limit of intermediate transport distances grains are often rounded and "nugget" shaped.

(iv) Placer gold that has undergone prolonged transport (30-100km).

Prolonged transport of placer gold produces a dough-like texture, and numerous scratches on the surface with folding of previously flattened and deformed edges.

(v) Gold particles which have travelled long distances (>100km).

After long transport distances, placer gold grains are hammered into characteristically thin sheets (approximately 10 μ m thick).

Other studies of the shape-characteristics found in placer gold include those by Bogdanova (1975), Sagon *et al.* (1985), and Guisti (1986). Bogdanova (1975) recognised two distinct morphological types of placer gold from the Panagyuvishte

district, Bulgaria. These morphological types were: (i) nugget- and flake-shaped grains with "spongy" or "porous" surfaces, and grains having a compositional range of 960 to 1000 fine; and (ii) irregularly shaped placer gold grains with a fineness range between 525 to 700. Sagon *et al.* (1985) in an SEM study of the shape of detrital gold grains from Limousin, France, showed that some grains were directly inherited from source rocks (that is the placer gold showed no evidence of attrition), but the majority of grains showed evidence of attrition. Guisti (1986), in a detailed study of the shape of placer gold (using Corey shape analysis) from the Athabasca and Saskatchewan rivers, Alberta, Canada, concluded that for the Athabasca river samples, size fractions of +35, +60, and +120 mesh show an increase in the average Corey shape factor; that is, the gold particles become more flattened as they decrease in size, whereas for the Saskatchewan river samples no such relationship was observed. This difference between the samples from the two rivers was related to the degree of sedimentological maturity of the placer gold; the placer gold from the Athabasca river being more mature than the Saskatchewan river gold. These papers illustrate how shape analysis of placer gold can be used to obtain provenance information.

The work of Hallbauer and Utter (1977) was used as a guideline in identifying the morphological characteristics of the alluvial gold from the Southern Uplands. This placer gold was collected from first order streams of no greater than 5-10km in length. In parallel with this study, alluvial gold from North Wales was also morphologically characterised using the same criteria. The placer gold from North Wales was collected at known distances from two working gold mines (1km from Clogau Mine, and 10km from Gwynfynydd Mine). This alluvial gold, therefore, provides samples collected at known distances from source for comparison with the placer gold from the Southern Uplands.

In total, eighteen morphological characteristics were identified in the placer gold from North Wales and the Southern Uplands (table 8.1). These were divided into two groups; macro-morphological characteristics, that is the overall shape and texture of the grains; and micro-morphological characteristics, that is the surface detail observed at high magnification of the grains.

The morphology exhibited by the Southern Uplands gold was compared with the morphological data for recent placer gold examined by Hallbauer and Utter (1977) and the morphology of the placer gold from North Wales. The characteristics of each group were arranged on an empirical basis in an approximate order of increasing comminution, abrasion, and deformation. Each morphological characteristic was allocated an arbitrary number (1 to 8 for the macro-morphological characteristics, and 9 to 18 for the micro-morphological characteristics), the allocation of numbers to particular morphological features enables the data to be treated as *categorical statistical data*.

An individual gold grain may exhibit more than one morphological characteristic, and when this occurs all of the observed morphological characteristics are included in the data set. This is because the data are categorical and it is meaningless to assign a mean to categorical data (categorical data can have a mode and a median but not a mean). All of the morphological characteristics observed (as opposed to just recording the minimum or maximum morphological characteristic) on a single gold grain were recorded so that the total variation within a data set could be examined as opposed to biasing the data by only choosing a single morphological characteristic to record.

When the data were collected for a suite of placer gold samples, before statistical analysis was attempted, the data were assigned to suitable sample populations for analysis. A sample population is defined as consisting of the morphological data from a minimum of 30 placer gold grains, where a sample population may contain (i) a number of grains from one locality or (ii) a number of grains from a number of localities. For example, the placer gold from North Wales consisted of a number of gold grains collected from two localities (sample population (i) above) and the Southern Uplands gold comprised mainly individual gold grains collected from over 100 localities (sample population (ii) above).

In using the above approach it is important that the allocation of morphological

characteristic to placer gold grains is consistent and that the sample population chosen for analysis contains data from enough gold grains.

The eighteen morphological characteristics listed in table 8.1 are described below.

8.3 Description of the Morphological Characteristics of Placer Gold from the Southern Uplands and North Wales.

8.3.1 Macro-morphological Characteristics.

Morphological Characteristic 1 (Placer gold with a "glazed" surface).

Relatively undeformed and unabraded grains have a surface which appears "glazed" due to the smooth unworn nature of the surfaces of the grains. This feature is illustrated in plates 8.1a to 8.1d. The grains illustrated show a wide variation in shape, but they can all be identified by their smooth glazed surface.

Placer gold grains that exhibit this feature are envisaged as being proximal to their original source, because: (i) the placer gold grains illustrated in plates 8.1a to 8.1d were collected at 1km from its probable source, Clogau Mine, and gold grains collected from the River Mawddach, 10km from its source (Gwynfynydd Mine), do not exhibit this feature (plates 8.1e to 8.1h); (ii) gold removed from vein quartz (plates 8.2a to 8.2d) by hydrofluoric acid digestion, using the method of Neuerberg (1979) has very similar textural features to the placer gold from Clogau Mine (plates 8.1a to 8.1d); and (iii) abrasion in the fluvial environment easily removes the "glazed" surface of pristine gold grains, because of the low hardness and ductile nature of native gold.

Morphological Characteristic 2 (Placer gold which preserves much of the original crystalline morphology).

Gold grains which preserve most of their original crystalline morphology (plates 8.3a to 8.3d) also vary considerably in shape from obviously angular grains with an irregular surface (plates 8.3a and 8.3b) to angular grains with smooth, unworn surfaces (plates 8.3c and 8.3d). However, they do exhibit certain characteristic features;

a general absence of scratches on the surface, and very little abrasion and plastic deformation at their edges and vertices.

The wide variation in shape of grains in this category is probably a reflection of original morphology. For example, if the gold grains grew in vugs and veins in quartz they will exhibit typomorphic crystallographic features (cubes, tetrahedra etc., cf. plate 8.1a), whereas gold which forms emulsoid droplets in pyrite, will, when released from pyrite, exhibit a globular shape (cf. plate 8.1b).

Morphological Characteristic 3 (Deformed crystalline gold).

Placer gold that exhibits a deformed crystalline texture is illustrated in plates 8.4a to 8.4d. Gold grains which exhibit this type of morphology again show a wide range in overall shape and a variety of textures. Plate 8.4a illustrates a grain which preserves a large proportion of its original morphology; its surface is smooth and unworn, and its surface in places is still glazed, but it has been slightly bent and folded. Plate 8.4b shows a grain with similar features, but the smooth, unworn surfaces and crystal faces are confined to areas which have been protected by surrounding protruberances. Plates 8.4c and 8.4d exhibit more extreme deformation, the surface is generally worn, protruberances have been plastically deformed, and smooth unworn surfaces are only just preserved.

Morphological Characteristic 4 (Irregularly shaped grains).

Irregularly shaped placer gold grains retain little of their original morphology. However, remnants of a crystalline texture are locally preserved (plates 8.5a and 8.5b). Plate 8.5a illustrates an irregular grain with a generally smooth but scratched original crystalline texture. Plate 8.5b shows an irregularly shaped grain, which although abraded on all surfaces, retains some of its original shape (note the arrowed tetrahedron). However, the smooth and unworn surface has been destroyed. More commonly observed are the features exhibited by the placer gold grains illustrated in plates 8.5c and 8.5d, where no original features are preserved and the surface is irregular (plate 8.5c), or smooth and worn (plate 8.5d).

Morphological Characteristic 5 (Abraded, subrounded grains that show evidence of folding, and "hammering" of edges and vertices).

Plates 8.6a to 8.6d illustrate placer gold grains which are abraded and subrounded. Grains that exhibit this feature are often folded, and this folding can trap other mineral grains, such as illite and kaolinite. Protruberances on these grains are usually bent and hammered, and the surface is scratched (plates 8.6c and 8.6d). The only remnants of original morphology that are locally preserved are minor irregularities in grain shape, and small areas (20 μ m x 20 μ m) where smooth, unworn surfaces are still retained (plate 8.6c).

Morphological Characteristic 6 (Placer gold with a general elongate shape).

Placer gold grains which have a general elongate/cylindrical shape (plates 8.7a to 8.7d) show a variation in texture from grains which preserve some of their original features (plates 8.7a and 8.7b), where smooth or unworn areas (approximately 40 μ m x 40 μ m) can be observed, to grains where the surface is smooth and worn (plates 8.7c and 8.7d) and no original features such as crystal faces and smooth, unworn areas can be observed.

Morphological Characteristic 7 (Rounded "nugget" shaped grains).

Placer gold grains which have undergone a relatively high degree of abrasion and deformation are generally rounded and "nugget" shaped, as illustrated in plates 8.8a to 8.8d. Original textures are rarely preserved and the surface is smooth and worn.

Morphological Characteristic 8 (Flattened flake shaped grains).

Flake-shaped placer gold grains are illustrated in plates 8.9a to 8.9d. Placer gold grains which exhibit this type of morphology are hammered into characteristically thin (10-30 μ m) sheets, the surface is nearly always smooth and worn, and the grains can show evidence of repeated folding.

8.3.2 Micro-morphological Features.

Micro-morphological features are classified according to the different types of surface texture observed at high magnification (>500x). Each of these features is described in turn.

Morphological Characteristic 9 (Grains with a smooth or unabraded surface at high magnification).

Placer gold grains which exhibit smooth or unworn surfaces at high magnification (plates 8.10a to 8.10d) have suffered little or no abrasion or deformation. Plate 8.10a illustrates a grain with the original morphology perfectly preserved; there are no surficial scratches, and irregularities on the surface are not deformed or abraded. Plate 8.10b shows a similar grain, but in this case there are a small number of scratches on the surface, and the protruberances on that surface show evidence of deformation and attrition. Plates 8.10c and 8.10d illustrate grains where original unworn irregularities are preserved on the surface of the grain; plate 8.10c shows cubic crystalline forms, and plate 8.10d an irregular smooth surface with no obvious typomorphic crystalline features. Placer gold grains which exhibit the above morphological feature are generally restricted to grains that fall into categories 1 to 3 of the macro-morphological characteristics; that is, placer gold grains which still retain a large proportion of their original characteristics.

Morphological Characteristic 10 (The inclusion of primary minerals and the presence of inclusion scars).

The inclusion of primary minerals and the presence of inclusion scars are illustrated in plates 8.11a to 8.11d. Plate 8.11a and 8.11b illustrate the inclusion of two small quartz grains and an euhedral twinned quartz grain. Plate 8.11c shows a scar left by a small cubic or prismatic mineral, and plate 8.11d shows a placer gold grain, from the River Mawddach, North Wales, in which a small vein of quartz is preserved.

The occurrence of these features are rare in the material examined; and when these features are observed it might be expected that the presence of primary inclusions

and inclusion scars would be associated with placer gold grains which preserve original features. This is not the case. It is, therefore, tentatively suggested that any attached mineral grains are removed before or soon after the placer gold was introduced into the placer environment, and that when this feature is observed, it may be the result of mechanical abrasion exposing inclusions in the core of the placer gold grains. Support for this is shown in plates 8.11a to 8.11d where the placer gold grains all show evidence of abrasion and deformation, and contain original inclusions and inclusion scars, whereas grains which retain their original morphology (plates 8.1a to 8.1d) have no original inclusions or inclusion scars.

The shape-types (macro-morphological features) associated with placer gold grains that exhibit this micro-morphological feature are placer gold which is irregularly shaped to placer gold that has a rounded "nugget" morphology (Characteristics 4 to 7). This micro-morphological characteristic is totally absent from placer gold grains which are flattened into flakes (Characteristic 8).

Morphological Characteristic 11 (Grains with an irregular surface at high magnification).

Placer gold grains with an irregular surface at high magnification (plates 8.12a to 8.12d) vary from angular, irregular surfaces which have suffered little abrasion (plate 8.12a) to irregular surfaces where the protruberances are rounded (plates 8.12b and 8.13d). Sometimes surface irregularities protect original features and crystal faces can be observed (plate 8.12c).

Placer gold which exhibits this micro-morphological feature is generally associated with macro-morphological features 1 to 5.

Morphological Characteristic 12 (Trapped mineral grains).

This micro-morphological feature is often associated with grains that are irregularly shaped, and grains which are subrounded and show evidence of folding (Characteristics 4 and 5); it is these grains that often trap other minerals such as kaolinite, illite, and rutile. These minerals are not primary in origin and have been introduced

whilst the gold grains have been in the placer environment. Plate 8.13a shows small kaolinite/illite flakes that have formed in pits and crevasses in an irregularly shaped grain, and plates 8.13b to 8.13d show the typical variation in this feature in the Southern Uplands placer gold.

Morphological Characteristic 13 (Flaky surface at high magnification).

The presence of a flaky surface texture at high magnification is illustrated in plates 8.14a to 8.14d. The surfaces of gold grains exhibiting this feature have numerous thin (approximately 1µm) ridges, which give the surface its flaky appearance. These ridges are probably formed by shearing and flattening of surface irregularities (such as those which characterise feature 12). Placer gold that exhibits this micro-morphological feature is generally restricted to grains which are rounded or flake shaped (Characteristics 7 and 8).

Morphological Characteristics 14 and 15 (Presence of a smooth, generally worn surface [14], and the presence of random scratches [15], at high magnification).

The feature of a smooth, worn surface at high magnification is illustrated in plates 8.15a and 8.15b. In each of the two plates no original features are preserved, and the surface has been polished smooth by abrasion. Plates 8.15c and 8.15d show grains with random scratches on the surface.

Grains exhibiting the above micro-morphological features occur in a variety of shape-types; from irregularly shaped, to flake-shaped grains (Characteristics 4 to 7). However, placer gold grains that exhibit a smooth worn surface and random scratches tend not to preserve their original shape.

Morphological Characteristic 16 (Formation of a "dough"-like texture at high magnification).

Grains which exhibit a "dough"-like texture are illustrated in plates 8.16a to 8.16d. The salient features of this characteristic are that the surface of the grain is intermediate between "irregular" and "smooth/worn"; and any protruberances on the grain are deformed and rounded giving the surface the appearance of kneaded bread.

This micro-morphological characteristic is associated with all shape-types except undeformed crystalline grains and flakes (Characteristics 1, 2, and 8), and is most commonly associated with subrounded grains.

Morphological Characteristic 17 (Development of a layered texture at high magnification).

Placer gold which develops a layered texture (cf. plate 8.1f from Hallbauer and Utter, 1977) is rare in the material examined and only one example was found. However, examination of plates 8.9a to 8.9d shows that some of the grains are beginning to develop a layered texture through repeated folding. This texture represents the final surficial morphological change of placer gold in the attrition cycle.

Morphological Characteristic 18 (Presence of a porous/spongy surface at high magnification).

The morphological characteristic of a porous/spongy surface at high magnification is dealt with last as it is difficult to envisage a mechanical process which would form the fine porous texture illustrated in plate 8.18a, and hence the ranking of this feature in terms of the degree of attrition and deformation cannot be determined.

This morphological characteristic shows a variation in its surficial textures; from grains (plates 8.18a and 8.18b) where the porous texture is coarse (holes 10 μ m in diameter), to grains (plates 8.18c to 8.18d) where the pores are fine (approximately 1 μ m in diameter).

This micro-morphological characteristic has a restricted shape association; it is generally associated with rounded "nugget"-shaped grains and flake-shaped grains.

8.4 Discussion of Morphological Characteristics.

8.4.1 Macro-morphological Features.

The macro-morphological features, that is, the shape characteristics, show a distinct sequence of changes from crystalline gold to highly abraded gold, which is

illustrated by the destruction of original features (crystal faces, and smooth, uneven surfaces) firstly to form irregularly shaped grains, followed by the formation of rounded grains, and finally to form flakes.

There are a number of caveats which must be taken into account when interpreting the above general sequence in terms of estimating transport distances of placer gold and the proximity of placer gold to its original deposit:

(i) the original shape of the grain will heavily influence the final shape. For example, pristine rounded grains (cf. plate 8.3c) will only form rounded abraded grains and flakes, and original flakes will only form flakes.

(ii) Pristine gold grains may or may not be derived from a hypogene source and could have a supergene origin, or may have grown *in situ* in the placer.

(iii) Size will heavily influence how rapidly an individual gold grain responds to deformation and attrition. Gold grains will behave sedimentologically in the same manner as the size fraction in the sediment load of the stream or river to which the gold grains are hydraulically equivalent (Tyrell, 1912, p.597; Mackie, 1923, p.139-140; Rubey, 1933; and Rittenhouse, 1943, p.1741). Tourtelot (1968) showed that 1000 μ m (1mm) gold grains will behave as pebbles in the main sediment load, and therefore their main mode of attrition will be by "sand blasting", whereas 200 μ m (0.2mm) gold grains are hydraulically equivalent to the coarse sand fraction and the main mode of attrition will be by saltation. Thus, at a given rate of attrition, the larger a gold grain is the more rapid its comminution will be.

(iv) Yeend (1975), in an experimental study of the abrasion rates of placer gold, showed that the initial degradation of placer gold is rapid and then equilibrium is attained, after which no further decrease in size is observed. Yeend (1975) also showed that the rate at which equilibrium is attained is dependent on stream/river velocity; a fourfold increase in velocity producing a tenfold increase in hourly abrasion rates. Therefore it would be

expected that morphological changes in placer gold should reflect these experimental abrasion rates; that is, the morphology of gold grains should change rapidly from undeformed grains to abraded grains, and when equilibrium is attained little further morphological change should take place.

(v) The morphological features described by Hallbauer and Utter (1977) are representative, according to their data, of placer gold that has travelled between 5 and 200km. However the morphological features described in the preceding section, which are very similar to those described by Hallbauer and Utter (1977) apply to placer gold subjected to fluvial transport distances of less than 20km (this distance is based on the lengths of the first order streams from which the Southern Uplands gold was collected, and the known distances from working gold mines where the Welsh placer gold was collected). This indicates that the morphological changes described by Hallbauer and Utter (1977) do not form over large transport distances (up to 200km) but happen rapidly over short transport distances (approximately 20km), and also that the conclusions made by Yeend (1975) on experimental abrasion rates of placer gold are applicable to rates of morphological change.

(vi) Guisti (1986), in a morphological study of placer gold from Alberta, Canada, recognised that gold in placers may be polycyclic in origin; that is, some of the gold grains may be derived from a pre-existing placer. Thus, some placer gold may have a long history in the placer environment and be derived from a pre-existing placer.

The above caveats show that it is unwise to try and estimate transport distances over the wide range (1-200 km) proposed by Hallbauer and Utter (1977), because the influence exerted by the different variables which control shape (e.g., stream velocity through time, size, and original shape) cannot be easily quantified. However, the experimental work of Yeend (1975), and general observations on the placer gold from North Wales, show that original crystalline textures are rapidly lost, probably within the first few kilometres of transport, and hence the preservation of these original features is a good indicator of proximity of placer gold to its original source. Therefore, in any one

sample population the proportion of placer gold grains exhibiting proximal characteristics will be indicative of how close that sample population is to its original source, and also examination of the distribution of morphological characteristics within that population can also yield information on the provenance of that placer gold.

8.4.2 Micro-morphological Features.

The relationship between micro-morphological features and macro-morphological features is shown in figure 8.1. In most cases an individual micro-morphological characteristic is associated with three or more macro-morphological characteristics. This shows that the surface textures of placer gold are not sensitive enough indicators of provenance to be used on their own, and must be used in conjunction with the macro-morphological characteristics. However, two micro-morphological characteristics, the presence of a smooth, unworn surface (characteristic 9) and the presence of a spongy/porous texture (characteristic 18) at high magnification, have restricted shape associations. Characteristic 9 is almost exclusively associated with grains which preserve original features and its presence is a useful diagnostic tool in identifying pristine gold grains. Characteristic 18 is restricted to rounded "nugget"-shaped and flake-shaped grains. It has no obvious mechanical origin, and could therefore have a chemical origin. Similar surficial textures to characteristic eighteen have been described by Hallbauer and Utter (1977), Guisti and Smith (1984), and Guisti (1986), and in these three articles it was concluded that this texture has a chemical origin.

8.5 Petrography.

A number of workers have shown that the colour and reflectance of native gold is related to composition (e.g., Eales, 1968; Squair, 1965; and Ramhdor, 1969). The reflectance of native gold increases with silver content, and the colour changes from deep yellow to white with increasing silver content. Variations in the colour and reflectance which can be detected by the naked eye represent changes in silver content of 5 to 7 wt.%

silver between two adjacent areas in a single grain (Desborough, 1970). Therefore variations in composition within grains can be determined qualitatively using high magnification reflected light microscopy. One variation that is frequently observed is a rim which is deeper yellow in colour than the core of the grain; this is common in all types of placer gold. This is a gold-enrichment rim and shows considerable variations in thickness, continuity, and homogeneity, with the rim being porous or filamentous. Within the core of the grain, zonation and irregular heterogeneities may be observed. Zonation and heterogeneities of this type have been described by Desborough *et al.* (1971) who considered them to be primary in origin.

Within the core of the grain there may be inclusions of primary minerals, and their identification may prove useful in characterising some gold deposits. However their usefulness is limited because of the low probability of intersecting any inclusions during polishing (Desborough *et al.*, 1971).

8.6 Composition of Native Gold.

Variation in the silver content of native gold has been known for centuries. Generally, variations in the composition of native gold have chiefly been evaluated by fire assay or by methods which require more material than electron probe micro-analysis. These methods show that the bulk fineness of placer gold increases downstream from the source (Boyle, 1979). However, assay methods yield no information on how composition varies on the micro-scale within grains and between grains, whereas micro-analysis techniques used in conjunction with high magnification microscopy provide a realm of investigation that allows analysis of areas as small as 10µm in diameter (Desborough, 1970).

A number of workers (e.g., Fisher, 1935; Petrovskaya and Fastalovich, 1955; Stumpfl and Clark (1965) Ramdohr, 1965; and Desborough *et al.*, 1970) have shown that placer gold often shows a rim to core variation in silver content, with gold grains having a gold-rich "rind" (gold-enrichment rim) that is usually greater than 980 fine.

However, Stumpfl and Clarke (1965) have shown that the gold-enrichment rim is not always present. They observed that it is absent from some gold grains in gold-platinum placers from southeast Borneo.

When present, the boundary between the gold-enrichment rim and the core material is sharp with compositional gradients of the order of 1 to 7 wt.% Ag/micron for grains with an interior silver content of between 10 and 46 weight percent silver (Desborough, 1970). The extent of the gold enrichment rim can be investigated in three ways: firstly, high magnification microscopy indicates the two dimensional extent of the rim; secondly, SEM investigations coupled with energy dispersive micro-analysis show variations in surface composition; and thirdly, electron probe micro-analysis yields an accurate composition of both the core and the rim. Differences between the core composition obtained by electron probe micro-analysis, and the surface composition obtained by SEM analysis, will indicate the three dimensional extent of the rim and the presence of a thin ($<1\mu\text{m}$) enrichment rim when no rim is visible microscopically.

In recent years, a number of studies using electron probe micro-analysis techniques, have been undertaken on placer gold (e.g., Stumpfl and Clark, 1965; Saager, 1969; Desborough, 1970; Desborough *et al.*, 1970; Desborough *et al.*, 1971; Czmanske *et al.*, 1973; Craig *et al.*, 1982; Guisti and Smith, 1984; Bowles *et al.*, 1984; Guisti, 1986).

Desborough *et al.* (1971) showed that placer gold from the north-eastern part of the Colorado mineral belt exhibits striking contrasts in silver and copper contents, and that these contrasts are related to different lode-sources. In a similar study of silver and copper distributions in six gold deposits in the Western United States, Desborough *et al.* (1971) concluded that:

Regardless of primary zoning within crystals or aggregates of crystals, gold grains from a single deposit may show a wide range in silver content or may exhibit remarkable compositional homogeneity. A major conclusion is that there may or may not be a wide range of silver content in the gold grains of a single deposit. The detection of such characteristics from assay data or bulk analysis is not possible. Microprobe analysis is one of the few methods available for determining these characteristics.

Czmanske *et al.* (1973) were able to estimate the time-temperature constraints of gold-formation in the original deposit by comparing concentration profiles of heterogeneous placer gold grains with concentration profiles which were experimentally determined. Czmanske *et al.* (1973), using this method, were also able to show that the formation of gold-enrichment rims is a low temperature (<100°C) phenomenon.

Craig *et al.* (1982), in a microprobe study of alluvial gold from the central and southern Appalachian mountains, U.S.A., concluded that individual gold-bearing districts have characteristic compositional signatures in terms of fineness and copper content, and that the measured core compositions of placer gold grains are reliable indicators of the placer gold's original composition.

Guisti and Smith (1984) concluded that placer gold from the Saskatchewan and Athabasca rivers, Alberta, Canada was derived from multiple sources. This conclusion was based on the variation in silver and copper contents of the cores of placer gold grains.

The above literature shows that core compositions of placer gold preserve the primary composition, and that variations in core composition, with respect to gold, silver, and copper, can be used to "fingerprint" placer gold and aid in provenancing placer gold. For example, Bowles *et al.* (1984), in an electron probe micro-analysis study of placer gold from Sumatra, related the composition of placer gold to two different styles of gold mineralisation. Low-silver placer gold was found in rivers which drain the Pre-Tertiary Sumatra Orogen. Here gold-quartz mineralisation which was related to contact metamorphism has a silver/gold ratio of 0.8:1. High-silver placer gold, on the other hand, was found in rivers which drain the younger (Tertiary) Sunda Orogen. Here the gold mineralisation is associated with abundant sulphides and tellurides, and the silver/gold ratio is between 17:1 and 400:1. Where placer gold was found in rivers which drain both styles of mineralisation, both high and low silver to gold ratios were observed.

The study of Czmanske *et al.* (1973) is of particular interest because if primary heterogeneities (i.e., differences in silver content of the placer gold grain) are present in the core of placer gold grains, time-temperature estimations can be made on the original mineralisation from which the placer gold was derived. This is achieved by analysing the observed variation in silver content across the heterogeneity, using electron probe micro-analysis to produce a quantitative line concentration profile. The rate of change in silver content along the measured profile records the annealing history of that grain, and by comparing measured diffusion profiles with experimentally determined diffusion rates for gold-silver alloys at different temperatures, an estimation of the temperature at which the heterogeneity formed can be made. Since some of the placer gold from the Southern Uplands has these heterogeneities, the techniques developed by Czmanske *et al.*, (1973) can be used to elucidate some of the conditions of ore-formation which gave rise to the Southern Uplands placer gold.

8.7 Concluding Remarks.

This chapter has described the methods used in the investigation of the characteristics of the Southern Uplands gold. For each individual grain, a number of data can be collected; firstly, SEM examination yields data on the shape-characteristics and the surface composition; secondly, high magnification microscopy provides information on the two-dimensional shape of the grain, the type (if any) of gold-enrichment rim, and the presence of primary inclusions within the core of the grain; and thirdly, electron probe micro-analysis of the core of the grain reveals intra- and inter- grain variations in composition. The intra-grain variations can be related to provenance, and internal heterogeneities can be used to estimate the original conditions of formation of the placer gold grains. The investigative approach described yields, for an individual placer gold grain, information on the changes which have happened to that grain in the placer environment and the conditions which originally formed that grain. When these data are combined with similar data for other grains in a sample population of placer gold, the processes which have formed that sample population can be elucidated. The data

obtained for the Southern Uplands and North Wales samples using the above methodology are described and discussed in the following chapter.

CHAPTER 9.

**MORPHOLOGICAL,
PETROLOGICAL AND
MINERALOGICAL DATA FOR
THE SOUTHERN UPLANDS
PLACER GOLD.**

9.1 Introduction.

During the late 1970's the Institute of Geological Sciences (now the British Geological Survey) conducted an extensive stream sediment sampling survey of two areas of the Southern Uplands in Scotland: the Loch Doon-Glenkens area southwest Scotland (Dawson *et al.*, 1977), and the Abington-Biggarr-Moffat area south central Scotland (Dawson *et al.*, 1979).

Figures 9.1 and 9.2 show the distribution of placer gold identified in the two areas; each point on the maps represents a locality where placer gold was observed in pan concentrates. Generally, where gold was observed in the pan, the pan only contained one grain of gold. The gold collected from these two surveys was examined using the techniques described in Chapter 8 to identify different populations of placer gold based on morphology and composition, and elucidate the type or types of mineralisation that originally formed the gold. The data discussed in this chapter are presented in Appendix 5.

9.2 Loch Doon-Glenkens Area.

9.2.1 General Geology and Distribution of Gold.

The general geology of the area and the distribution of placer gold are illustrated in figure 9.1. The sediments in the area comprise mainly Ordovician and Silurian greywackes and black shales, with the former being volumetrically the more important. These sediments have been intruded by the Loch Doon and Cairnsphairn granitoids. These two intrusions are broadly similar in that they both have a central acid phase surrounded by a variety of more basic rocks. The granitoids have thermally metamorphosed the sedimentary country rocks to hornfels.

The distribution of gold shows an approximate correlation with geology: 73% of all the gold grains are located within the metamorphic aureoles of the granites and a 2km halo surrounding the metamorphic aureoles. Within the metamorphic aureoles of the granites the placer gold is not evenly distributed. There are two distinct clusters of placer

gold associated with the Cairnsphairn and Fleet granitoids, and a more dispersed cluster surrounding the small granitoid stocks at Burnhead and Mid Hill. This area described above only occupies 27% of the total project area. Also 70% of all the placer gold grains are within 2km of a black shale horizon.

The above simple analysis shows that there are strong spatial associations between the geographical distribution of placer gold and the contact metamorphosed shales and greywackes.

9.2.2 Morphology of the Loch Doon-Glenkens Placer Gold.

The placer gold from the Loch Doon Glenkens area was prepared for scanning electron microscope examination according to the method described in Appendix 3. Each individual grain was characterised according to the morphological features observed.

The morphological data for all the gold grains examined in the Loch Doon area are illustrated in figures 9.3 and 9.4. Figure 9.3 shows the morphological distribution for the macro-morphological features of the Loch Doon gold. The distribution is bimodal with the larger population having a mode in macro-morphological feature 4 (i.e., irregularly shaped gold grains) and the subsidiary population having a mode centred on macro-morphological characteristic 7 (i.e., gold grains that are well rounded or "nugget" shaped). The micro-morphological characteristics of the Doon-Glenkens gold shows three distinct populations (fig. 9.4), centred on morphological characteristics 11 (irregular surface at high magnification), 14 (surface generally smooth and worn at high magnification) and 18 (presence of a porous surface at high magnification).

The geographical distribution of the various morphological characteristics was determined by dividing the morphological characteristics into five groups, each group corresponding to the range of morphological characteristics within an individual population. These groups are as follows: characteristics 1 to 4; 5 to 8; 9 to 13; 14 to 17; and 18 only. These groups were then plotted on a geological map of the Doon-Glenkens

area (figs. 9.5 and 9.6). Visually the two diagrams show that there are no clusters or associations of morphology with geographical locality and that the clusters of placer gold associated with the Cairnsmore of Cairnsphairn and Fleet granites contain placer gold that has both proximal and distal morphological features. However, if the geographical distribution of gold grains that show the least evidence of attrition are plotted then the morphological features show a geographical cluster around the granitoids (fig 9.7). These morphological types of placer gold are placer gold grains that have morphological characteristics 1, 2 and 3 (i.e., placer gold with a glazed surface (1), placer gold that preserves crystalline features (2) and placer gold with slightly deformed crystalline features (3)).

9.2.3 Scanning Electron Microscope Fineness Data for the Doon-Glenkens Placer Gold.

In addition to the morphological examination of the gold grains the surface of each gold grain was also semi-quantitatively analysed using a Link Systems energy dispersive X-ray analyser (cf. Appendix 2 for analysis techniques), which was attached to the scanning electron microscope.

Surface analysis of the grains was employed to examine any systematic differences in surface composition of the grains (the penetration of the electron beam on the scanning electron microscope operated at 20Kv is approximately 2 μ m for pure gold) and to examine the development of a gold enrichment rim, the extent of which is shown by differences in core and rim composition. Figure 9.8 is a histogram showing the distribution of surface fineness of the placer gold from the Loch Doon area. The histogram shows: (i) that as fineness increases there are an increasing number of placer gold grains which have that range of fineness; for example, only 9% grains have a fineness less than 825 but 64% grains have a fineness greater than 950; and (ii) that there are no distinct sub-populations of different finenesses. This indicates that the majority of gold grains have developed a gold-enrichment rim that masks the core composition.

As well as the geographical distribution of morphology the geographical distribution of surface fineness was also investigated (fig 9.9). The surface fineness of the placer gold was divided into two populations, one having finenesses greater than 950 and the other less than 950. The reason for choosing this dividing line is that, if the fineness is less than 950 it is reasonable to assume that the gold enrichment rim is only poorly developed. Conversely, if the fineness is greater than 950 then the enrichment rim is well developed. Thus this dividing line is a useful way of examining the geographical distribution of gold enrichment rims on the placer gold. Figure 9.9 shows that the lower (<950) fineness population shows two distinct clusters around the Cairnsmore of Cairnsphairn and Fleet Granitoids.

9.2.4. Petrography of The Doon-Glenkens Placer Gold

Reflected light microscopy was used to study the petrography of the placer gold grains from the Loch Doon area, to examine the internal homogeneity of individual grains (excluding variations that can be assigned to the gold enrichment rim), the type of gold enrichment rim, and the presence of any primary or secondary inclusions within the core of the placer gold grains.

The large majority of placer gold grains are homogeneous, that is, they exhibit no intragrain variations in colour or reflectivity other than colour and reflectance variations that can be assigned to the gold enrichment rim. However, a small number of grains show a striking variation in colour and reflectance. These variations are caused by differences in silver content within the grain, and appear as thin white to pale yellow veinlets (2-5 μ m wide) and patches (5-10 μ m in diameter) in deep yellow gold grains (plate 9.1). The variation in silver content across these heterogeneities was subsequently examined using electron probe micro-analysis, and the results are discussed in detail later in this chapter.

In all of the placer gold grains examined, extensive development of a gold enrichment rim was not observed (i.e., an enrichment rim that surrounds over 75% of the

placer gold grain, and is generally over 10 μ m thick). However, some degree of gold enrichment was observed in the majority of placer gold grains with the zones of gold enrichment being confined to very thin (1-2 μ m) incomplete rims and patches on the margins of the gold grains (plate 9.2). Where the silver-rich heterogeneities intersect gold enrichment rims the gold enrichment rim occurs on both the silver-rich and gold-rich portions of the grain.

The large majority of placer gold grains from the Loch Doon area have no inclusions within their cores. Where inclusions are observed they are generally very small (<5 μ m across) and difficult to identify. However, inclusions of native bismuth (plate 9.3) were identified by using energy dispersive analysis.

9.2.5. Composition of the Doon-Glenkens Placer Gold.

The summary statistics for the fineness of the Doon-Glenkens placer gold are presented in table 9.1. The fineness of the Loch Doon-Glenkens placer gold varies from 511 fine to 992 fine with a mean of 885 fine. The frequency distribution (fig. 9.10) shows that the fineness of the Loch Doon-Glenkens placer gold has a bimodal distribution, with the two populations having finenesses of 913 fine and 988 fine (mid-points of the intervals 900-925 fine and 975 to 1000 fine). The geographical distribution of these two populations shows no relationship to the underlying geology (fig. 9.11). However, there does appear to be a loose association of low (<800) fineness placer gold with the margins of the granite plutons. The heterogeneous gold grains are also associated with the cluster of low fineness gold grains near the northern margin of the Fleet granitoid. The silver-rich part of the heterogeneous gold grains corresponds to the composition of the placer gold grains which form the compositional clusters associated with the granitoids (i.e., <800 fine).

There is generally no correlation between morphology and fineness. However, a small number of gold grains comprise almost pure gold (980 fine to 1000 fine), and these gold grains have morphologies that are described by macro-morphological features

7 and 8 (flakes and nuggets) and micro-morphological feature 18 (porous surface at high magnification).

The composition profiles of the heterogeneous gold grains are illustrated in figures 9.12a to 9.12e. These grains show variations in silver content from 13 to 30 weight percent silver over distances of 7 to 35 microns within a single grain. Each of the profiles illustrated records the diffusion of silver and gold atoms across the original heterogeneity from the time that the heterogeneity was formed to the present day. The rate at which atoms will diffuse across the original discontinuity is dependent on time, temperature and composition; that is, the observed Au-Ag gradients are the result of annealing an original discontinuity. Experimental work by Czmannske *et al.* (1973) has shown that diffusion profiles in heterogeneous gold grains can be used to estimate time-temperature constraints of the process that formed the gold (the details of this method are outlined in Appendix 3).

Czmannske *et al.* (1973) stated that any data derived using their method is subject to the following constraints: (i) preserved diffusion profiles, such as those illustrated in Figures 9.12a to 9.12e, are not necessarily the result of diffusion and may be original compositional gradients; (ii) preserved diffusion profiles, regardless of origin, provide maximum time-temperature limits; and (iii) heterogeneous gold grains subjected to metamorphism should show no chemical heterogeneities.

The data obtained using the method of Czmannske *et al.* (1973) are presented graphically in figure 9.13. The two axes represent the time and temperature at which a heterogeneous gold grain was held to produce the measured Au-Ag profile. Each measured diffusion profile is represented on the graph by a curve that is defined by the time a heterogeneous gold grain would have to be held at a given temperature to produce the observed Au-Ag gradient.

The gold grains all exhibit high rate of change in silver content over a given distance and fall into a narrow band of curves on the time-temperature graph. Thus, if the

limits of 10,000 years to 1,000,000 years are taken as the limits of the time that the gold grains were held at an elevated temperature (i.e., during ore deposition) then the heterogeneities must have formed in a temperature range of 150 to 235°C. This range indicates that the formation of the heterogeneities is a relatively low temperature phenomenon. These low temperatures are also indicated by the presence of euhedral native bismuth inclusions within some of the gold grains, because gold and native bismuth only co-exist in equilibrium below 113°C (gold and bismuth react to form maldonite (Au_2Bi) above this temperature (Vaughan and Craig, 1978). Also the preservation of such heterogeneities indicates that the primary formation of the heterogeneous placer gold post-dates metamorphism.

9.3 Abington-Biggar-Moffat Area.

9.3.1 General Geology and Distribution of Gold.

The Abington-Biggar-Moffat area includes parts of the Northern and Central Belts of the Southern Uplands and is composed mainly of sediments of Ordovician and Silurian age comprising thick sequences of near-vertical greywackes, siltstones with rare belts of black shales, cherts and volcanic rocks (the Moffat Shale Group). The Moffat Shale Group is associated with the Leadhills Line. No major igneous intrusives of Caledonian age occur within the area (the general geology of the area, and the distribution of gold are illustrated in fig. 9.3).

Placer gold was discovered just outside the area in the Leadhills-Wanlockhead mining district at the beginning of the sixteenth century, where it was mined during the reign of James V. Within the area, placer gold was worked (at approximately the same time as the gold at Leadhills) in the Glengaber Burn, a north tributary of the Megget Water.

The British Geological Survey, in a stream sediment sampling survey of the area, recovered gold from 48 out of a total of 182 streams that were panned. 35% of the placer gold grains are associated with Ordovician rocks. However, of the 17 localities in

the Northern Belt that yielded placer gold, 12 of them are from streams that cut the Moffat Shales.

2.3.2 Morphology of the Abington-Biggarr-Moffat Placer Gold.

The total morphological data set for the placer gold examined in the Abington-Biggarr-Moffat area is illustrated in figures 9.14 and 9.15.

The histogram for the macro-morphological features (fig. 9.14) shows a similar distribution to the placer gold from the Loch Doon area (cf. fig. 9.3). That is, two populations of placer gold centred on morphological characteristics 4 and 7 (irregular and "nugget" shaped grains). However, placer gold from the Abington-Biggarr-Moffat area has a higher proportion of placer gold that is "nugget" shaped. The histogram for the micro-morphological features (fig. 9.15) is again similar to the distribution for the placer gold from the Loch Doon area (cf. fig. 9.4) with three morphological populations centered on micro-morphological features 11, 14 and 18; that is, placer gold with an irregular surface, a smooth worn surface and porous surface at high magnification. However, in the Abington-Biggarr-Moffat placer gold, the distribution of morphological characteristics is more tightly clustered around the three modes, and the ratio of the number of observations between the two areas is different. In the Loch Doon area the ratio between the number of grains that exhibit characteristics 4 and 7 is 2.5, whereas in the Abington Biggar Moffat area the ratio is 0.7.

The geographical distribution of morphology of the Abington-Biggarr-Moffat placer gold was examined using the same method as for the Loch Doon placer gold. Figures 9.16 and 9.17 illustrate this geographical distribution; in both diagrams there is no clustering of similar morphological characteristics or spatial association with geology.

2.3.3 SEM Fineness Data for the Abington-Biggarr-Moffat Area.

The distribution of the SEM fineness data for the Abington-Biggarr-Moffat area

(fig. 9.18) is different to the distribution for the Loch Doon area, in that all of the placer gold has a surface fineness greater than 950 fine, with 83% of the grains having a fineness greater than 980 fine. This indicates that most of the gold has developed at least a thin (2 μ m) gold enrichment rim.

9.3.4 Petrography of the Abington-Biggarr-Moffat Placer Gold.

In all of the placer gold examined from the Abington-Biggarr-Moffat area, no heterogeneous gold grains or inclusions of native bismuth were observed. Thus, it was not possible to estimate conditions of gold formation in the manner used for the Loch Doon placer gold.

In a significant number of gold grains no gold enrichment rims were observed. In these grains the surface colour of the gold was deep yellow, indicating that this gold is of high fineness.

9.3.5 Composition of the Abington-Biggarr-Moffat Placer Gold.

The fineness distribution of gold from the Abington-Biggarr-Moffat area has a fineness range of 854 to 1000 fine with a mean of 952 fine (the summary statistics are presented in table 9.2). The bar chart (fig. 9.19) shows that the distribution is bimodal, with fineness populations centred on 938 and 988 fine (mid-points of the intervals 925 to 950 and 975 to 1000). Of the two populations, 60% are in the lower fineness population (<950 fine) and 40% in the higher fineness population (>950 fine). The geographical distribution (fig. 9.20) of these two populations shows no clustering or correlation with the underlying geology.

9.4 Comparison of the Doon-Glenkens and the Abington-Biggarr-Moffat Placer Gold.

There are a number of differences and similarities in the properties of the placer gold from the two project areas as outline below:

(i) the geographical distribution of the Doon-Glenkens placer gold shows clustering around the Cairnsphairn and Fleet granitoids, and no clustering was observed in the Abington-Biggarr-Moffat placer gold.

(ii) The frequency distributions of the morphological characteristics of the placer gold from the two project areas are very similar. However, the ratio of morphological characteristics is different; the Doon-Glenkens gold contains a higher proportion of placer gold that exhibits proximal morphological characteristics than the Abington-Biggarr-Moffat placer gold (66% of the Doon-Glenkens placer gold has proximal features as opposed to 32% of the Abington-Biggarr-Moffat placer gold). Also the Doon-Glenkens placer gold shows geographical clustering of morphological features around the smaller granitoid intrusions, whereas the Abington-Biggarr-Moffat shows no such association with the underlying geology.

(iii) Petrographically, the main difference between the two project areas is the absence of heterogeneous placer gold in the Abington-Biggarr-Moffat area.

(iv) The surface and the core fineness of the Doon-Glenkens placer gold shows a wider range in fineness (surface: 759 fine to 1000 fine, core: 511 fine to 992 fine) than the Abington-Biggarr-Moffat placer gold (surface: 941 fine to 1000 fine, core: 854 fine to 1000 fine). The distribution of core fineness between the two project areas are broadly similar in that they are both bimodal with modes centred on 913 fine and 988 fine for the Doon-Glenkens area, and 938 fine and 988 fine for the Abington-Biggarr-Moffat area, but in the Doon-Glenkens area 16% of the grains analysed have a fineness of less than 850 fine, whereas in the Abington-Biggarr-Moffat area none of the placer gold analysed is less than 850 fine.

2.5 Origin of the Southern Uplands Placer Gold.

The morphology of the placer gold from the two project areas shows that the

placer gold comprises a proximal and a distal population (fig. 9.21), and the frequency distribution of the fineness of the placer gold consists of a high fineness (>975 fine) and a lower fineness (<975) population. These observations indicate that there are two types of placer gold with different sedimentological histories, and two compositional types of placer gold.

The relationship between composition and morphology was examined by comparing the frequency distributions of the morphological characteristics between the high fineness and low fineness placer gold. Figures 9.22 and 9.23 show that the two fineness populations have similar macro-morphological distributions, in that the macro-morphological characteristics of both fineness populations are bimodal and one of the modes is coincident (characteristic 7, i.e., "nugget" shaped grains) and the other mode is nearly coincident (characteristics 3 and 4, i.e., irregularly shaped grains and grains exhibiting a deformed crystalline texture). However, the high fineness population contains a higher proportion of "nugget"- and flake-shaped grains than the low fineness population (64% of the observed morphological characteristics are either characteristic 7 or 8 in the high fineness population as opposed to 26% in the low fineness population). Also, in the high fineness population the micro-morphological characteristic of a porous surface at high magnification comprises 29% of the observed morphological characteristic as opposed to only 6% in the low fineness population. Thus, although, the two types of gold have similar compositional signatures, detailed examination shows that "nugget"- and flake-shaped grains, and grains with a porous surface at high magnification, are associated with high fineness placer gold.

As the placer gold examined in this work was collected within 1 to 5 km of the headwaters of first or second order streams it is reasonable to assume that the placer gold has undergone similar distances of fluvial transport and hence similar degrees of comminution. Thus, it would be expected that the distribution of morphological characteristics would not be bimodal, but as the distribution of the morphological characteristics is bimodal then some of the placer gold has probably had a previous sedimentological history. This could be either in a pre-existing placer, but this is

considered to be unlikely as the gold was collected from first or second order streams, or that some of the placer gold has been involved in glaciation. However, it is not known how glaciation affects the morphology of placer gold as there are no data in the literature for comparison and none of the placer gold from the Southern Uplands was collected from glacial till for examination. Another interpretation of the data is that the "nugget"- and flake-shaped gold with its associated high fineness represents "supergene" gold; that is, gold that has been remobilised in groundwater solutions during the oxidation process of hypogene orebody. This hypothesis is supported by the following:

(i) the association of a placer gold with a porous surface at high magnification, a morphological feature which appears to have a chemical origin, with high fineness gold. Placer gold of high fineness is thought to be supergene in origin (e.g., Mackay, 1944; Pit'luko, 1976; Boyle, 1979; Evans, 1981; Wilson, 1981; Mann 1984; Herail, 1984; Michel, 1987).

(ii) The fact that from the known *in situ* occurrences of gold mineralisation in the Southern Uplands, particulate gold has only rarely been observed and that not all of the gold in assay can be accounted for by this particulate gold, and some of the gold occurs in solid solution or submicroscopic grains in sulphides. Weathering of this gold will release gold into groundwater and hence provide a source of gold from which supergene gold can form.

(iii) The recorded occurrence of large (up to 30 to 60g) nuggets associated with the Leadhills placer gold (MacLaren, 1902). Large nuggets are thought to be the result of secondary enrichment processes and not related to hypogene ore-forming processes (Boyle, 1979; Wilson, 1981).

(iv) There is no known *in situ* source for the Leadhills placer gold, despite much searching in both the sixteenth century, when the gold was mined, and more recently. This indicates that the Leadhills gold is the result of an already eroded ore deposit, or the placer gold is the result of supergene processes.

It is concluded that there are two types of placer gold in the Southern Uplands: low-fineness placer gold with a hypogene origin and high-fineness placer gold that has a supergene origin. Also that removal of this placer gold from its original deposit, be it a zone of supergene enrichment or primary ore, may have involved both glacial and alluvial processes.

The close geographical association of metamorphic aureoles, proximal morphological characteristics, and low-fineness gold indicates that the primary source of the placer gold, which is considered to be hypogene in origin, is mineralisation associated with the metamorphic aureoles of granites. This is supported by the fact that *in situ* mineralisation has been observed associated with the contact between the Cairnsphairn (Sharp, 1986) and The Loch Doon (Leake *et al.*, 1981) granitoids and that low fineness placer gold is associated with the northern margin of the Fleet granitoid. This would also seem a probable site for the location of *in situ* gold mineralisation. The time-temperature data obtained from this placer gold show that the fluids that formed the heterogeneous placer gold were low temperature (150 to 235°C). Where similar heterogeneous gold grains have been provenanced to a hypogene deposit (e.g., by Bowles *et al.*, 1984; Ivoilov *et al.*, 1982) the *in situ* mineralisation is epithermal. This suggests that some of the Southern Uplands placer gold represents relict epithermal gold mineralisation.

CHAPTER 10.

**DISCUSSION OF THE SOUTHERN
UPLANDS PLACER GOLD.**

10.1 Critique of the Methodology Developed in Chapter 8.

The use of the core fineness of placer gold for studying and delineating different populations of placer gold is well established (e.g., Stumpfl and Clark, 1965; Saager, 1968; Desborough, 1970; Desborough *et al.*, 1970; Desborough *et al.*, 1971; Czmanske *et al.*, 1973; Craig *et al.*, 1984; Guisti and Smith, 1984; Bowles *et al.*, 1984; Guisti, 1986). However the use of morphology, in the manner used in this work, to characterise different populations of placer gold has not been described before, although studies by Hallbauer (1981), Utter (1979), Hallbauer and Utter (1977), Bogdanova (1975), Sagon *et al.* (1985), and Guisti (1986) have shown that morphology is related to the degree of attrition and that shape can be used to discriminate between different sedimentological populations of placer gold.

The classification by morphology using different characteristics, and the arrangement of these characteristics into an order of approximately increasing degree of comminution is based on empirical observation and not on experimental data. Hence, the relationship between morphology and the degree of attrition is not precisely determined. However, the morphological characteristics of non-abraded "pristine" gold grains have been determined by examining the morphological characteristics of lode gold dissolved from quartz. Thus the morphological characteristics of placer gold that has undergone little mechanical abrasion can be related to the morphological features exhibited by "pristine" gold. The relationship between morphology and the degree of attrition has been described by Hallbauer (1981), Utter (1979), and Hallbauer and Utter (1977) and in the present work, by the comparison of the morphology of placer gold collected from the Hirgwm and Mawddach rivers in north Wales, where the distance from lode gold to the point of collection of the placer gold is known.

10.2 Discussion of the Southern Uplands Placer Gold Data.

The data for the Southern Uplands placer gold can be summarised as follows:

- (i) compositionally there are two populations of placer gold: a low to high fineness population (500-950 fine); and a very high fineness population (950-1000 fine).
- (ii) The morphological characteristics indicate that there are proximal and distal populations of placer gold, and a significant number of grains exhibit the micro-morphological feature of a porous surface at high magnification.

All of the above types of placer gold are present in both of the project areas studied. The difference between the two project areas is the proportion of the various types of placer gold. In the Loch Doon-Glenkens area there is a higher proportion of low-fineness and proximal placer gold than in the Abington-Biggarr-Moffat area, and the Abington-Biggarr-Moffat placer gold has a higher proportion of grains that exhibit the micro-morphological feature of a porous surface at high magnification.

The compositional data for the Southern Uplands placer gold indicate that the placer gold has two origins: a hypogene origin that is associated with the contact between the granite plutons, and a supergene origin.

Hypogene Origin.

The hypogene origin is indicated by the spatial association between placer gold exhibiting proximal morphological characteristics and the contact between granite and country rock. This placer gold has a distinct fineness range (<950). This hypogene origin is also indicated by the spatial association of the heterogeneous placer gold with the Fleet granite. The heterogeneities exhibited by this gold are interpreted as being primary in origin on petrographic grounds, and by analogy with recorded occurrences of heterogeneous placer gold in the literature (cf. Czamnske *et al.*, 1973 and Bowles *et al.*, 1984). Heterogeneous placer gold has been described from *in situ* occurrences in

epithermal Au-Ag vein type deposits in Japan (Shikazono, 1985). The annealing history limits obtained from the heterogeneous placer gold show that the placer gold grains originally formed at temperatures between 165-235°C. The comparison with data published in the literature and the temperatures obtained from the heterogeneous placer gold indicate that the primary mineralisation that formed some of the Southern Uplands placer gold may have been epithermal.

Supergene origin.

The morphological feature of a porous or spongy surface at high magnification has been observed by a number of workers (Bogdanova, 1975; Hallbauer and Utter, 1983; Herail, 1984; Guisti, 1986; and Michel, 1987). Michel (1987) and Herail (1984) observed this morphological feature in placer gold recovered from lateritic weathering profiles, and concluded that the placer gold originated from alteration of auriferous sulphides from an underlying orebody. Mann (1984) in a study of the mobility of gold in lateritic weathering profiles observed the occurrence of high fineness gold and Wilson (1981) attributed the formation of high fineness nugget of gold to the transport of gold in, and the precipitation of gold from, groundwater solutions. Hence, the association, in the Southern Uplands, of high fineness (<950) placer gold with the morphological characteristic of a porous surface at high magnification indicates that this gold has formed by secondary processes.

10.3 Limitations of the Technique.

The most important limitation of the technique is that the presence of an individual morphological characteristic cannot be used to estimate the distance of transport of placer gold grains in the fluvial environment, as there are too many variables that influence the shape of placer gold (e.g., stream velocity, climate, size and original shape). Thus it is not possible to estimate how far placer gold grains have travelled from a hypogene deposit.

The technique also requires a reasonably large sample to allow a reliable statistical interpretation of the data. For example, in the Southern Uplands where generally only one grain of gold was found at any particular locality, comparisons of morphological data between individual localities cannot be made. Hence, the comparisons possible using the data from the Southern Uplands are mainly restricted to comparisons of the frequency distributions of morphological characteristics and composition between the two project areas, and the relationship between morphology and composition. For example, the relationship between morphology and composition is illustrated by the association of the morphological characteristic of a porous surface at high magnification with high fineness placer gold.

Future Work.

As the relationship between morphology and degree of attrition is based on empirical observations there is a need to test the empirical observations experimentally. This could be achieved by conducting tumbling experiments similar to those undertaken by Yeend (1969) , but using pristine gold dissolved from ore as starting material instead of placer gold. This would enable comparison of gold grains that have undergone known degrees of attrition with the morphological features of placer gold.

Further work should also be aimed at examining placer gold from areas where the location of *in situ* gold mineralisation is known so that the geographical distribution of morphological characteristics can be directly related to the geographical distribution of *in situ* gold mineralisation.

REFERENCES.

- Allen, P.M., 1979, Mineral exploration in the Harlech Dome, North Wales. *Mineral Reconnaissance Programme Rep. Inst. Geol. Sci.*, No. 29, 172p
- Allen, P.M. and Easterbrook, G.D., 1978, A mineralised breccia pipe and other intrusion breccias in the Harlech Dome, North Wales. *Trans. Instn. Min. Metall.*, Sect. B. Vol. 85, 100-108.
- Allen, P.M. and Jackson A.A., 1978, Bryn-teg Borehole, North Wales. *Bull. Geol. Surv. G.B.*, No. 61, 55p.
- Allen, P.M. and Jackson A.A., 1985, Geology of the country around Harlech. Memoir for 1:50 000 geological sheet 135 with part of sheet 149.
- Allen, P.M., Bide, P.J., Cooper, D.C., Parker, M.E., Easterbrook, G.D. and Haslam, H.W., 1981b, Copper-bearing intrusive rocks at Cairngarroch Bay, south-west Scotland. *Mineral Reconnaissance Programme Rep. Inst. Geol. Sci.*, No. 39.
- Allen, P.M., Cooper, D.C., Fuge, R., and Rea, W.E., 1976, Geochemistry and relationships to mineralisation of some igneous rocks of the Harlech Dome. *Trans. Instn. Min. Metall.*, Sect. B. Vol. 85, 100-108.
- Allen, P.M., Cooper, D.C., Parker, M.E. and Haslam, H.W., 1982, Mineral exploration in the area of the Fore Burn igneous complex, south-western Scotland. *Mineral Reconnaissance Programme Rep. Inst. Geol. Sci.*, No. 55.
- Allen, P.M., Jackson A.A. and Rushton A.W.A., 1981a, The stratigraphy of the Mawddach Group in the Cambrian succession of North Wales. *Proc. Yorkshire Geol. Soc.*, Vol. 43, 295-329.
- Andrew, A.R., 1910, The geology of the Dolgelley Gold Belt, North Wales. *Geol. Mag.*, Vol. 7, 159-171, 201-211, 261-271.

- Ashton, J.H., 1976, *Wallrock Geochemistry and Ore Geology of Certain Mineralised Veins in North Wales*. Unpublished Ph.D Thesis, University of Aberystwyth.
- Bancroft, G.M. and Jean, G.E., 1982, Gold deposition at low temperature on sulphide minerals. *Nature*, Vol. 298, 730-731.
- Barnes, R.P., Rock, N.M.S. and Gaskarth, J.W., 1986, The Caledonian dyke-swarms in Southern Scotland: new field and petrological data for the Wigtown peninsula, Galloway. *Geological Journal* , Vol. 21, 101-25.
- Barton, P.B. Jr, 1970, Sulphide petrology. *Min. Soc. Amer. Spec. Pap.* No. 3, 187-198
- Barton, P.B. Jr., and Skinner, B.J., 1979, Sulphide mineral stabilities. In: Barnes H.L. (Editor), *Geochemistry of Hydrothermal Ore Deposits*, 2nd edition. Pp. 278-403, New York, John Wiley.
- Barton, P.B. Jr., and Toulmin, P., 1964, The electrom-tarnish method for the determination of fugacity of sulphur in laboratory systems. *Geochim. et Cosmochim. Acta* , Vol. 28, 619-640.
- Beckinsale, R.D. and Rundle, C.C., 1980, K-Ar ages for amphibole separates from the Rhobell Volcanic Group (Upper Tremadocian) Harlech Dome, North Wales. *Geological Journal* , Vol. 10, 165-175.
- Bogdanova, R., 1975, Morphological features and composition of placer gold from the Panagyurishte district. *Rudoobraz. Prosesi Miner. Nakhodishta* , Vol. 3, 3-8 (in Bulgarian with English summary and figure captions). C.A. 85(22):163528.
- Bottrell, S.H., 1986, *The origin of the gold mineralization of the Dolgellau region, North Wales: the chemistry and role of fluids* . Unpublished Ph.D Thesis, University of East Anglia.

- Bottrell, S.H., Shepherd, T.J., Yardley, B.W.D and Dubessy, J., 1988, A fluid inclusion model for the genesis of the ores of the Dolgellau Gold Belt, North Wales. *J. Geol. Soc. London*, Vol. 145, 139-145.
- Bowles, J.F.W, Cameron, B.A., Beddoe-Stevens, B. and Young, R.D., 1984, Alluvial gold, platinum, osmium-iridium, copper-zinc and copper-tin alloys from Sumatra - their origin and genesis. *Trans. Instn. Min. Metall.*, Sect. B. Vol. 93, 23-30.
- Boyle, R.W., 1979, The geochemistry of gold and its deposits (together with a chapter on geochemical prospecting for the element). *Geol. Surv. Canada Bulletin*, No. 280, 584p.
- Brown, G.C., Cassidy, J., Tindle, A.G. and Hughes, D.J., 1979a, The Loch Doon Granite: an example of granite petrogenesis in the British Caledonides. *J. Geol. Soc. London*, Vol. 136, 745-753.
- Brown, M.J., Leake, R.C., Parker, M.E. and Fortey, N.J., 1979b, Porphyry copper style mineralisation at Black Stockarton Moor, south-west Scotland. *Mineral Reconnaissance Programme Rep. Inst. Geol. Sci.*, No. 30.
- Clarkson, C.M., Craig, G.Y. and Walton, E.K., 1975, The Silurian rocks bordering Kirkcudbright Bay, south-west Scotland. *Trans. R. Soc. Edinburgh*, Vol. 69, 313-325.
- Cooper, D.C., Parker, M.E. and Allen P.M., 1982, Investigations of small intrusions in southern Scotland. *Mineral Reconnaissance Programme Rep. Inst. Geol. Sci.*, No. 58.
- Cox, A.H. and Wells, A.K, 1927, The geology of the Dolgelley district, Merionethshire. *Proc. Geol. Assoc.*, Vol. 38, 265-318.
- Craig, G.Y., 1983, *Geology of Scotland* (2nd. Edition), Scottish Academic Press, Edinburgh, 472p.

- Craig, J.R. and Barton, P.B. Jr., 1973, Thermochemical approximations for sulphosalts. *Econ. Geol.*, Vol. 68, 493-506.
- Craig, J.R., Solberg, T.N. and Linden, M.A., 1982, Appalachian gold: ore mineralogy and chemistry of central and southern deposits. *Trans. Soc. Min. Engrs.*, Vol. 274, 1870-1872.
- Czmanske, G.K., Desborough, G.A. and Goff, F.E., 1973, Annealing history limits for inhomogeneous native gold grains as determined from Au-Ag diffusion rates. *Econ. Geol.*, Vol. 65, 1275-1288.
- Dawson, J., Floyd, J.D. and Phillip, P.R., 1979, A mineral reconnaissance survey of the Abington-Biggarr-Moffat area, south-central Scotland. *Mineral Reconnaissance Programme Rep. Inst. Geol. Sci.*, No. 28.
- Dawson, J., Floyd, J.D. Phillip, P.R., Burley, A.J., Allsop, J.M., Bennett, J.R.P., Marsden, G.R., Leake, R.C. and Brown, M.J., 1977, A mineral reconnaissance survey of the Loch Doon-Glenkens area south-west Scotland. *Mineral Reconnaissance Programme Rep. Inst. Geol. Sci.*, No. 18.
- Deer, W.A., 1935, The Cairnsmore of Cairnsphairn igneous complex. *Q. J. Geol. Soc. London*, Vol. 91, 47-46.
- Desborough, G.A., 1970, Silver depletion indicated by microanalyses of gold from placer occurrences, Western U.S.A.. *Econ. Geol.*, Vol. 65, 304-311.
- Desborough, G.A., Heidel, P.H., Raymond, W.H. and Tripp, J., 1971, Primary distribution of Au and Cu in native gold from six deposits in the Western U.S.A. *Mineral. Deposita*, Vol. 6, 321-334.
- Desborough, G.A., Raymond, W.H. and Iagmin, P.J., 1970, Distribution of silver and copper in placer gold derived from the north-eastern part of the Colorado Mineral Belt. *Econ. Geol.*, Vol.65, 937-944.

- Duller, P.R., 1984, Turbidite hosted gold mineralization (abs.). Mineral Deposits Studies Group of the Geological Society of London, Annual General Meeting, Aberdeen University.
- Dunham, K., Beer, K.E., Ellis, R.A., Gallagher, M.J., Nutt, M.J.C. and Webb, B.C., 1979, United Kingdom. Pp 263-317. In: Bowie, S.H.U., Kvalheim, A. and Haslam, H.W. (Editors.), *Mineral Deposits of Europe*, Vol. 1, Instn. Min. Metall. and Mineral Soc. London.
- Dunkley, P.N., 1979, Ordovician volcanicity of the S.E. Harlech Dome. Pp. 597-601. In: *The Caledonides of the British Isles - Reviewed*. Harris, A.L., Holland, C.H. and Leake B.E. (Editors). *Spec. Pub. Geol. Soc. London*, No. 8.
- Eales, H.V., 1968, Determining fineness variation characteristics of gold by reflectometry. *Econ. Geol.*, Vol. 63, 688-699.
- Evans, D.L., 1981, Laterization as a possible contributor to gold placers. *Eng. Min. J.*, Vol. 182, 86-91.
- Eyles, V.A., Simpson, J.B. and MacGregor, A.G., 1929, The igneous geology of Central Ayrshire. *Trans. Geol. Soc. Glasgow*, Vol. 18, 361-381.
- Eyles, V.A., Simpson, J.B. and MacGregor, A.G., 1949, Geology of Central Ayrshire. *Mem. Geol. Surv. Scotland*, 157pp.
- Fisher, M.S., 1935, The origin and composition of alluvial gold, with special reference to the Morobe gold field, New Guinea. *Trans. Instn. Min. Metall.*, Vol. 44, 337-420.
- Fisher, N.H., 1945, The fineness of gold with special reference to the Morobe gold field, New Guinea. *Econ. Geol.*, Vol. 40, 449-495.

- Fitch, F.J., Miller, J.A., Evans, A.L., Grasty, R.L. and Meneisy, M.Y., 1969, Isotopic age determinations on rocks from Wales and the Welsh Borders. In: *The Pre-Cambrian and Lower Palaeozoic rocks of Wales*. 23-45, University of Wales Press.
- Floyd, J.D., 1982, Mineral reconnaissance survey of the Loch Doon-Glenkens area south-west Scotland. *Trans. Instn. Min. Metall.*, Sect. B. Vol. 86, 219-220.
- Gallagher, M.J., Michie, U. McL., Smith, R.T., Harries, L., Garson, M.S. and May, F., 1971, New evidence of uranium and other mineralisation in Scotland. *Trans. Instn. Min. Metall.*, Sect. B. Vol. 80, 150-173.
- Gallagher, M.J., Stone, P., Kemp, A.E.S., Hills, M.G., Jones, R.C., Smith, R.T., Peachey, D., Vickers, B.P., Parker, M.E., Rollin, K.E. and Skilton, B.R.H., 1983, Stratabound arsenic and vein antimony mineralisation in Silurian greywackes at Glendinning south Scotland. *Mineral Reconnaissance Programme Rep. Inst. Geol. Sci.*, No. 59.
- Gardiner, C.J. and Reynolds, S.H., 1937, The Cairnsmore of Fleet granite and its metamorphic aureole. *Geol. Mag.*, Vol. 74, 280-300.
- Gather, B. and Blachnik, R., 1974, The gold-bismuth-tellurium system. *Z. Metallkunde*, Vol. 65, 653-656.
- Gilbey, J.W.G., 1969, *The Mineralogy, Paragenesis, and Structure of the Ores of the Dolgellau Gold Belt, Merionethshire, and Associated Wallrock Alteration*. Unpublished Ph.D Thesis, University of London.
- Greenly, E., 1897, Incipient metamorphism in the Harlech Grits. *Trans. Edinb. Geol. Soc.*, 254
- Greenly, E., 1919, The geology of Anglesey. *Mem. geol. Survey Great Britain*, 2 Vols., 980p.

- Gregory, J.W., 1928, The nickel-cobalt ore of Talnotry, Kirkcudbrightshire. *Trans. Instn. Min. Metall.*, Vol. 37 178-195.
- Guisti, L., 1986, The morphology, mineralogy and behavior of "fine grained" gold from placer deposits of Alberta: sampling and implications for mineral exploration. *Canad. J. Earth Sci.*, Vol. 23, 166-1672.
- Guisti, L. and Smith, D.G.W., 1984, An electron microprobe study of some alberta placer gold. *Tschermaks Mineral. Petrog. Mitt.*, Vol. 33, 187-202.
- Hall, G.W., 1975, *The gold mines of Merioneth*. (Gloucester: Griffin Publications.) 120pp.
- Hallbauer, D.K., 1981, Geochemistry and morphology of mineral components from the fossil gold and uranium placers of the Witswatersrand. *U.S. Geol. Surv. Prof. Pap.*, 116-M, M1-M22.
- Hallbauer, D.K. and Utter, T., 1977, Geochemical and morphological characteristics of gold particles from recent river deposits and the fossil placers of the Witswatersrand. *Mineral. Deposita*, Vol. 12, 293-306.
- Halliday, A.N., Stephens, W.E. and Harmon, R.S., 1980, Rb, Sr, and O isotope relationships in three zoned Caledonian granitoids from the Southern Uplands, Scotland: evidence for magma mixing. *J. Geol. Soc. London*, Vol. 137, 329-348.
- Herail, G., 1984, *Geomorphologie et géologie de l'or detritique (piemonts et bassins intramontagneux du nord-ouest de L'Espagne)*. Editions C.N.R.S., 456p.
- Holland, C.H., 1979, *A Geology of Ireland*. Scottish Academic Press, Edinburgh.
- Ineson, P.R. and Mitchell, J.G., 1974, K-Ar isotopic age determinations from some Scottish mineral localities. *Trans. Instn. Min. Metall.*, Sect. B. Vol. 83, 13-18.

- Ineson, P.R. and Mitchell, J.G., 1975, K-Ar isotopic age determinations from some Welsh mineral localities. *Trans. Instn. Min. Metall.*, Sect. B. Vol. 84, 7-16.
- Ivoilov, A.S., Zav'yalova, L.L., Lipskaya, V.I., Khramchenko, S.I. and Barankevich, V.G., 1982, Composition of the gold in placers and their possible sources. *Geologiya i Geofizika*, Vol. 23, 53-56.
- Jackson, J.S., 1979, Metallic ores in Irish prehistory: copper and tin. In: Ryan (Editor). *The Origins of Metallurgy in Western Europe*. 107-125.
- Jean, G.E. and Bancroft, G.M., 1985, An XPS and SEM study of gold deposition on mineral surfaces: concentration of gold by adsorption/reduction. *Geochim. et Cosmochim. Acta*, Vol. 49, 979-987.
- Jones, O.T., 1924, Lead and zinc ores in the slaty rocks of Britain. *Trans. Instn. Min. Engrs.*, Vol. 66, 219-242.
- Kelling, G., 1961, The stratigraphy and structure of the Ordovician rocks of the Rhinns of Galloway. *Q. J. Geol. Soc. London*, Vol. 117, 37-75.
- Kelling, G., 1962, The petrology and sedimentation of Upper Ordovician rocks of the Rhinns of Galloway. *Trans. R. Soc. Edinburgh*, Vol. 67, 107-37.
- Kinahan, G.H., 1883, On the possibility of gold being found in quantity in County Wicklow. *Sci. Proc. R. Dublin Soc.*, Vol. 4, 39-42.
- Knipe, R.J. and Needham, D.T., 1985, Deformation processes in accretionary wedges - examples from the southwestern margin of the Southern Uplands, Scotland. In: *Collision Tectonics*. Coward, M.P. and Ries, A.C. (Editors). *Spec. Pub. Geol. Soc. London*, No.8.
- Kokelaar, B.P., 1977, *The Igneous History of the Rhobell Fawr Area, Merionethshire, North Wales*. Unpublished Ph.D Thesis, University of Wales, Aberystwyth.

- Kokelaar, B.P., 1979, Tremadoc to Llanvirn volcanism on the south east side of the Harlech Dome (Rhobell Fawr), North Wales. In: *The Caledonides of the British Isles - Reviewed*. Harris, A.L., Holland, C.H. and Leake B.E. (Editors). *Spec. Pub. Geol. Soc. London*, No. 8.
- Kokelaar, B.P., Fitch, F.J. and Hooker, P.J., 1982, A new K-Ar age from the uppermost Tremadoc, North Wales. *Geol. Mag.*, Vol. 119. No.2, 207-211.
- Leake, R.C., Auld, H.A., Stone, P. and Johnson, C.E., 1981, Gold mineralisation at the southern margin of the Loch Doon granitoid complex, south-west Scotland. *Mineral Reconnaissance Programme Rep. Inst. Geol. Sci.*, No.46, 41p.
- Leake, R.C. and Brown, M.J., 1979, Porphyry - style copper mineralisation at Black Stockarton Moor, south-west Scotland. *Trans. Instn. Min. Metall.*, Sect. B. Vol. 88, 177-181.
- Lebedeva, N.V., 1982, The study of the processes of gold deposition on bismuth and tellurobismuthite. Deposited Doc., Viniti 6348-82, avail. Viniti, 169-176 (in Russian: CA 100(24):195243v).
- Leggett, J.K., 1987, The Southern Uplands as an accretionary prism: the importance of analogues in reconstructing palaeogeography. *J. Geol. Soc. London*, Vol. 144, 737-752.
- Leggett, J.K., McKerrow, W.S. and Casey, D.M., 1982, The anatomy of a Lower Palaeozoic accretionary forearc: the Southern Uplands of Scotland. In: Leggett, J.K. (Editor), *Trench Fore-arc Geology. Spec. publ. geol. Soc. London*, Vol. 10, 495-520.
- Leggett, J.K., McKerrow, W.S., and Eales, M.H., 1979a, The Southern Upland of Scotland: a Lower Palaeozoic accretionary prism. *J. Geol. Soc. London*, Vol. 138, 167-176.

- Leggett, J.K., McKerrow, W.S., Morris, J.H., Oliver, G.J. and Philips W.E.A., 1979b, The northwestern margin of the Iapetus Ocean. In: *The Caledonides of the British Isles - Reviewed*. Harris, A.L., Holland, C.H. and Leake B.E. (Editors). *Spec. Pub. Geol. Soc. London*, No. 8.
- Lindsay, W.L., 1867, The gold and goldfields of Scotland. *Trans. Edinburgh geol. Soc.*, Vol. 1, 105-115.
- Lowell, J.D. and Guilbert, J.M., 1970, Lateral and vertical alteration, and mineralisation zoning in porphyry ore deposits. *Econ. Geol.*, Vol. 65, 383-403.
- Lyburn, E. St. J., 1901, Prospecting for gold in County Wicklow, and an examination of rocks for gold and silver. *Sci. Proc. R. Dublin Soc.*, Vol. 9, 422-433.
- Mackay, R.A., 1944, The purity of native gold as criterion in secondary enrichment. *Econ. Geol.*, Vol. 39, 56-68.
- MacKay, R.A., 1959, The Leadhills-Wanlockhead mining district. In: *Symposium on the Future of Non-ferrous Mining in Great Britain and Ireland.*, Instn. Min. Metall., 49-64.
- Mackie, W., 1923, The principles that regulate the distribution of heavy particles of heavy minerals in sedimentary rocks, as illustrated by the sandstones of the north east of Scotland. *Trans. geol. Soc. Edinburgh* , Vol. 11, 138-164.
- MacLaren, J.M., 1902, The occurrence of gold in Great Britain and Ireland. *Trans. Instn. Min. Engrs.*, Vol. 25, 435-508.
- Mann, A., 1984, Mobility of gold and silver in lateritic weathering profiles: some observations from Western Australia. *Econ. Geol.*, Vol. 79, 86-91.
- Matley, C.A., and Wilson, T.S., 1946, The Harlech Dome north of the Barmouth estuary. *Q. J. Geol. Soc. London*, Vol. 102, 1-40.

- McArdle, P. and Warren, W.P., 1987, Iron formation as a bedrock source of gold in southeast Ireland and its implications for exploration. *Trans. Instn. Min. Metall.*, Sect. B. Vol. 96, 195-200.
- McKerrow, W.S., Leggett, J.K. and Eales, M.H., 1977, Imbricate thrust model of the Southern Uplands. *Nature*, Vol. 267, 273-289.
- Michel, D., 1987, Concentration of gold in *in situ* laterites from Mato Grosso. *Mineral. Deposita*, Vol. 22, 185-189.
- Mills. K.C., 1974, *Thermodynamic Data for Inorganic Sulphides, Selenides and Tellurides*. London, Butterworths, 845p.
- Moorbath, S., 1962, Lead isotope abundance studies on mineral occurrences in the British Isles and their geological significance. *Phil. Trans. Roy. Soc. London*, Vol. 245B, 295-360.
- Morris, J.H., 1987, The Northern Belt of the Longford-Down Inlier, Ireland and Southern Uplands, Scotland: an Ordovician back-arc basin. *J. Geol. Soc. London*, Vol. 144, 773-786.
- Morrison, T.A., 1975, *Gold Mining in Western Merioneth*. Merioneth Historical and Record Society, Llandysul, 98p.
- Muir, W.L.G., 1972, Sb mineralization at Hare Hill, New Cumnock, Ayrshire. Open file B.G.S. Report, Edinburgh.
- Murchison, Sir R.I., 1839, *The Silurian System*.
- Needham, D.T. Knipe, R.J., 1986, Accretion and collision related deformation in the Southern Uplands accretionary wedge. *Geology*, Vol. 14, 303-306.
- Neuerberg, G.J., 1979, A procedure, using hydrofluoric acid, for quantitative mineral separations from silicate rocks. *J. Res. U.S. Geol. Surv.*, Vol. 3, 337-378.

- Oliver, G.J.H. and Leggett, J.K., 1980, Metamorphism in an accretionary prism: prehnite-pumpellyite facies metamorphism of the Southern Uplands of Scotland. *Trans. R. Soc. Edinburgh* , Vol. 71, 235-246.
- Parker, M.E., 1977, Geophysical surveys around the Talnotry Mine, Kirkcudbright, Scotland. *Mineral Reconnaissance Programme Rep. Inst. Geol. Sci.*, No. 10, 10p.
- Parslow, G.R., 1968, The physical and structural features of the Cairnsmore of Fleet Granite and its aureole. *Scott. J. Geol.*, Vol. 4, 91-108.
- Parslow, G.R., 1971, Variations of mineralogy and major elements in the Cairnsmore of Fleet Granite, south-west Scotland. *Lithos*, Vol. 4, 43-45.
- Petrovskaya, N.V. and Fastalovich, A.I., 1955, Changes in the internal texture of native gold buried in placers. *Vop. Geol. Azii.*, No.2, 245-256.
- Phillips, L., 1918, *Report to the comptroller of the department for the development of mineral resources in the United Kingdom*. Ministry of Munitions of War, London, HMSO.
- Pitu'ko, V.M., 1976, The behavior of gold in the oxidation zones of deposits in the Far North. *Geochem. International*, Vol. 13, 157-163.
- Ramdohr, P., 1965, Rheingold als seifenmineral. *Jahrb. Geol. Landesamt. Baden Wurtemberg* , Vol. 1, 81-95.
- Ramdohr, P., 1969, *The Ore Minerals and their Intergrowths*. Pergamon Press, 1182p
- Ramsay, Sir A., 1881, The geology of North Wales. *Mem. Geol. Surv. Great Britain*, Vol. 3, 611p.
- Read. H.H., 1931, The geology of Central Sutherland. *Memoir of the Geological Survey of Scotland.*, 238p.

- Readwin, T.A., 1888, On the occurrence of gold in Wales. *Proc. Geol. Assoc.*, Vol. 10, 339-344.
- Reeves, T.J., 1971, Gold in Ireland. *Bull. geol. Surv. Ireland*, Vol. 1, 73-85.
- Rice, R. and Sharp, G.J., 1976, Copper mineralisation in the forest of Coed-y-Brenin, North Wales. *Trans. Instn. Min. Metall.*, Sect. B. Vol. 85, 1-13.
- Rittenhouse, G., 1943, The transportation and deposition of heavy minerals. *Geol. Soc. Amer.*, Vol. 54, 1725-1780.
- Robie, R.A. and Waldbaum, D.R., 1968, Thermodynamic properties of minerals and related substances at 298.15 K (25°C) and one atmosphere (1.013 bars) and at higher temperatures. *U.S. geol. Survey Bull.*, No. 1259, 256p.
- Rock, N.M.S., 1984, Nature and origin of the calc-alkaline lamprophyres, minettes, vogesites, kersantites and spessarites. *Trans. R. Soc. Edinburgh*, Vol. 74, 193-227.
- Rock, N.M.S., 1987, Discussion. In: Leggett, J.K., The Southern Uplands as an accretionary prism: the importance of analogues in reconstructing palaeogeography. *J. Geol. Soc. London*, Vol. 144, 751-752.
- Rock, N.M.S., Gaskarth, J.W. and Rundle, C.C., 1986, Late Caledonian dyke-swarms in southern Scotland: a regional zone of K-rich lamprophyres and associated vents. *J. Geol.*, Vol. 94, 505-522.
- Rubey, W.W., 1933, Settling velocities of gravel, sand and silt particles. *Amer J. Sci.*, Vol. 25, 325-338.
- Saager, R., 1969, The relationship of silver and gold in the basal reef of the Witwatersrand System, South Africa. *Mineral. Deposita*, Vol. 4, 93-113.

- Sagon, J.P., Chaker, M., Dewulf, P. Floc'h, J.P., Malechaux, L., Quinton, M. and Santallier, D., 1975, Origin and concentration of alluvial gold in the Armorican Massif and Limousin, France. *Chron. Rech. Min.*, Vol. 40, 449-495.
- Salter, J.N., 1865, Explanation of a map of the faults in the gold district of Dolgellau. *Rept. Brit. Assn. Adv. Sci. (Transactions of the Sections)*, 73-74.
- Sawyer, J.B.P. and Dickinson, R.A., 1976, Mount Nausen. In: *Porphyry Copper Deposits of The Canadian Cordillera*, Sutherland-Brown, A. (Editor), Canad. Inst. Min. Metall. Special vol. 15, 366-343.
- Sedgwick, A., 1844, On the older Palaeozoic (Protozoic) rocks of North Wales. *Q. J. Geol. Soc. London*, Vol. 1, 5-22.
- Seward, T.M., 1973, Thio complexes of gold in hydrothermal ore solutions. *Geochim. et Cosmochim. Acta* , Vol. 37, 379-399.
- Seward, T.M., 1984, The transport and deposition of gold in hydrothermal systems. In: Foster R.J. (Ed.) *Gold '84* .
- Sharp, J.G., 1986, *Gold Exploration in the Southern Uplands of Scotland*. Unpublished M.Sc. Thesis, Cambourne School of Mines.
- Shepherd, T.J. and Allen, P.M., 1985, Metallogensis in the Harlech Dome, North Wales: a fluid inclusion interpretation. *Mineral. Deposita*, Vol. 20, 150-168.
- Shikazono, N. 1985, A comparison of temperatures estimated from the electrum-sphalerite-pyrite-argentite assemblage, and filling temperatures of fluid inclusions from epithermal Au-Ag vein type deposits in Japan. *Econ. Geol.*, Vol. 80, 1415-1424.
- Soper, N.J. and Hutton, D.M.W., 1984, Late Sinistral displacements in Britain. Implications for a three plate collision model. *Tectonics*, Vol. 3, 781-794.

- Squair, H., 1965, A reflectometric method of determining the silver content of natural gold alloys. *Trans. Instn. Min. Metall.*, Vol. 74, 917-931.
- Stanley C.J., Symes, R.F., and Jones, G.C., 1987, Nickel-cobalt mineralisation at Talnotry, Newton Stewart, Scotland. *Mineralogy and Petrology*, Vol. 37, 293-313.
- Stanley,C.J., 1979, *Mineralogical Studies of Copper, Lead, Zinc and Cobalt Mineralisation in the English Lake District*. Unpublished Ph.D. Thesis, University of Aston
- Steed, G.M., 1982, Gold Mineralisation within the Clontibret Area - Mineralogical and Geochemical Results - Part 2. Munster Base Metals Ltd., Unpublished Company Report, 15p.
- Steed, G.M., and Annels, A.E., 1980, *The Ogofau Gold Mines. Mining Field Centre Guide*. University College Cardiff Publications, 4p.
- Steed, G.M., Annels, A.E., Shrestha, P.L. Tatler, P.S., 1976, Geochemical and biogeochemical prospecting in the area of the Ogofau Gold Mines, Dyfed, Wales. *Trans. Instn. Min. Metall.*, Sect. B. Vol. 109-117.
- Stephens, W.E. and Halliday, A.N., 1980, Compositional variation in the Galloway plutons. In: Atherton, M.P. and Tarney, J. (Editors), *Origin of Granite Batholiths: Geochemical Evidence*. Shiva Publishing Ltd.,9-17.
- Stone, P., Floyd, J.D., Barnes, R.P. and Lintern, B.C., 1987, A sequential back-arc and foreland basin thrust duplex model for the Southern Uplands of Scotland. *J. Geol. Soc. London*, Vol. 144, 753-764.
- Stumpfl, E.F. and Clark, A.M.. 1965, Electron-probe microanalysis of gold platinoid concentrates from southeast Borneo. *Trans. Instn. Min. Metall.*, Vol. 74, 933-946.

- Temple, A.K., 1956, The Leadhills-Wanlockhead lead and zinc deposits. *Trans. R. Soc. Edinburgh*, Vol. 63, 85-133.
- Tourtelot, H.A., 1968, Hydraulic equivalence of grains of quartz and heavier minerals, and implications for the study of placers. *U.S. Geol. Prof. Pap.*, 594-F, F1-13.
- Tyrrell, J.B., 1912, The law of the pay streak in placer deposits. *Trans. Instn. Min. Metall.*, Vol. 21, 593-605.
- Utter, T., 1979, The morphology and silver content of gold from the Upper Witwatersrand and Ventersdorp Systems of the Klerksdorp gold field, South Africa. *Econ. Geol.*, Vol. 74, 27-44.
- Vaughan, D.J. and Craig, J.R., 1978, *Mineral Chemistry of Metal Sulphides*. Cambridge University Press, 493p.
- Wells, A.K., 1925, The geology of the Rhobell Fawr district, Merioneth. *Q. J. Geol. Soc. London*, Vol. 81, 463-538.
- Wheatley, C.J.V., 1978, Ore mineral fabrics in the Avoca polymetallic sulphide deposit south-east Ireland. In: Verwoerd, W.J. (Editor), *Geol. Soc. South Africa Spec. Publ.*, No. 4, 529-544.
- Willan, R.C.R and Hall, A.J., 1980, Sphalerite geobarometry and trace element studies on stratiform sulphide from McPhuns Cairn, Loch Fyne, Argyll, Scotland. *Trans. Instn. Min. Metall.*, Sect. B. Vol. 90, 31-40.
- Wilson, A., 1981, The economic significance of non-hydrothermal transport of gold, and the accretion of large gold nuggets in laterite and other weathering profiles in Australia: Internat. Conf. Appl. Mineralogy, Johannesburg 1981, 1-15.
- Wilson, G.V. and Flett, J.S., 1921, Lead zinc copper and nickel ores of Scotland. *Spec. Rept. Min. Res. Great Britain.*, Vol. 17, 13p.

Wilson. G.V., 1920, Arsenic and antimony ores. *Spec. Rept. Min. Res. Great Britain.*,
Vol. 15.

Yeend, W., 1975, Experimental abrasion rates of detrital gold. *J Res. U.S. Geol. Surv.*,
Vol. 3, 203-212.